1077

SECTION COPY
MANEUVER LOADS BRANCH COPY

NATIONAL ADVISORY COMMITTEE FOR AERONAUTICS

TECHNICAL NOTE

No. 1077

JET-BOUNDARY AND PLAN-FORM CORRECTIONS FOR PARTIAL-SPAN MODELS WITH REFLECTION PLANE, END PLATE, OR NO END PLATE IN A CLOSED CIRCULAR WIND TUNNEL

By James C. Sivells and Owen J. Deters

Langley Memorial Aeronautical Laboratory
Langley Field, Va.

Washington
June 1946

NATIONAL ADVISORY COMMITTEE FOR AERONAUTICS

TECHNICAL NOTE NO. 1077

JET-BOUNDARY AND PLAN-FORM CORRECTIONS FOR PARTIAL-SPAN MODELS WITH REFLECTION PLANE, END PLATE, OR NO END PLATE IN A CLOSED CIRCULAR WIND TUNNEL

By James C. Sivells and Owen J. Deters

SUMMARY

A method is presented for determining the jet-boundary and plan-form corrections necessary for application to test data for a partial-span model with a reflection plane, an end plate, or no end plate in a closed circular wind tunnel. Examples are worked out for a partial-span model with each of the three end conditions in the Langley 19-foot pressure tunnel and the corrections are applied to measured values of lift, drag, pitching-moment, rolling-moment, and yawing-moment coefficients. A comparison of the corrected aerodynamic characteristics for all three end conditions indicates that good agreement is obtained with flaps neutral at values of lift coefficient below the stall and that somewhat less satisfactory agreement is obtained in the region of maximum lift coefficient or with flaps deflected. Except for the corrections to the rolling-moment coefficient, the jet-boundary corrections were somewhat smaller for the reflection-plane condition than for either of the other end conditions because the induced upwash angle was the lowest; also, the plan-form corrections for this end condition were considerably smaller because the wing lift distribution was the least altered as compared with that for a complete wing. From every consideration, the use of a reflection plane gave the best results for tests of a partial-span model.

INTRODUCTION

Because of the demand for greater load-carrying capacity, the size of bomber and transport airplanes is being steadily increased. In order to test models of

these airplanes in existing wind tunnels at Reynolds numbers as large as possible, greater use is being made of semispan or partial-span models. The use of such models effectively increases the Reynolds number at which tests can be made to two or more times the test Reynolds number for complete-span models. Such models are used to best advantage to determine the aerodynamic characteristics of wings, flaps, lateral-control devices, and ducts.

In many previous tests of partial-span models, wind-tunnel corrections to the test data have been neglected entirely. In some instances, however, these corrections may amount to as much as 20 percent of the uncorrected value and therefore every effort should be made to determine and apply the corrections. Davison and Rosenhead (reference 1) developed a method for determining the jet-boundary corrections to the angle of attack and drag of semispan models with a reflection plane in an open-jet circular wind tunnel. Kondo (reference 2) by a different method also determined these corrections for open and closed circular wind tunnels. Swanson and Toll (reference 3) determined these and several other corrections for models in a closed rectangular wind tunnel.

The purpose of the present report is to give a method for determining the jet-boundary and plan-form corrections to be applied to wind-tunnel data for partial-span models with a reflection plane, an end plate, or no end plate in a closed circular wind tunnel. For the jet-boundary corrections the methods of reference 3 are fairly closely followed in many respects after the basic methods of determining the jet-boundary-induced upwash angle have been established. In order to determine the jet-boundary-induced upwash angle for the reflection-plane condition, the method of reference 1 is revised to apply to a closed circular wind tunnel and extended so that corrections to rolling and yawing moments may be obtained. The jet-boundary-induced upwash angle for the conditions with an end plate and no end plate is determined by the usual methods for closed circular wind tunnels. The plan-form corrections described herein are those which must be applied to partial-span-wing data in order that the completely corrected data be applicable to complete-span wings.

The corrections derived herein have been applied to the data from tests in the Langley 19-foot pressure tunnel of a partial-span model with each of the three types of end condition: reflection plane, end plate, and no end plate. Included for purposes of comparison are rolling-moment data from tests of a complete-span model of the same airplane. A comparison of other aerodynamic characteristics with those of the complete-span model is not given because the model configurations were not comparable.

COEFFICIENTS AND SYMBOLS

The coefficients and symbols used herein are defined as follows:

C_{L_u} uncorrected lift coefficient $\left(\frac{\text{Measured lift}}{qS}\right)$

C_{D_u} uncorrected drag coefficient $\left(\frac{\text{Measured drag}}{qS}\right)$

C_{m_u} uncorrected pitching-moment coefficient

$$\left(\frac{\text{Measured pitching moment}}{qSc'}\right)$$

C_{l_u} rolling-moment coefficient corrected for asymmetry only

$$\left(\frac{\text{Measured rolling moment} - (\text{Measured rolling moment})_{\delta_a = 0^\circ}}{q(2S)b}\right)$$

C_{n_u} yawing-moment coefficient corrected for asymmetry only

$$\left(\frac{\text{Measured yawing moment} - (\text{Measured yawing moment})_{\delta_a = 0^\circ}}{q(2S)b}\right)$$

C_L lift coefficient; no corrections applied $\left(C_{L_u}\right)$

C_D drag coefficient completely corrected $\left(C_{D_u} + \Delta C_D\right)$

C_m pitching-moment coefficient corrected for plan form $\left(C_{m_u} + \Delta C_{m_p}\right)$

C_{l_c} corrected rolling-moment coefficient for semispan model with reflection plane

C_l rolling-moment coefficient completely corrected

C_n yawing-moment coefficient completely corrected $\left(C_{n_u} + \Delta C_n\right)$

where

q dynamic pressure $\left(\frac{1}{2}\rho V^2\right)$

ρ mass density of air

V airspeed

S model wing area

c' mean aerodynamic chord of complete wing

b twice model span

ΔC_D complete drag-coefficient correction $\left(\Delta C_{D_j} + \Delta C_{D_p}\right)$

ΔC_{D_j} jet-boundary correction to drag coefficient

ΔC_{D_p} plan-form correction to drag coefficient

ΔC_{m_p} plan-form correction to pitching-moment coefficient

ΔC_n complete correction to yawing-moment coefficient

$$\left(\left(\Delta C_{n_p}\right)_1 + \left(\Delta C_{n_p}\right)_2 + \left(\Delta C_{n_i}\right)_2 + \left(\Delta C_{n_i}\right)_3\right)$$

$\left(\Delta C_{n_p}\right)_1$ plan-form correction to yawing-moment coefficient due to end condition

$\left(\Delta C_{n_p}\right)_2$ plan-form correction to yawing-moment coefficient due to aspect ratio, taper ratio, and ratio of aileron span to wing span

$\left(\Delta C_{n_i}\right)_1$ yawing-moment-coefficient correction due to reflection plane

$\left(\Delta C_{n_i}\right)_2$ yawing-moment-coefficient correction due to boundary-induced aileron upwash and wing loading

$\left(\Delta C_{n_i}\right)_3$ yawing-moment-coefficient correction due to boundary-induced wing upwash and aileron loading

and

w induced vertical velocity; positive upward

v induced lateral velocity; positive toward wing tip

Γ circulation

r radius of circular jet

c_l section lift coefficient

c section chord

$\bar{c}$ mean geometric chord

x longitudinal coordinate or complex coordinate used in transformation

y lateral coordinate

y' lateral coordinate, fraction of model span $\left(\frac{y}{b/2}\right)$

z vertical coordinate

$\Delta\alpha_j$ jet-boundary correction to induced angle of attack

$\Delta\alpha_{s.c.}$ streamline-curvature correction to angle of attack

$\Delta\alpha_p$ plan-form correction to angle of attack

$\Delta\alpha$ complete correction to angle of attack $\left(\Delta\alpha_j + \Delta\alpha_{s.c.} + \Delta\alpha_p\right)$

α_o angle of attack for infinite aspect ratio

α_u uncorrected angle of attack

α corrected angle of attack $(\alpha_u + \Delta\alpha)$

α_i induced angle of attack

m_o section lift-curve slope per radian $(57.3a_o)$

m_u uncorrected lift-curve slope per radian $(57.3a_u)$

m corrected lift-curve slope per radian $(57.3a)$

a_o section lift-curve slope per degree $\left(\frac{dc_l}{d\alpha_o}\right)$

a_u uncorrected lift-curve slope per degree $\left(\frac{dC_L}{d\alpha_u}\right)$

a corrected lift-curve slope per degree $\left(\frac{dC_L}{d\alpha}\right)$

A aspect ratio

λ taper ratio; ratio of tip chord to root chord

E edge-velocity correction factor $\left(\frac{\text{Semiperimeter}}{\text{Span}}\right)$

u induced-drag correction factor (reference 4)

$x_{a.c.}$ distance from reference point to aerodynamic center

H factor used to determine $x_{a.c.}$ (reference 4)

Λ angle of sweepback of quarter-chord line

ΔC_{l_j} jet-boundary correction to rolling-moment coefficient

ΔC_{l_p} plan-form correction to rolling-moment coefficient

ΔC_l complete correction to rolling-moment coefficient

ΔC_{l_r} one-half rolling-moment-coefficient correction due to reflection plane

C_{l_δ} rate of change of rolling-moment coefficient with aileron deflection $\left(\frac{\partial C_l}{\partial \delta_a}\right)_\alpha$

δ_a aileron deflection

k rate of change of section angle of attack with aileron deflection $\left(\frac{\partial \alpha_o}{\partial \delta_a}\right)_{c_l}$

K factor used to determine induced yawing-moment coefficient (reference 5)

ξ complex coordinate in transformed plane

η lateral coordinate in transformed plane

ζ vertical coordinate in transformed plane

$\gamma = \tan^{-1}\frac{h}{d}$

h semiheight of reflection plane or end plate

d distance of reflection plane or end plate from center line of tunnel

e distance of wing tip from center line

s spanwise location of trailing vortex

σ spanwise location of trailing vortex in transformed plane

ϕ velocity potential function

ψ stream function

f factor used to determine lift-curve slope (reference 4)

R Reynolds number ($\rho V c'/\mu$)

μ coefficient of viscosity

M Mach number (V/V_c)

V_c speed of sound in air

Subscripts:

i induced

j jet boundary

p plan form

M model

2M wing of twice model span

W complete wing

e end plate

s.c. streamline curvature

u uncorrected

All pitching-moment coefficients, measured or corrected, are about the quarter-chord point of the mean aerodynamic chord of the complete wing. Corrected rolling-moment and yawing-moment coefficients are about the projection of this point in the plane of symmetry of the complete wing, although these moments were measured about the projection of this point in the plane at the root end of the model parallel to the plane of symmetry.

DERIVATION OF CORRECTIONS

The corrections to be applied to data from tests of partial-span models are of two types: jet boundary and plan form. The jet-boundary corrections are due to the influence of the tunnel wall on the induced velocities, which in turn affect the aerodynamic characteristics of the model. The main factors contributing to the jet-boundary corrections are the shape of the tunnel wall

and the size of the model relative to the tunnel. The geometric characteristics of the model also contribute to the corrections. The plan-form corrections may be divided into two parts. The first part is due to differences in the span loading of a complete wing and that of the model with a reflection plane, end plate, or no end plate. The second part is due to differences in aspect ratio, taper ratio, and the ratio of aileron span to wing span if the model span is less than the semispan of the complete wing.

For the sake of simplicity, not only in deriving the corrections but also in applying them to data, the lift due to flaps is not separated herein from the lift of the plain wing as in reference 3 which derives separate corrections for each part of the lift. Instead, the total lift is considered and the alteration of the span loading due to flaps is neglected. This neglect introduces a slight error in the results but is believed to be warranted by the resulting simplification. Several other corrections are also neglected when the magnitude of the corrections is within the limits of accuracy of the measurements.

The derivation of nearly all of the corrections begins with the spanwise lift distribution of the wing. In order to simplify the computations, the lift distribution for a lift coefficient of 1.0 is used. The lift distributions used herein were determined by lifting-line theory. For straight tapered wings, the tables of additional lift L_a in reference 4 are probably the most readily available source of information for the present purpose.

The distribution of the jet-boundary-induced upwash angle along the span must then be determined. This angle, in radians, is the ratio of the induced vertical velocity to the stream velocity. For a particular type of tunnel, tables may be devised that give the boundary-induced vertical velocity at any point in the tunnel due to a vortex of unit circulation placed at any point in the tunnel. The model generally is located close to the horizontal center line of the tunnel; consequently, the induced-vertical-velocity distribution along this center line only needs to be computed. The lift distribution is broken into several steps and each increment is multiplied by the proper value of induced vertical velocity per unit circulation to obtain an increment

of induced vertical velocity. The summation at each spanwise point of these increments due to all the image vortices is the induced vertical velocity at that point.

The induced upwash angle per unit lift coefficient at each point in a circular tunnel is expressed as

$$\frac{w}{VC_L} = \frac{\bar{c}}{2r}\sum \frac{wr}{\Gamma}\,\Delta\frac{c_l c}{C_L \bar{c}} \qquad (1)$$

where wr/Γ is the induced vertical velocity per unit circulation for a tunnel of unit radius.

Angle of attack.- The jet-boundary correction to the induced angle of attack is defined in reference 1 as

$$\Delta\alpha_j = \frac{1}{L}\int \frac{w}{V}\,dL$$

but the lift L of a partial-span model may be expressed as

$$L = q\bar{c}\frac{b}{2}\int_0^1 \frac{c_l c}{\bar{c}}\,dy'$$

$$= q\bar{c}\frac{b}{2}C_L$$

and

$$dL = qc_l c\,\frac{b}{2}\,dy'$$

After substitution and rearrangement, the induced angle of attack is, in radians,

$$\Delta\alpha_j = C_L \int_0^1 \frac{w}{VC_L} \frac{c_l c}{C_L \bar{c}} dy'$$

or, in degrees,

$$\Delta\alpha_j = 57.3 C_L \int_0^1 \frac{w}{VC_L} \frac{c_l c}{C_L \bar{c}} dy'$$

The correction for streamline curvature must be added to the jet-boundary correction to the induced angle of attack. The streamline-curvature correction, as used herein, is applied entirely to the angle of attack instead of partly to the angle of attack and partly to the lift coefficient as in reference 3. This procedure simplifies the computations of the data, and any differences in the results obtained by the two methods are well within the experimental accuracy. The magnitude of the curvature is obtained from reference 6 in which derivations are made for a circular tunnel and for a 1.41:1 elliptical tunnel. The derivation for the circular tunnel produces a nondimensional constant, proportional to the curvature, which in terms of this report is

$$\frac{1}{\frac{w}{VC_L}} \frac{d\frac{w}{VC_L}}{d\frac{x}{2r}} = 2.1$$

A similar constant for the elliptical tunnel is derived on the basis of the tunnel width but, when converted to the basis of the tunnel height, becomes identical with that for the circular tunnel. This fact indicates that this constant is a function of the tunnel height and is relatively independent of the tunnel width. Since only the width of a circular tunnel is affected by the introduction of a reflection plane, for the purpose of this report it is assumed that the constant derived in reference 6 applies whether or not the reflection plane is used.

The curvature of the streamlines is practically constant along the wing chord. The streamline-curvature correction for the wing may be determined from the difference between the induced upwash angle at the quarter-chord point where the lifting line is assumed to be located and the induced upwash angle at the three-quarter-chord point where the tangent to the streamline is the zero-lift line. This difference in the angles is

$$\Delta\left(\frac{w}{VC_L}\right)_{s.c.} = \frac{w}{VC_L}\,\frac{1}{\frac{w}{VC_L}}\,\frac{d\frac{w}{VC_L}}{d\frac{x}{2r}}\,\frac{0.75c - 0.25c}{2r}$$

$$= 1.05\frac{c}{2r}\,\frac{w}{VC_L}$$

This angle must be added to the induced angle at the lifting line so that the complete correction to the angle of attack due to the jet boundary is

$$\Delta\alpha_j + \Delta\alpha_{s.c.} = 57.3C_L \int_0^1 \frac{w}{VC_L}\left(1 + 1.05\frac{c}{2r}\right)\frac{c_l c}{C_L \bar{c}}\,dy'$$

or approximately

$$\Delta\alpha_j + \Delta\alpha_{s.c.} = 57.3C_L \left(1 + 1.05\frac{\bar{c}}{2r}\right)\int_0^1 \frac{w}{VC_L}\,\frac{c_l c}{C_L \bar{c}}\,dy' \qquad (2)$$

This approximation and the assumptions made for the use of the constant of reference 6 are sufficiently accurate for the present purpose, since the streamline-curvature correction is only a small fraction of the complete correction to the angle of attack.

Although the greatest accuracy would theoretically be obtained if the lift distribution of the model in the tunnel were used, the free-air lift distribution gives a result that is well within the accuracy of either experiment or the lifting-line theory. If the tunnel lift distribution is desired, an approximate result may be obtained from the free-air distribution by the equation

$$\frac{c_l' c}{C_L' \bar{c}} = \frac{c_l c}{C_L \bar{c}} \frac{m}{m_u} + m\left(1 + 1.05\frac{c}{2r}\right) \frac{w}{VC_L} \frac{c_l c}{C_L \bar{c}} \qquad (3)$$

where the primed values refer to the tunnel distribution and the unprimed values refer to the free-air distribution. This equation weights the induced upwash angle according to the lift distribution and would be exact if the quantity $\left(1 + 1.05\frac{c}{2r}\right) \frac{w}{VC_L}$ were constant along the span. For the conditions usually encountered in a wind tunnel, a very close approximation is obtained by using this equation. This equation may be used for a partial-span model with or without an end plate, for which cases other methods, such as the influence lines of reference 7 as used in reference 3, are not applicable.

The plan-form correction to the angle of attack is the correction to the slope of the lift curve necessary because of differences in aspect ratio between the model and the complete wing; that is,

$$\Delta\alpha_p = \left(\frac{1}{a_W} - \frac{1}{a_M}\right) C_L \qquad (4)$$

where the model or wing lift-curve slope is

$$a = \frac{\frac{a_o}{E}}{1 + \frac{57.3\frac{a_o}{E}}{\pi A}} \qquad (5)$$

and corresponding values of E and A are used. This equation was developed for an elliptic wing in reference 7 but is used herein for other plan forms because it has been shown to give good results even for the model with no end plate. For the model with an end plate, neither E nor A is known and the lift-curve slope is obtained by use of the lifting-line theory, as is shown later.

The complete correction to the angle of attack is

$$\Delta\alpha = \Delta\alpha_j + \Delta\alpha_{s.c.} + \Delta\alpha_p \tag{6}$$

Drag coefficient.- The jet-boundary correction to the drag coefficient involves the same integral as that for the angle of attack before the streamline-curvature correction is added; that is,

$$\Delta C_{D_j} = C_L^2 \int_0^1 \frac{w}{VC_L} \frac{c_l c}{C_L \bar{c}} dy' \tag{7}$$

The plan-form correction to the drag coefficient is that due to the difference in the induced drag of the complete wing and the model; it may be expressed as

$$\Delta C_{D_p} = C_{D_{i_W}} - C_{D_{i_M}} \tag{8}$$

For the reflection-plane condition

$$\Delta C_{D_p} = \left(\frac{1}{\pi A_W u_W} - \frac{1}{\pi A_{2M} u_{2M}} \right) C_L^2 \tag{9}$$

where u is obtained from reference 4. For the other end conditions $C_{D_{i_M}}$ may be obtained from lifting-line theory.

The complete correction to the drag coefficient is

$$\Delta C_D = \Delta C_{D_j} + \Delta C_{D_p} \tag{10}$$

Pitching-moment coefficient.- The correction to the pitching-moment coefficient is entirely due to plan form since the effects of streamline curvature may be neglected when the wing alone (no tail) is involved. The plan-form correction is a function of the sweep of the wing and would be zero for zero sweep. The correction is the ratio of the difference between the chordwise locations of the aerodynamic center of the model and that of the complete wing to the chord upon which the pitching-moment coefficient is based; that is,

$$\Delta C_{m_p} = \frac{x_{a.c._M} - x_{a.c._W}}{c'} C_L \tag{11}$$

Both $x_{a.c._M}$ and $x_{a.c._W}$ must be measured from the same point and are considered positive in the direction of the air stream. These distances may be obtained by the following equations:

$$x_{a.c.} = 2H\frac{b}{2} \tan \Lambda + \text{Constant} \tag{12}$$

$$= \frac{b}{2} \tan \Lambda \int_0^1 \frac{c_l c}{c_l \bar{c}} y' \, dy' + \text{Constant} \tag{13}$$

The value of the constant is the distance between a chosen reference point and the quarter-chord point of the root chord. For a model and reflection plane, the value of H may be obtained from reference 4. For the other end conditions, the integration (equation (13)) must be performed to obtain H.

Aileron distributions.- In order to determine the corrections to be applied to the rolling-moment and yawing-moment coefficients, two additional distributions are necessary: the lift distribution due to aileron deflection and the induced-upwash-angle distribution due to this lift distribution. The aileron lift distribution for a complete wing may be determined from lifting-line theory or by use of the influence lines of reference 7. This distribution must be altered to account for the effects of the reflection plane or other end condition. A reflection plane "reflects" the distribution over the model so that the model distribution is the same as would be obtained for a complete wing with both ailerons deflected in the same direction. The distribution for a model with a reflection plane therefore is obtained by adding the increment due to the "image" wing to the distribution of the "real" wing (reference 3). For a wing with or without an end plate, such a reflection is not present and the aileron lift distribution must be obtained directly from lifting-line theory. After the shape of the aileron lift distribution is determined, for convenience the ordinates are multiplied by a constant that makes the moment of the area equal to 4 if the abscissas are in fractions of the model span. This operation converts the ordinates to the load coefficient $\frac{c_l c}{C_l \bar{c}}$ and the rolling-moment coefficient to unity.

The induced-upwash-angle distribution due to the aileron lift distribution is obtained in the same manner as for the wing. The aileron lift distribution is broken into several steps, each increment is multiplied by the value of induced velocity per unit increment, and the summation is made of all the increments at each point; thus,

$$\frac{w}{VC_l} = \frac{\bar{c}}{2r} \sum \frac{wr}{\Gamma} \Delta \frac{c_l c}{C_l \bar{c}} \qquad (14)$$

where wr/Γ is the induced vertical velocity per unit circulation for a tunnel of unit radius.

Rolling-moment coefficient.- The jet-boundary correction to the rolling-moment coefficient is the moment of the increment in the aileron lift distribution due to the induced velocity; that is,

$$\Delta C_{l_j} = -\frac{1}{L} m C_{l_u} \int_0^1 \frac{w}{V C_l} \left(1 + 1.05 \frac{c}{2r}\right) \frac{c_l c}{C_L \bar{c}} y' \, dy' \qquad (15)$$

The increment in aileron lift distribution is similar to the increment in wing lift distribution given as the last term in equation (3). For this reason, equation (15) is approximate in the same sense as equation (3). A more accurate method of determining this correction to the rolling-moment coefficient could be used for the reflection-plane condition (see reference 3) but such a method would not be readily applicable for the end-plate and no-end-plate conditions. In reference 3 an aerodynamic-induction factor J is introduced that is approximately equal to 2 for a semispan or partial-span model. In equation (15) the three-dimensional lift-curve slope m is therefore approximately equal to $\frac{m_o A}{A + J}$ and the wing load coefficient $\frac{c_l c}{C_L \bar{c}}$ approximately accounts for the difference in the loadings of the actual wing and an elliptic wing. Although these conditions would not exist for a complete-span model, equation (15) may be used with sufficient accuracy for a semispan or partial-span model. As in the case of the wing, the tunnel distribution should theoretically be used to obtain this correction but, practically, the free-air distribution may be used.

The plan-form correction to the rolling-moment coefficient is, for convenience, divided into two parts; the first part corrects for the effect of the end condition on the aileron lift distribution and the second corrects for the difference in aspect ratio and taper ratio of the partial-span model and of the complete wing. The first part $\frac{C_{l_{\delta_{2M}}}}{C_{l_{\delta_M}}}$ is the ratio of the rolling-moment

coefficient per unit aileron deflection for a full-span model of twice the model span to that for the actual model. For the reflection-plane condition this correction is equal to the reciprocal of the correction $1 + \frac{2\Delta C_{l_r}}{C_{l_c}}$ of reference 3. For the end-plate or no-end-plate condition, this correction may be obtained from lifting-line theory. The second part of the plan-form correction is required only if the model is not a true semispan model and may be obtained from figure 16 of reference 8. For the particular aspect ratio and taper ratio of either a wing of twice model span or the complete wing, a value of C_{l_δ}/k is obtained by taking the difference between the values of C_{l_δ}/k for the outboard and inboard ends of the aileron. The desired correction is the ratio of the value of C_{l_δ}/k for the complete wing to that for the wing of twice model span.

The completely corrected value of the rolling-moment coefficient is

$$C_l = C_{l_u}\left(1 + \frac{\Delta C_{l_j}}{C_{l_u}}\right)\frac{C_{l_{\delta_{2M}}}}{C_{l_{\delta_M}}}\frac{\left(\frac{C_{l_\delta}}{k}\right)_W}{\left(\frac{C_{l_\delta}}{k}\right)_{2M}} \qquad (16)$$

Yawing-moment coefficient.- The jet-boundary corrections to the yawing-moment coefficient are derived as in reference 3 and are due to the interaction of the wing and aileron lift and induced-upwash-angle distributions. The equations for the corrections are

$$\left(\Delta C_{n_i}\right)_2 = -\frac{C_L C_{l_u}}{4}\int_0^1 \frac{w}{V C_l}\frac{c_l c}{C_L \bar{c}}\, y'\, dy' \qquad (17)$$

and

$$\left(\Delta C_{n_i}\right)_3 = -\frac{C_L C_{l_u}}{4} \int_0^1 \frac{w}{V C_L} \frac{c_l c}{C_l \bar{c}} y' \, dy' \tag{18}$$

The plan-form correction to the yawing-moment coefficient is divided into two parts in the same manner as that for the rolling-moment coefficient. The first part, due to the end condition, may be expressed as

$$\left(\Delta C_{n_p}\right)_1 = C_{n_{2M}} - C_{n_M}$$

$$= -K_{2M} C_L C_{l_{2M}} + K_M C_L C_{l_M}$$

$$= C_L C_{l_{2M}} \left(-K_{2M} + K_M \frac{C_{l_{\delta_M}}}{C_{l_{\delta_{2M}}}} \right) \tag{19}$$

where

$$K_{2M} = \frac{1}{4} \int_0^1 \left(\frac{c_l c}{C_{L_{2M}} \bar{c}} \frac{a_i}{C_{l_{2M}}} + \frac{c_l c}{C_{l_{2M}} \bar{c}} \frac{a_i}{C_{L_{2M}}} \right) y' \, dy' \tag{20}$$

$$K_M = \frac{1}{4} \int_0^1 \left(\frac{c_l c}{C_{L_M} \bar{c}} \frac{a_i}{C_{l_M}} + \frac{c_l c}{C_{l_M} \bar{c}} \frac{a_i}{C_{L_M}} \right) y' \, dy' \tag{21}$$

and the distributions of the lift and induced angle (in radians) per unit coefficient are identified by C_L for the wing and C_l for the aileron in the denominators. For the reflection-plane condition, the correction

$\left(\Delta C_{n_p}\right)_1$ is equal to the correction $\left(\Delta C_{n_i}\right)_1$ of reference 3. For the end-plate or no-end-plate conditions, the integrations for K_M and K_{2M} must be performed, the value of K_{2M} being independent of the end condition.

For the second part of the plan-form correction, due to differences in aspect ratio and taper ratio between the complete wing and a wing of twice model span, values of K may be obtained from figure 13 of reference 5. Interpolation is simplified by plotting K for the inboard end of the aileron against 1/A since such a plot is practically a straight line. If the outboard end of the aileron is some distance from the wing tip, the value of K must be modified as indicated in reference 5. The equation for this part of the correction is

$$\left(\Delta C_{n_p}\right)_2 = C_{n_W} - C_{n_{2M}}$$

$$= -K_W C_L C_{l} + K_{2M} C_L C_{l_{2M}}$$

$$= C_L C_{l} \left[-K_W + K_{2M} \frac{\left(\frac{C_{l_\delta}}{k}\right)_{2M}}{\left(\frac{C_{l_\delta}}{k}\right)_W} \right] \qquad (22)$$

The value of K_{2M} from equation (20) may differ slightly from that obtained from reference 5 because of slight differences in the methods of computation. If this value does differ, the value from equation (20) should be used in equation (19) and the value from reference 5 in equation (22).

The complete correction to the yawing-moment coefficient is

$$\Delta C_n = \left(\Delta C_{n_p}\right)_1 + \left(\Delta C_{n_p}\right)_2 + \left(\Delta C_{n_i}\right)_2 + \left(\Delta C_{n_i}\right)_3 \qquad (23)$$

CORRECTIONS FOR MODEL WITH REFLECTION PLANE

Determination of Induced Upwash Angle

A reflection plane used with a partial-span model in a circular wind tunnel reflects both the model and the tunnel; therefore the effect is that of a wing of twice the model span in a bipolar tunnel (fig. 1). This reflection satisfies the condition that the stream function must be constant over that part of the boundary of a closed tunnel formed by the reflection plane. In order to satisfy this condition over the circular-arc part of the bipolar tunnel, vortices that are images of the vortices inside the tunnel must be introduced outside the tunnel. The locations of these image vortices and their effects within the tunnel are well known for a circular tunnel. This knowledge may be used to determine their effects within a bipolar tunnel by transforming the interior of the bipolar tunnel into the interior of a circular tunnel by means of the conformal transformation of reference 1.

The transformation may be expressed as

$$\tan^{-1}\zeta = n \tan^{-1}\frac{x}{r \sin \gamma}$$

where, in the yz plane (bipolar tunnel),

$$x = y + iz$$

in the $\eta\zeta$ plane (circular tunnel),

$$\xi = \eta + i\zeta$$

and

$$n = \frac{\pi}{2(\pi - \gamma)}$$

Also,

$$h = r \sin \gamma$$

$$d = r \cos \gamma$$

It should be noted that the axes of reference 1 have been revised to agree with the standard wind axes used in figure 1. A point η on the η-axis that corresponds to a point y on the y-axis may be obtained by the relation

$$\tan^{-1}\eta = n \tan^{-1}\frac{y}{r \sin \gamma}$$

Furthermore, if there are vortices of strength $\pm\Gamma$ at the points $y = \pm s$ on the y-axis, there are vortices of equal strength at the points $\eta = \pm\sigma$ on the η-axis where

$$\tan^{-1}\sigma = n \tan^{-1}\frac{s}{r \sin \gamma}$$

The complex potential due to the vortices $\pm\Gamma$ at $\eta = \pm\sigma$ is

$$\phi_1 + i\psi_1 = \frac{i\Gamma}{2\pi} \log \frac{\xi - \sigma}{\xi + \sigma}$$

The complex potential due to the image vortices in the $\eta\zeta$ plane is

$$\phi_2 + i\psi_2 = \frac{i\Gamma}{2\pi} \log \frac{\xi - \frac{1}{\sigma}}{\xi + \frac{1}{\sigma}}$$

The condition that ψ is constant at the boundary of the jet can be easily seen since $|\xi| = 1$ at the boundary and $\psi_1 + \psi_2$ becomes equal to zero. The complex potential due to the original vortices in the yz plane at $y = \pm s$ is

$$\phi_3 + i\psi_3 = -\frac{i\Gamma}{2\pi} \log \frac{x - s}{x + s}$$

The complex potential due to the jet boundary is the difference between that in the $\eta\zeta$ plane and that in the yz plane; that is,

$$\phi + i\psi = \phi_1 + \phi_2 - \phi_3 + i\left(\psi_1 + \psi_2 - \psi_3\right)$$

The induced vertical velocity at the y-axis due to the jet boundary is one-half that due to vortices extending to infinity in both directions; that is

$$w = -\frac{1}{2} \frac{d\psi}{dy}$$

The induced velocity due to ψ_1 is

$$w_1 = -\frac{1}{2} \frac{d\psi_1}{dy}$$

$$= -\frac{1}{2} \frac{d\psi_1}{d\eta} \frac{d\eta}{dy}$$

$$= \left(-\frac{1}{2}\right)\left(-\frac{\Gamma}{2\pi}\right)\left(\frac{1}{\eta - \sigma} - \frac{1}{\eta + \sigma}\right)\frac{d\eta}{dy}$$

where

$$\frac{d\eta}{dy} = \frac{n(1 + \eta^2)}{r \sin \gamma \left(1 + \frac{y^2}{r^2 \sin^2 \gamma}\right)}$$

By collecting terms,

$$w_1 = \frac{\Gamma}{2\pi r} \frac{\sigma}{\eta^2 - \sigma^2} \frac{n(1 + \eta^2)}{\sin \gamma \left(1 + \frac{y^2}{r^2 \sin^2 \gamma}\right)}$$

The induced velocity due to ψ_2 is, similarly,

$$w_2 = -\frac{1}{2} \frac{d\psi_2}{d\eta} \frac{d\eta}{dy}$$

$$= -\frac{\Gamma}{2\pi r} \frac{\sigma}{\eta^2\sigma^2 - 1} \frac{n(1 + \eta^2)}{\sin \gamma \left(1 + \frac{y^2}{r^2 \sin^2 \gamma}\right)}$$

and the induced velocity due to $-\psi_3$ is

$$w_3 = -\frac{1}{2} \frac{d\left(-\psi_3\right)}{dy}$$

$$= -\frac{\Gamma}{2\pi r} \frac{\frac{s}{r}}{\left(\frac{y}{r}\right)^2 - \left(\frac{s}{r}\right)^2}$$

The net induced velocity is

$$w = w_1 + w_2 + w_3$$

It may be noticed that the value of w according to the final equations for w_1 and w_3 becomes indeterminate of the form $\infty - \infty$ at the point $y = s$ or $\eta = \sigma$. This is the only point at which singularities occur inside the tunnel. At this point, however, w may be determined in the following manner: Before the terms are combined,

$$w_1 + w_3 = \frac{\Gamma}{4\pi}\left[\left(\frac{1}{\eta - \sigma} - \frac{1}{\eta + \sigma}\right)\frac{d\eta}{dy} - \left(\frac{1}{y - s} - \frac{1}{y + s}\right)\right]$$

$$= \frac{\Gamma}{4\pi}\left(\frac{1}{y + s} - \frac{1}{\eta + \sigma}\frac{d\eta}{dy}\right) - \frac{\Gamma}{4\pi}\left(\frac{1}{y - s} - \frac{1}{\eta - \sigma}\frac{d\eta}{dy}\right)$$

Only the second term of this equation is indeterminate and may be written as

$$\frac{-\frac{\Gamma}{4\pi}\left[(\eta - \sigma) - (y - s)\frac{d\eta}{dy}\right]}{(y - s)(\eta - \sigma)}$$

and evaluated at the limit by taking the second derivative of both the numerator and the denominator; that is,

$$\lim_{y \to s} \frac{-\frac{\Gamma}{4\pi}\left[(\eta - \sigma) - (y - s)\frac{d\eta}{dy}\right]}{(y - s)(\eta - \sigma)} = \frac{\Gamma}{4\pi}\frac{n\sigma r \sin\gamma - s}{r^2 \sin^2\gamma + s^2}$$

At the point $y = s$, therefore,

$$w = \frac{\Gamma}{2\pi r}\left\{\frac{1}{4\frac{s}{r}} - \left(\frac{1}{4\sigma} + \frac{\sigma}{\sigma^4 - 1}\right)\frac{n(1+\sigma^2)}{\sin\gamma\left(1 + \frac{s^2}{r^2\sin^2\gamma}\right)} + \frac{n\sigma\sin\gamma - \frac{s}{r}}{2\left[\sin^2\gamma + \left(\frac{s}{r}\right)^2\right]}\right\}$$

The induced velocity may be expressed as

$$w = \frac{\Gamma}{2\pi r}F$$

where

$$F = f(y,s,\eta,\sigma)$$

It is convenient to use the nondimensional form

$$\frac{wr}{\Gamma} = \frac{F}{2\pi}$$

which, for a tunnel of unit radius, is the induced velocity per unit circulation. Values of wr/Γ are given in table I and are plotted in figure 2 for a reflection-plane location of $\frac{d}{r} = 0.73026$. Table II and figure 3 present values for a reflection-plane location of $\frac{d}{r} = 0.49781$. These values of d/r correspond to 83.25 inches and 56.75 inches, respectively, in a tunnel 19 feet in diameter.

Illustrative Example

An example of the procedure involved in the determination of the corrections is worked out herein for a reflection-plane location of 83.25 inches from the center line of the Langley 19-foot pressure tunnel (fig. 4) and for the model shown in figure 5.

Angle of attack.- The wing lift distribution is shown in figure 6 for both free-air and tunnel conditions. The boundary-induced upwash angle shown in figure 7, from equation (1), is

$$\frac{w}{VC_L} = \frac{\bar{c}}{2r} \sum \frac{wr}{\Gamma} \Delta \frac{c_l c}{C_L \bar{c}}$$

The jet-boundary correction to the angle of attack, from equation (2), is

$$\Delta\alpha_j + \Delta\alpha_{s.c.} = 57.3 C_L \left(1 + 1.05 \frac{\bar{c}}{2r}\right) \int_0^1 \frac{w}{VC_L} \frac{c_l c}{C_L \bar{c}} \, dy'$$

The integral $\int_0^1 \frac{w}{VC_L} \frac{c_l c}{C_L \bar{c}} \, dy'$ (equation (2)) is the area under the curve obtained by multiplying the values of figure 6 by those of figure 7 and, in this case, has a numerical value of 0.01542. Therefore,

$$\Delta\alpha_j + \Delta\alpha_{s.c.} = 57.3 C_L (1.153)(0.01542)$$

$$= 1.019 C_L$$

The uncorrected lift-curve slope obtained experimentally is

$$a_u = 0.1041$$

This slope is corrected for the jet-boundary effects by the relation

$$\frac{1}{a_{2M}} - \frac{1}{a_u} = \frac{\Delta\alpha_j + \Delta\alpha_{s.c.}}{C_L}$$

so that

$$\frac{1}{a_{2M}} - \frac{1}{0.1041} = 1.019$$

and

$$a_{2M} = 0.0941$$

This slope is used to obtain the two-dimensional slope by substitution in equation (5) as

$$a_{2M} = \frac{\frac{a_o}{E_{2M}}}{1 + \frac{57.3\frac{a_o}{E_{2M}}}{\pi A_{2M}}}$$

$$0.0941 = \frac{\frac{a_o}{1.039}}{1 + \frac{57.3\frac{a_o}{1.039}}{\pi \times 10.84}}$$

from which

$$a_o = 0.1162$$

This two-dimensional slope is used in the same formula to determine the slope for the complete wing of aspect ratio 11.09, which is

$$a_W = 0.0945$$

The plan-form correction is then obtained from equation (4) as

$$\Delta\alpha_p = \left(\frac{1}{a_W} - \frac{1}{a_{2M}}\right) C_L$$

$$= \left(\frac{1}{0.0945} - \frac{1}{0.0941}\right) C_L$$

$$= -0.038 C_L$$

The complete correction for the angle of attack, from equation (6), is

$$\Delta\alpha = \Delta\alpha_j + \Delta\alpha_{s.c.} + \Delta\alpha_p$$

$$= (1.019 - 0.038) C_L$$

$$= 0.981 C_L$$

which is added to the geometric angle of attack of the model in the tunnel.

Drag coefficient.- The jet-boundary correction to the drag coefficient, from equation (7), is

$$\Delta C_{D_j} = C_L^2 \int_0^1 \frac{w}{VC_L} \frac{c_l c}{C_L \bar{c}} dy'$$

$$= 0.01542 C_L^2$$

The plan-form correction, from equation (9), is

$$\Delta C_{D_p} = \left(\frac{1}{\pi A_W u_W} - \frac{1}{\pi A_{2M} u_{2M}} \right) C_L^2$$

$$= \left(\frac{1}{\pi \times 11.09 \times 0.974} - \frac{1}{\pi \times 10.84 \times 0.976} \right) C_L^2$$

$$= -0.00062 C_L^2$$

The complete correction to drag coefficient, obtained from equation (10), is

$$\Delta C_D = \Delta C_{D_j} + \Delta C_{D_p}$$

$$= (0.01542 - 0.00062) C_L^2$$

$$= 0.0148 C_L^2$$

which is added to the uncorrected drag coefficient.

Pitching-moment coefficient.- The value of H taken from reference 4 is 0.202 for both the model and the complete wing. The location of the aerodynamic center, from equation (12), is

$$x_{a.c.} = 2H\frac{b}{2} \tan \Lambda + \text{Constant}$$

The reference point is taken as the 0.25 chord of the root chord of the complete wing so that for the model

$$x_{a.c._M} = (2 \times 0.202 \times 15 \times 0.21552) + 0.186$$

$$= 1.491 \text{ feet}$$

and for the complete wing

$$x_{a.c._W} = 2 \times 0.202 \times 15.862 \times 0.21552$$

$$= 1.380 \text{ feet}$$

The correction to the pitching-moment coefficient is obtained from equation (11) as

$$\Delta C_{m_p} = \frac{x_{a.c._M} - x_{a.c._W}}{c'} C_L$$

$$= \frac{1.491 - 1.380}{3.226} C_L$$

$$= 0.0344 C_L$$

which is added to the uncorrected pitching-moment coefficient.

Rolling-moment coefficient.- The aileron lift distribution is shown in figure 8 for both free-air and tunnel conditions. The boundary-induced upwash angle shown in figure 9 is obtained from equation (14):

$$\frac{w}{VC_l} = \frac{\bar{c}}{2r}\sum \frac{wr}{\Gamma}\Delta\frac{c_l c}{C_l \bar{c}}$$

The jet-boundary correction to the rolling-moment coefficient, from equation (15), is

$$\Delta C_{l_j} = -\frac{1}{4}mC_{l_u}\int_0^1 \frac{w}{VC_l}\left(1 + 1.05\frac{c}{2r}\right)\frac{c_l c}{C_L \bar{c}}\, y'\, dy'$$

$$= -\frac{1}{4}(5.392)\left(C_{l_u}\right)(0.0605)$$

$$= -0.0816C_{l_u}$$

The plan-form correction due to the effect of the reflection plane on the aileron lift distribution is obtained from figure 10, which was taken from reference 3, as

$$\frac{C_{l_{\delta_{2M}}}}{C_{l_{\delta_M}}} = \frac{1}{1 + \frac{2\Delta C_{l_r}}{C_{l_c}}}$$

$$= \frac{1}{1.054}$$

$$= 0.949$$

From figure 16 of reference 8, values of C_{l_δ}/k were found to be

$$\left(\frac{C_{l_\delta}}{k}\right)_W = 0.395$$

and

$$\left(\frac{C_{l_\delta}}{k}\right)_{2M} = 0.423$$

The corrected value of the rolling-moment coefficient from equation (16) is

$$C_l = C_{l_u}\left(1 + \frac{\Delta C_{l_i}}{C_{l_u}}\right)\frac{C_{l_{\delta_{2M}}}}{C_{l_{\delta_M}}}\frac{\left(\frac{C_{l_\delta}}{k}\right)_W}{\left(\frac{C_{l_\delta}}{k}\right)_{2M}}$$

$$= C_{l_u}\,(1 - 0.0816)\,0.949\,\frac{0.395}{0.423}$$

$$= 0.814\,C_{l_u}$$

Yawing-moment coefficient.- The two parts of the yawing-moment-coefficient correction due to the jet boundary are, from equation (17),

$$\left(\Delta C_{n_i}\right)_2 = -\frac{C_L C_{l_u}}{4}\int_0^1 \frac{w}{V C_l}\,\frac{c_l c}{C_L \bar{c}}\,y'\,dy'$$

$$= -\frac{0.05408}{4}\,C_L C_{l_u}$$

$$= -0.0135 C_L C_{l_u}$$

and, from equation (18),

$$\left(\Delta C_{n_i}\right)_3 = -\frac{C_L C_{l_u}}{4} \int_0^1 \frac{w}{VC_L} \frac{c_l c}{c_l \bar{c}} y' \, dy'$$

$$= -\frac{0.0776}{4} C_L C_{l_u}$$

$$= -0.0194 C_L C_{l_u}$$

The plan-form correction due to the reflection plane is obtained from figure 11, which was also taken from reference 3

$$\frac{\left(\Delta C_{n_p}\right)_1}{C_L C_{l_{2M}}} = \frac{\left(\Delta C_{n_i}\right)_1}{C_{l_c} C_L}$$

$$= -0.0070$$

In order to determine the plan-form correction due to aspect ratio and taper ratio, values of K were found from figure 13 of reference 5 to be

$$K_W = 0.075$$

and

$$K_{2M} = 0.077$$

so that this plan-form correction (equation (22)) is

$$\left(\Delta C_{n_p}\right)_2 = C_L C_l \left[-K_W + K_{2M} \frac{\left(\frac{C_{l_\delta}}{k}\right)_{2M}}{\left(\frac{C_{l_\delta}}{k}\right)_W} \right]$$

$$= C_L C_l \left(-0.075 + 0.077 \frac{0.423}{0.395} \right)$$

$$= 0.007 C_L C_l$$

The complete correction to yawing-moment coefficient, from equation (23), is

$$\Delta C_n = \left(\Delta C_{n_p}\right)_1 + \left(\Delta C_{n_p}\right)_2 + \left(\Delta C_{n_i}\right)_2 + \left(\Delta C_{n_i}\right)_3$$

$$= -0.0070 C_L C_{l_{2M}} + 0.007 C_L C_l - 0.0135 C_L C_{l_u} - 0.0194 C_L C_{l_u}$$

It is usually most convenient to express the correction to the yawing-moment coefficient in terms of the final corrected value of the rolling-moment coefficient; therefore,

$$\Delta C_n = \left[-0.0070 \frac{\left(\frac{C_{l_\delta}}{k}\right)_{2M}}{\left(\frac{C_{l_\delta}}{k}\right)_W} + 0.007 - 0.0135 \frac{C_{l_u}}{C_l} - 0.0194 \frac{C_{l_u}}{C_l} \right] C_L C_l$$

$$= \left(-0.0070 \frac{0.423}{0.395} + 0.007 - 0.0135 \frac{1}{0.814} - 0.0194 \frac{1}{0.814}\right) C_L C_l$$

$$= -0.04100 C_L C_l$$

which is added to the uncorrected yawing-moment coefficient.

CORRECTIONS FOR MODEL WITH END PLATE

Determination of Lift Distribution

The lift distributions are considerably more difficult to obtain for a model with an end plate than for a model with a reflection plane. The method used herein is described in reference 9. In this method, the wing is represented by a lifting line that is perpendicular to another lifting line representing the end plate. In addition to the vortices trailing from these lifting lines, image vortices outside the tunnel are introduced to satisfy the condition of constant stream function at the jet boundary. The complete trailing-vortex system is shown in figure 12. According to the Biot-Savart law, the induced velocities are related to the strength of the vortices by the following equations, which are given in the symbols of this report as

$$\left(\frac{w}{V}\right)_{y_1} = \frac{\bar{c}}{8\pi}\int_{-d}^{e} \frac{d\left(\frac{c_l c}{\bar{c}}\right)_y}{dy}\,\frac{1}{y - y_1}\,dy \qquad \text{(due to wing)}$$

$$- \frac{\bar{c}}{8\pi}\int_{-d}^{e} \frac{d\left(\frac{c_l c}{\bar{c}}\right)_y}{dy}\,\frac{1}{\frac{r^2}{y} - y_1}\,dy \qquad \text{(due to wing images)}$$

$$+ \frac{\bar{c}}{8\pi}\int_{-h}^{h} \frac{d\left(\frac{c_l c}{\bar{c}}\right)_z}{dz}\,\frac{y_1 + d}{(y_1 + d)^2 + z^2}\,dz \qquad \text{(due to end plate)}$$

$$- \frac{\bar{c}}{8\pi}\int_{-h}^{h} \frac{d\left(\frac{c_l c}{\bar{c}}\right)_z}{dz}\,\frac{r^2 d + y_1\left(z^2 + d^2\right)}{r^4 + 2y_1 r^2 d + y_1{}^2\left(z^2 + d^2\right)}\,dz \qquad (24)$$

(due to end-plate images)

and

$$\left(\frac{c_l c}{\bar{c}}\right)_{y_1} = \frac{m_o c}{\bar{c}}\left[\alpha + \left(\frac{w}{V}\right)_{y_1}\right] \qquad (25)$$

Also

$$\left(\frac{v}{\bar{V}}\right)_{z_1} = \frac{\bar{c}}{8\pi}\int_{-h}^{h} \frac{d\left(\frac{c_l c}{\bar{c}}\right)_z}{dz}\,\frac{1}{z - z_1}\,dz \qquad \text{(due to end plate)}$$

$$-\frac{\bar{c}}{8\pi}\int_{-h}^{h} \frac{d\left(\frac{c_l c}{\bar{c}}\right)_z}{dz}\,\frac{\frac{r^2 z}{z^2 + d^2} - z_1}{\frac{r^4 - 2r^2\left(d^2 + zz_1\right)}{z^2 + d^2} + z_1^2 + d^2}\,dz$$

(due to end-plate images)

$$+\frac{\bar{c}}{8\pi}\int_{-d}^{e} \frac{d\left(\frac{c_l c}{\bar{c}}\right)_y}{dy}\,\frac{z_1}{z_1^2 + (y + d)^2}\,dy \qquad \text{(due to wing)}$$

$$-\frac{\bar{c}}{8\pi}\int_{-d}^{e} \frac{d\left(\frac{c_l c}{\bar{c}}\right)_y}{dy}\,\frac{z_1}{z_1^2 + \left(\frac{r^2}{y} + d\right)^2}\,dy \qquad (26)$$

(due to wing images)

and

$$\left(\frac{c_l c}{\bar{c}}\right)_{z_1} = \frac{2\pi c}{\bar{c}}\left(\frac{v}{\bar{V}}\right)_{z_1} \qquad (27)$$

In the last equation, 2π is used as the lift-curve slope of the end plate for want of a more exact value.

If the free-air lift distribution is desired, the terms due to the image vortices are omitted. The only practicable method of solution of these equations is graphical by means of successive approximations. The evaluation of the integral over the region near $y = y_1$ may be approximated by means of the expression

$$\int_{y_1-\Delta y}^{y_1+\Delta y} \frac{d\left(\frac{c_l c}{\bar{c}}\right)_y}{dy} \frac{1}{y - y_1} dy = \frac{d\left(\frac{c_l c}{\bar{c}}\right)_{y_1+\Delta y}}{dy} - \frac{d\left(\frac{c_l c}{\bar{c}}\right)_{y_1-\Delta y}}{dy}$$

where Δy is a small spanwise increment. After the lift distribution is obtained for some value of the angle of attack, the distribution may easily be converted for a lift coefficient of unity.

Illustrative Example

An example of the method used in determining the corrections is given herein for the model shown in figure 5 to which an end plate is attached (fig. 13). The lift distribution for this model arrangement for both tunnel and free-air conditions is shown in figure 14.

Angle of attack.- It should be theoretically possible to obtain the correction to the angle of attack by taking the difference between the angles of attack at unit lift coefficient for the tunnel and free-air conditions. The accuracy involved, however, in obtaining the lift distributions for this end condition generally is insufficient for the purpose of this report and, in addition, such a correction would not include the streamline-curvature correction. The jet-boundary correction to the angle of attack from equation (2)

$$\Delta\alpha_j + \Delta\alpha_{s.c.} = 57.3C_L\left(1 + 1.05\frac{\bar{c}}{2r}\right)\int_0^1 \frac{w}{VC_L}\frac{c_l c}{C_L \bar{c}}\,dy'$$

is used; in this case, w/VC_L is the upwash angle along the model span due to the images of the wing and the end plate. This upwash-angle distribution is shown in figure 15. For the end-plate condition,

$$\Delta\alpha_j + \Delta\alpha_{s.c.} = 57.3C_L(1.153)(0.01845)$$

$$= 1.219C_L$$

Applying this correction to the experimental value of lift-curve slope of 0.0935 results in a lift-curve slope of 0.0839 per degree or 4.809 per radian.

The plan-form correction is obtained from equation (4)

$$\Delta\alpha_p = \left(\frac{1}{a_W} - \frac{1}{a_M}\right)C_L$$

although in this case a_W and a_M are obtained in a different manner from that for the reflection-plane condition. The edge-velocity correction factor E cannot be determined for the model with an end plate; therefore, lifting-line theory without the aid of this factor is employed to obtain a_W and a_M. The section-lift-curve slope of 0.122, obtained from tests in two-dimensional flow, is used. In the solution of equations (24) through (27) an angle of attack of 0.2 radian gave a lift coefficient of 1.042 for the model in free air; therefore,

$$a_M = \frac{1.042}{0.2 \times 57.3}$$

$$= 0.0909$$

The correction factor E is not employed in the results of reference 4; these results can therefore be used to determine a_W for the complete wing. The equation

$$a_W = \frac{fa_o}{1 + \frac{57.3a_o}{\pi A}}$$

accordingly is used for the complete wing, where f is the factor obtained from reference 4. Then,

$$a_W = \frac{0.997 \times 0.122}{1 + \frac{57.3 \times 0.122}{\pi \times 11.09}}$$

$$= 0.1013$$

Therefore,

$$\Delta\alpha_p = \left(\frac{1}{0.1013} - \frac{1}{0.0909}\right)C_L$$

$$= -1.127C_L$$

The complete correction to the angle of attack is

$$\Delta\alpha = (1.219 - 1.127)C_L$$

$$= 0.092C_L$$

Drag coefficient.- The jet-boundary correction to the drag coefficient, obtained as for the reflection-plane condition from equation (7), is

$$\Delta C_{D_j} = C_L^2 \int_0^1 \frac{w}{VC_L} \frac{c_l c}{C_L \bar{c}} dy'$$

$$= 0.0185 C_L^2$$

For the plan-form correction, the induced drag of the model is obtained by the relation

$$C_{D_{i_M}} = C_L^2 \int_0^1 \frac{\alpha_i}{C_L} \frac{c_l c}{C_L \bar{c}} dy'$$

where α_i/C_L is the self-induced angle of the model and the end plate in free air. Then

$$C_{D_{i_M}} = 0.0466 C_L^2$$

The plan-form correction to the drag coefficient is obtained from equation (8) as

$$\Delta C_{D_p} = C_{D_{i_W}} - C_{D_{i_M}}$$

$$= (0.0295 - 0.0466) C_L^2$$

$$= -0.0171 C_L^2$$

where the value $C_{D_{i_W}} = 0.0295$ is the same as previously used in the case of the reflection plane. In addition to these corrections, there is in this case the induced drag due to both the jet-boundary-induced angle and the self-induced angle over the span of the end plate. This correction is a combination jet-boundary and plan-form correction and may be determined as a single value by use of

$$\Delta C_{D_e} = C_L^2 \int_{-h}^{h} \frac{v}{VC_L} \left(\frac{c_l c}{C_L \bar{c}} \right)_e dz$$

where v/VC_L is the total induced angle over the span of the end plate due to the model, the end plate itself, and all images; $\left(\frac{c_l c}{C_L \bar{c}} \right)_e$ is the tunnel lift distribution over the end plate; and all values are based upon the model dimensions so that ΔC_{D_e} is based upon the model area. For the example

$$\Delta C_{D_e} = 0.0030 C_L^2$$

The complete correction to the drag coefficient is

$$\Delta C_D = (0.0185 - 0.0171 + 0.0030) C_L^2$$

$$= 0.0044 C_L^2$$

Pitching-moment coefficient.- The location of the aerodynamic center is obtained from equation (13)

$$x_{a.c._M} = \frac{b}{2} \tan \Lambda \int_0^1 \frac{c_l c}{C_L \bar{c}} y' \, dy' + \text{Constant}$$

which gives $x_{a.c._M} = 1.569$ feet from the quarter-chord point of the complete-wing root chord. The value $x_{a.c._W} = 1.380$ feet is the same as previously used in the determination of the correction for the reflection-plane condition. From equation (11),

$$\Delta C_{m_p} = \frac{x_{a.c._M} - x_{a.c._W}}{c'} C_L$$

$$= \frac{1.569 - 1.380}{3.226} C_L$$

$$= 0.0586 C_L$$

Rolling-moment coefficient.- The aileron lift distribution is obtained by the same general formulas as the wing lift distribution for the model with the end plate and is shown in figure 16. The upwash angle due to the jet boundary is shown in figure 17. The jet-boundary correction, from equation (15), is

$$\Delta C_{l_j} = -\frac{1}{4} m C_{l_u} \int_0^1 \frac{w}{V C_l} \left(1 + 1.05 \frac{c}{2r}\right) \frac{c_l c}{C_L \bar{c}} y' \, dy'$$

$$= -\frac{1}{4}(4.809)\left(C_{l_u}\right)(0.0681)$$

$$= -0.0819 C_{l_u}$$

The plan-form correction due to the effect of the end-plate on the aileron lift distribution was found from equations (24) through (27) for the model and from

conventional lifting-line theory for the wing of twice model span. The resulting ratio is

$$\frac{c_{l_{\delta_{2M}}}}{c_{l_{\delta_M}}} = 0.956$$

The plan-form corrections due to aspect ratio and taper ratio are independent of the end condition so that the corrected value of rolling-moment coefficient from equation (16) is

$$c_l = c_{l_u}\left(1 + \frac{\Delta c_{l_j}}{c_{l_u}}\right)\frac{c_{l_{\delta_{2M}}}}{c_{l_{\delta_M}}}\frac{\left(\frac{c_{l_\delta}}{k}\right)_W}{\left(\frac{c_{l_\delta}}{k}\right)_{2M}}$$

$$= c_{l_u}(1 - 0.0819)0.956\,\frac{0.395}{0.423}$$

$$= 0.820c_{l_u}$$

Yawing-moment coefficient.- The corrections to the yawing-moment coefficient due to the jet boundary are, from equation (17),

$$\left(\Delta c_{n_i}\right)_2 = -\frac{c_L c_{l_u}}{4}\int_0^1 \frac{w}{V c_l}\,\frac{c_l c}{c_L \bar{c}}\,y'\,dy'$$

$$= \frac{-0.06064}{4}\,c_L c_{l_u}$$

$$= -0.01520 c_L c_{l_u}$$

and, from equation (18),

$$\left(\Delta C_{n_i}\right)_3 = -\frac{C_L C_{l_u}}{4} \int_0^1 \frac{w}{V C_L} \frac{c_l c}{c_l \bar{c}} y' \, dy'$$

$$= \frac{-0.07188}{4} C_L C_{l_u}$$

$$= -0.0180 C_L C_{l_u}$$

The plan-form correction due to the end plate is found from equation (19) through (21). From equation (20)

$$K_{2M} = 0.0741$$

and from equation (21)

$$K_M = 0.0650$$

The plan-form correction from equation (19) is

$$\left(\Delta C_{n_p}\right)_1 = C_L C_{l_{2M}} \left(-K_{2M} + K_M \frac{C_{l_{\delta_M}}}{C_{l_{\delta_{2M}}}}\right)$$

$$= C_L C_{l_{2M}} \left(-0.0741 + 0.0650 \frac{1}{0.956}\right)$$

$$= -0.0061 C_L C_{l_{2M}}$$

The plan-form correction due to aspect ratio and taper ratio is the same as for the model and reflection plane.

The complete correction to the yawing-moment coefficient, from equation (23), is

$$\Delta C_n = \left(\Delta C_{n_p}\right)_1 + \left(\Delta C_{n_p}\right)_2 + \left(\Delta C_{n_i}\right)_2 + \left(\Delta C_{n_i}\right)_3$$

$$= \left[-0.0061 \frac{\left(\frac{C_{l_\delta}}{k}\right)_{2M}}{\left(\frac{C_{l_\delta}}{k}\right)_W} + 0.007 - 0.0152 \frac{C_{l_u}}{C_l} - 0.0180 \frac{C_{l_u}}{C_l} \right] C_L C_l$$

$$= \left(-0.0061 \frac{0.423}{0.395} + 0.007 - 0.0152 \frac{1}{0.820} - 0.0180 \frac{1}{0.820} \right) C_L C_l$$

$$= -0.0400 C_L C_l$$

CORRECTIONS FOR MODEL WITH NO END PLATE

Determination of Induced Upwash Angle

For a model with no end plate, the determination of the jet-boundary-induced velocity is easier than for the other end conditions. In a closed circular tunnel, if there is a trailing vortex of strength Γ at a distance $y = s$, there is an image vortex of strength $-\Gamma$ at a distance $y = \frac{r^2}{s}$. The stream function due to the image vortex is

$$\psi = \frac{\Gamma}{2\pi} \log \left(y - \frac{r^2}{s} \right)$$

and the induced vertical velocity is

$$w = -\frac{\Gamma}{4\pi} \frac{1}{y - \frac{r^2}{s}}$$

Values of the boundary-induced vertical velocity per unit circulation for a tunnel of unit radius

$$\frac{wr}{\Gamma} = -\frac{1}{4\pi \left(\frac{y}{r} - \frac{1}{s/r} \right)}$$

are given in table III and plotted in figure 18. These values are for a counterclockwise vortex in the right-hand side of the tunnel and may be used for a clockwise vortex in the left-hand side of the tunnel by changing the signs of y and s. For vortices of signs opposite to these, the sign of the induced velocity must be changed: that is, the induced velocity is negative. These values may be used for any wing in a closed

circular wind tunnel. For a loading symmetrical about the vertical center line of the tunnel, a further simplification may be made by adding the induced velocities for negative values of y to the induced velocities for positive values of y and by using only the semispan loading.

Illustrative Example

An example of the procedure involved in the determination of the corrections is worked out for the model shown in figure 5 with no end plate. The lift distribution, obtained from lifting-line theory for this model configuration, is shown in figure 19 for both free-air and tunnel conditions. The spanwise distribution of the boundary-induced upwash angle, which is obtained for this model arrangement from equation (1)

$$\frac{w}{VC_L} = \frac{\bar{c}}{2r}\sum \frac{wr}{\Gamma}\Delta\frac{c_l c}{C_L \bar{c}}$$

is shown in figure 20.

Angle of attack.- The jet-boundary correction, from equation (2), is

$$\Delta\alpha_j + \Delta\alpha_{s.c.} = 57.3C_L\left(1 + 1.05\,\frac{\bar{c}}{2r}\right)\int_0^1 \frac{w}{VC_L}\,\frac{c_l c}{C_L \bar{c}}\,dy'$$

$$= 57.3C_L(1.153)(0.01979)$$

$$= 1.305C_L$$

The uncorrected lift-curve slope obtained experimentally is

$$a_u = 0.0800$$

This slope is corrected for the jet-boundary effects by the relation

$$\frac{1}{a_M} - \frac{1}{a_u} = \frac{\Delta\alpha_j + \Delta\alpha_{s.c.}}{C_L}$$

so that

$$\frac{1}{a_M} - \frac{1}{0.0800} = 1.305$$

and

$$a_M = 0.724$$

This value of a is used to obtain the two-dimensional slope from equation (5) as

$$a_M = \frac{\frac{a_o}{E_M}}{1 + \frac{57.3\,\frac{a_o}{E_M}}{\pi A_M}}$$

$$0.0724 = \frac{\frac{a_o}{1.186}}{1 + \frac{57.3\,\frac{a_o}{1.186}}{\pi \times 5.423}}$$

from which

$$a_o = 0.1136$$

This value of a_o agrees fairly well with the value of 0.1162 obtained for the reflection-plane condition. It should be noted that the aspect ratio of the model with no end plate is one-half that of the model with the reflection plane and the edge-velocity correction factor is increased since the root chord of the model is part of the perimeter when no end plate is used. The two-dimensional slope is used to determine the slope for the complete wing of aspect ratio equal to 11.09 as

$$a_W = \frac{\frac{0.1136}{1.039}}{1 + \frac{57.3 \frac{0.1136}{1.039}}{\pi \times 11.09}}$$

$$= 0.0927$$

The plan-form correction is then obtained from equation (4) as

$$\Delta\alpha_p = \left(\frac{1}{a_W} - \frac{1}{a_M}\right) c_L$$

$$= \left(\frac{1}{0.0927} - \frac{1}{0.0724}\right) c_L$$

$$= -3.014 c_L$$

The complete correction for the angle of attack, from equation (6), is

$$\Delta\alpha = \Delta\alpha_j + \Delta\alpha_{s.c.} + \Delta\alpha_p$$

$$= (1.305 - 3.014)C_L$$

$$= -1.709C_L$$

Drag coefficient.- The jet-boundary correction to the drag coefficient is obtained from equation (7) as

$$\Delta C_{D_j} = C_L^2 \int_0^1 \frac{w}{VC_L} \frac{c_l c}{C_L \bar{c}} dy'$$

$$= 0.01979C_L^2$$

The induced-drag coefficient of the model, obtained from the coefficients of the Fourier series determined in the solution of the lift distribution (reference 4), is

$$C_{D_{i_M}} = \frac{C_L^2}{\pi A_M} \sum_{n=1}^{\infty} \frac{nA_n^2}{A_1^2}$$

$$= \frac{C_L^2}{\pi \times 5.423} 1.0946$$

$$= 0.0643C_L^2$$

where A_1 is the first coefficient and A_n the n^{th} coefficient of the Fourier series. The induced-drag coefficient of the complete wing has been previously determined herein to be

$$C_{D_{i_W}} = 0.0295C_L^2$$

The plan-form correction, obtained from equation (8), is

$$\Delta C_{D_p} = C_{D_{i_W}} - C_{D_{i_M}}$$

$$= (0.0295 - 0.0643)C_L^2$$

$$= -0.0348C_L^2$$

The complete correction to the drag coefficient, from equation (10), is

$$\Delta C_D = \Delta C_{D_j} + \Delta C_{D_p}$$

$$= (0.0198 - 0.0348)C_L^2$$

$$= -0.0150C_L^2$$

Pitching-moment coefficient.- The location of the aerodynamic center is obtained from equation (13)

$$x_{a.c._M} = \frac{b}{2} \tan \Lambda \int_0^1 \frac{c_l c}{C_L \bar{c}} y' \, dy' + \text{Constant}$$

which gives $x_{a.c._M} = 1.682$ feet from the quarter-chord point of the complete-wing root chord. The value $x_{a.c._W} = 1.380$ feet was previously used in the determination of the correction for the reflection-plane condition. The plan-form correction to the pitching-moment coefficient is obtained from equation (11) as

$$\Delta C_{m_p} = \frac{x_{a.c._M} - x_{a.c._W}}{c'} C_L$$

$$= \frac{1.682 - 1.380}{3.226} C_L$$

$$= 0.0936 C_L$$

Rolling-moment coefficient.- The aileron lift distribution for the model with no end plate is shown in figure 21 for both free-air and tunnel conditions. The boundary-induced upwash angle shown in figure 22 is obtained from equation (14)

$$\frac{w}{V c_l} = \frac{\bar{c}}{2r} \sum \frac{wr}{\Gamma} \Delta \frac{c_l c}{c_l \bar{c}}$$

The jet-boundary correction, from equation (15), is

$$\Delta c_{l_j} = -\frac{1}{4} m c_{l_u} \int_0^1 \frac{w}{V c_l} \left(1 + 1.05 \frac{c}{2r}\right) \frac{c_l c}{C_L \bar{c}} y' \, dy'$$

$$= -\frac{1}{4}(4.149)\left(c_{l_u}\right)(0.0794)$$

$$= -0.0824 c_{l_u}$$

The plan-form correction due to the effect of no end plate on the aileron lift distribution was found from lifting-line theory to be

$$\frac{c_{l_{\delta_{2M}}}}{c_{l_{\delta_M}}} = 0.974$$

The plan-form correction due to aspect ratio and taper ratio is the same as for the other end conditions; hence, the rolling-moment coefficient for the complete wing, from equation (16), is

$$c_l = c_{l_u}\left(1 + \frac{\Delta c_{l_j}}{c_{l_u}}\right)\frac{c_{l_{\delta_{2M}}}}{c_{l_{\delta_M}}}\frac{\left(\frac{c_{l_\delta}}{k}\right)_W}{\left(\frac{c_{l_\delta}}{k}\right)_{2M}}$$

$$= c_{l_u}(1 - 0.0824)\,0.974\,\frac{0.395}{0.423}$$

$$= 0.835c_{l_u}$$

Yawing-moment coefficient.- The jet-boundary corrections to the yawing-moment coefficient are obtained from equation (17) as

$$\left(\Delta C_{n_i}\right)_2 = -\frac{C_L C_{l_u}}{4} \int_0^1 \frac{w}{V C_l} \frac{c_l c}{C_L \bar{c}} y' \, dy'$$

$$= -\frac{0.0664}{4} C_L C_{l_u}$$

$$= -0.0166 C_L C_{l_u}$$

and, from equation (18),

$$\left(\Delta C_{n_i}\right)_3 = -\frac{C_L C_{l_u}}{4} \int_0^1 \frac{w}{V C_L} \frac{c_l c}{c_l \bar{c}} y' \, dy'$$

$$= -\frac{0.0904}{4} C_L C_{l_u}$$

$$= -0.0226 C_L C_{l_u}$$

The plan-form correction due to no end plate is found from equations (19) through (21). From equation (20)

$$K_{2M} = 0.0741$$

From equation (21)

$$K_M = 0.0711$$

From equation (19)

$$\left(\Delta C_{n_p}\right)_1 = C_L C_{l_{2M}} \left(-K_{2M} + K_M \frac{C_{l_{\delta_M}}}{C_{l_{\delta_{2M}}}}\right)$$

$$= C_L C_{l_{2M}} \left(-0.0741 + 0.0711 \frac{1}{0.974}\right)$$

$$= -0.0011 C_L C_{l_{2M}}$$

The plan-form correction due to aspect ratio and taper ratio is the same as for the other end conditions so that the complete correction to the yawing-moment coefficient, from equation (23), is

$$\Delta C_n = \left(\Delta C_{n_p}\right)_1 + \left(\Delta C_{n_p}\right)_2 + \left(\Delta C_{n_i}\right)_2 + \left(\Delta C_{n_i}\right)_3$$

$$= \left[-0.0011 \frac{\left(\frac{C_{l_\delta}}{k}\right)_{2M}}{\left(\frac{C_{l_\delta}}{k}\right)_W} + 0.007 - 0.0166 \frac{C_{l_u}}{C_l} - 0.0226 \frac{C_{l_u}}{C_l}\right] C_L C_l$$

$$= \left(-0.0011 \frac{0.423}{0.395} + 0.007 - 0.0166 \frac{1}{0.835} - 0.0226 \frac{1}{0.835}\right) C_L C_l$$

$$= -0.0411 C_L C_l$$

APPLICATION TO TEST DATA

Model and Tests

The tests were conducted in the Langley 19-foot pressure tunnel for the partial-span tapered wing model shown in figure 5. The model represented 94.6 percent of the true semispan. The aspect ratios of the wing of twice model span and the complete wing were 10.84 and 11.09, respectively. The taper ratios of the model and complete wing were 0.26 and 0.25, respectively. The model was equipped with a full-span duplex-flap arrangement. The inboard slotted flap, the outboard balanced split flap, and the aileron were of constant chord and approximately 24, 20, and 15 percent, respectively, of the average wing chord over their portions of the wing span. The aileron was provided with a completely sealed internal aerodynamic balance.

The reflection-plane arrangement is shown in figures 4 and 23. The reflection plane was fastened to the tunnel at its top and bottom and extended beyond and behind the model as shown. The gap between the model and the reflection plane was automatically maintained at 0.09 ±0.03 inch, by a telescoping section in the end of the model. The end-plate arrangement is shown in figures 13 and 24. The end plate was elliptical in plan form and was rigidly fixed to the model. For the wing with no end plate, the model was tested as shown in figure 25.

The tests were conducted at a Reynolds number of approximately 8.9×10^6 and at a Mach number of 0.17. The angle-of-attack range was from -4° through maximum lift and the aileron deflection range was $\pm 20^\circ$.

The tests were made for three flap arrangements: flaps neutral and partial-span and full-span flaps deflected. The aileron tests were made at two angles of attack for each flap arrangement and end condition.

Uncorrected Characteristics

The uncorrected aerodynamic characteristics of the tapered-wing model for the three flap arrangements and the three end conditions are presented in figure 26 in terms of the uncorrected nondimensional coefficients.

Drag.- The uncorrected drag characteristics are presented in figure 26(a). The drag coefficient at zero lift coefficient is increased slightly for the model with no end plate and to a greater extent for the model with the end plate. These increases in drag coefficient are due to the abrupt tip form of the model with no end plate and to the drag of the end plate. The differences between the drag coefficients increase with lift coefficient because of the differences in the self-induced and the jet-boundary-induced drag for the three end conditions.

Lift.- The uncorrected lift characteristics are presented in figure 26(b). The slope of the lift curve is decreased for the model with the end plate and with no end plate because of changes in the effective aspect ratio. The maximum-lift-coefficient values for the three end conditions are reduced similarly because of the changes in the stalling characteristics. The angle of zero lift is slightly affected with the flaps neutral.

Pitching moment.- The uncorrected pitching-moment characteristics are presented in figure 26(c). The slope of the pitching-moment curve becomes more negative for the model with the end plate and still more negative for the model with no end plate. There is no change in the pitching-moment coefficient at zero lift with the flaps neutral.

Aileron.- The uncorrected rolling-moment and yawing-moment characteristics are presented in figures 27 to 29. The change in the rolling-moment and yawing-moment characteristics for the three end conditions is small. There is no consistent relationship between the characteristics for the various angles of attack and flap arrangements.

Corrected Characteristics

The corrected aerodynamic characteristics are presented in figure 30. The values of the corrections applied to the uncorrected coefficients are given in table IV. The absolute values of the data for partial-span models have certain limitations which are inherent in the test conditions and procedure. The determination of the effects of the tare and interference of the model support system was impractical for the model described

herein. The gap between the model and the reflection plane was kept to a practical minimum but may have introduced some slight errors in the data which could not be determined. For the end-plate and no-end-plate conditions the stalling characteristics were affected in a manner unsusceptible of correction.

Drag.- Application of the drag-coefficient corrections brings the characteristics (fig. 30(a)) into good agreement, with the flaps neutral. The main difference remaining is due to the drag of the end plate and to the tip drag for the model with no end plate. With partial-span and full-span flaps deflected, the agreement is not so good as with flaps neutral, although the corrected characteristics are in much better agreement than the uncorrected ones. The remaining discrepancies for these flap arrangements are due to differences in profile drag and induced drag not included in the corrections. The plan-form correction to the drag coefficient is lowest for the reflection-plane condition and it is therefore believed that this condition is the most representative of the complete wing. This fact is a point in favor of the use of a reflection plane rather than the other end conditions.

Lift.- The corrected lift characteristics are presented in figure 30(b). With the flaps neutral, the agreement of the characteristics for the three end conditions is very good below maximum lift. Contributing to the good agreement may have been the fact that no extremely low aspect ratio was involved even for the model with no end plate. The slight change in the angle of zero lift displaces the curves for the model with the end plate and with no end plate. The differences at and near maximum lift are due to alterations of the lift distribution for which corrections cannot be applied. With the partial-span and full-span flaps, the agreement of the characteristics for the three end conditions is not so good because of the change in the effectiveness of the inboard flap. The effectiveness of the outboard flap is approximately the same for all three end conditions. The greater maximum lift coefficient obtained with the reflection plane is another point in favor of the use of the reflection plane since the load distribution is most nearly that of a complete wing.

Pitching moment.- The corrected pitching-moment characteristics (fig. 30(c)) indicate only fair agreement for the three end conditions. The relative order of the curves for the three end conditions is reversed by the corrections. This reversal may be due to the effect of the sweepback on the lift distribution, which was not taken into account in the corrections. In any case, the differences between the characteristics are attributed to inaccuracies in the determination of the lift distributions and, since the lift distribution is least altered by the reflection plane, it is believed that the pitching-moment characteristics for the reflection-plane condition are the most nearly accurate.

Aileron.- The corrected rolling-moment and yawing-moment characteristics are presented in figures 31 to 33. The general relationship between the characteristics for the three end conditions is unchanged. The inconsistent relationship between the uncorrected characteristics for the three end conditions precludes any consistent relationship of the corrected characteristics. At the low angles of attack and with the flaps neutral, the characteristics for the three end conditions agree very well whereas, at the other angles of attack and with the flaps deflected, the characteristics agree slightly better in some cases and worse in other cases than the corresponding uncorrected characteristics.

The difference and inconsistent relationship between the characteristics are due in part to experimental inaccuracy and to the pronounced vibration of the model with the end plate and with no end plate.

Comparison of Aileron Effectiveness for Partial- and Complete-Span Models

The comparison of the rolling-moment characteristics determined for the partial-span model with a reflection plane and for a complete-span model is presented in figures 34 and 35. With the flaps neutral (fig. 34), the general agreement of the aileron effectiveness is good, except at the high angles of attack at which some differences exist. With the full-span flaps deflected (fig. 35), the agreement is good at the low angle of attack and rather poor at the high angle

of attack. The loss in effectiveness at the high angle of attack for the complete-span model is due to a change in the flow over the aileron as evidenced by a complete change in the stalling characteristics of the complete-span model. The change in the stalling characteristics is due in part to the decreased Reynolds number and to some difference in the models.

CONCLUDING REMARKS

A method is presented for determining the jet-boundary and plan-form corrections to be applied to test data for a partial-span model with a reflection plane, an end plate, or no end plate in a closed circular wind tunnel. These corrections have been applied to the measured values of lift, drag, pitching-moment, rolling-moment, and yawing-moment coefficients obtained from tests in the Langley 19-foot pressure tunnel of a partial-span model with each of the three end conditions.

With the exception of the corrections to the rolling-moment coefficient, the jet-boundary corrections were somewhat smaller for the reflection-plane condition than for either of the other end conditions because the induced upwash angle was smaller. For all corrections depending upon the wing lift distribution, the plan-form corrections were considerably smaller for the reflection-plane condition because the lift distribution was more nearly like that of a complete wing. Any errors in determining the lift distribution were therefore minimized and the corrected values of the data were the most representative of the complete wing.

From all these considerations, it was found that a reflection plane should be used wherever possible for tests of partial-span models. If it is necessary, from other considerations, to use an end plate or no end plate, it is possible by the methods described herein to determine suitable corrections to be applied in order to obtain reasonable results, particularly with flaps neutral and below maximum lift.

Langley Memorial Aeronautical Laboratory
National Advisory Committee for Aeronautics
Langley Field, Va., February 4, 1946

REFERENCES

1. Davison, B., and Rosenhead, L.: Wind Tunnel Correction for a Circular Open Jet Tunnel with a Reflexion Plate. Proc. Roy. Soc. (London), ser.A, vol. 177, no. 970, Feb. 24, 1941, pp. 366-382.

2. Kondo, Kazuo: The Wall Interference of Wind Tunnels with Boundaries of Circular Arcs. Rep. No. 126 (vol. X, 8), Aero. Res. Inst., Tokyo Imperial Univ., Aug. 1935.

3. Swanson, Robert S. and Toll, Thomas A.: Jet-Boundary Corrections for Reflection-Plane Models in Rectangular Wind Tunnels. NACA ARR No. 3E22, 1943.

4. Anderson, Raymond F.: Determination of the Characteristics of Tapered Wings. NACA Rep. No. 572, 1936.

5. Weick, Fred E., and Jones, Robert T.: Résumé and Analysis of N.A.C.A. Lateral Control Research. NACA Rep. No. 605, 1937.

6. Lotz, Irmgard: Correction of Downwash in Wind Tunnels of Circular and Elliptic Sections. NACA TM No. 801, 1936.

7. Jones Robert T.: Correction of the Lifting-Line Theory for the Effect of the Chord. NACA TN No. 817, 1941.

8. Pearson, Henry A., and Jones, Robert T.: Theoretical Stability and Control Characteristics of Wings with Various Amounts of Taper and Twist. NACA Rep. No. 635, 1938.

9. Katzoff, S., and Mutterperl, William: The End-Plate Effect of a Horizontal-Tail Surface on a Vertical-Tail Surface. NACA TN No. 797, 1941.

TABLE I.- BOUNDARY-INDUCED VELOCITY $\frac{wr}{\Gamma}$ ALONG HORIZONTAL CENTER LINE DUE TO UNIT COUNTERCLOCKWISE VORTEX AT VARIOUS DISTANCES $\frac{s}{r}$ FROM REFLECTION PLANE

$\left[\frac{d}{r} = 0.73026\right]$

y/r \ s/r	0.1	0.2	0.3	0.4	0.5	0.6	0.7	0.8	0.9	1.0	1.1	1.2	1.3	1.4	1.5	1.6
0	0.0083	0.0164	0.0243	0.0315	0.0387	0.0452	0.0511	0.0566	0.0618	0.0666	0.0709	0.0750	0.0787	0.0823	0.0855	0.0885
.1	.0082	.0160	.0238	.0312	.0383	.0449	.0508	.0564	.0616	.0664	.0708	.0749	.0787	.0823	.0856	.0886
.2	.0080	.0155	.0231	.0304	.0375	.0441	.0500	.0556	.0610	.0659	.0705	.0748	.0788	.0826	.0860	.0893
.3	.0076	.0149	.0224	.0295	.0366	.0428	.0488	.0545	.0600	.0652	.0700	.0746	.0789	.0830	.0868	.0905
.4	.0071	.0142	.0213	.0282	.0353	.0415	.0473	.0532	.0589	.0643	.0695	.0744	.0791	.0837	.0880	.0922
.5	.0067	.0135	.0202	.0267	.0335	.0397	.0458	.0515	.0576	.0632	.0688	.0743	.0795	.0847	.0896	.0944
.6	.0062	.0125	.0188	.0251	.0316	.0378	.0441	.0498	.0562	.0621	.0682	.0742	.0800	.0861	.0918	.0975
.7	.0058	.0117	.0176	.0235	.0298	.0360	.0422	.0482	.0550	.0613	.0678	.0745	.0811	.0879	.0946	.1013
.8	.0053	.0108	.0164	.0220	.0280	.0341	.0403	.0466	.0536	.0604	.0675	.0749	.0824	.0903	.0981	.1063
.9	.0049	.0100	.0152	.0206	.0263	.0324	.0386	.0450	.0522	.0596	.0669	.0753	.0840	.0932	.1026	.1126
1.0	.0046	.0093	.0141	.0192	.0247	.0307	.0369	.0434	.0510	.0589	.0670	.0763	.0862	.0971	.1083	.1208
1.1	.0042	.0086	.0131	.0180	.0233	.0291	.0353	.0421	.0498	.0582	.0672	.0773	.0891	.1020	.1157	.1314
1.2	.0039	.0079	.0122	.0168	.0219	.0276	.0338	.0407	.0488	.0577	.0674	.0788	.0928	.1085	.1251	.1456
1.3	.0036	.0074	.0114	.0158	.0207	.0262	.0324	.0395	.0478	.0572	.0680	.0806	.0976	.1175	.1378	.1651
1.4	.0033	.0069	.0105	.0148	.0195	.0249	.0311	.0382	.0468	.0568	.0686	.0828	.1030	.1280	.1544	.1927
1.5	.0031	.0064	.0099	.0139	.0184	.0237	.0298	.0371	.0460	.0567	.0699	.0864	.1090	.1401	.1771	.2381
1.6	.0029	.0060	.0093	.0131	.0174	.0226	.0287	.0361	.0453	.0567	.0712	.0902	.1161	.1539	.2089	.2730

TABLE II.- BOUNDARY-INDUCED VELOCITY $\frac{wr}{\Gamma}$ ALONG HORIZONTAL CENTER LINE DUE TO UNIT COUNTERCLOCKWISE VORTEX AT VARIOUS DISTANCES $\frac{s}{r}$ FROM REFLECTION PLANE

$$\left[\frac{d}{r} = 0.49781\right]$$

y/r \ s/r	0.1	0.2	0.3	0.4	0.5	0.6	0.7	0.8	0.9	1.0	1.1	1.2
0	0.0092	0.0177	0.0263	0.0346	0.0427	0.0506	0.0581	0.0653	0.0720	0.0786	0.0847	0.0906
.1	.0091	.0175	.0262	.0344	.0426	.0505	.0580	.0652	.0720	.0786	.0848	.0907
.2	.0089	.0174	.0261	.0340	.0420	.0501	.0577	.0650	.0720	.0787	.0852	.0913
.3	.0085	.0170	.0254	.0332	.0414	.0495	.0572	.0647	.0719	.0790	.0857	.0923
.4	.0083	.0166	.0248	.0325	.0407	.0489	.0567	.0644	.0719	.0794	.0866	.0938
.5	.0080	.0159	.0241	.0316	.0397	.0480	.0561	.0640	.0719	.0799	.0878	.0958
.6	.0077	.0154	.0232	.0308	.0386	.0470	.0555	.0636	.0719	.0807	.0894	.0985
.7	.0074	.0147	.0222	.0298	.0377	.0459	.0547	.0631	.0719	.0816	.0915	.1019
.8	.0070	.0141	.0214	.0288	.0366	.0448	.0536	.0628	.0719	.0830	.0940	.1063
.9	.0067	.0135	.0205	.0278	.0355	.0439	.0528	.0625	.0722	.0850	.0975	.1119
1.0	.0064	.0128	.0196	.0267	.0344	.0428	.0521	.0623	.0730	.0872	.1017	.1187
1.1	.0061	.0122	.0187	.0257	.0333	.0418	.0514	.0624	.0746	.0902	.1072	.1282
1.2	.0057	.0116	.0179	.0247	.0322	.0408	.0507	.0624	.0763	.0935	.1144	.1404

NATIONAL ADVISORY
COMMITTEE FOR AERONAUTICS

TABLE III.- BOUNDARY-INDUCED VELOCITY $\frac{wr}{\Gamma}$ ALONG HORIZONTAL CENTER LINE DUE TO UNIT COUNTERCLOCKWISE VORTEX AT VARIOUS DISTANCES $\frac{s}{r}$ FROM CENTER OF A CIRCULAR JET

y/r \ s/r	0.1	0.2	0.3	0.4	0.5	0.6	0.7	0.8	0.9
-0.9	0.0073	0.0135	0.0188	0.0234	0.0274	0.0310	0.0342	0.0370	0.0396
-.8	.0074	.0137	.0192	.0241	.0284	.0323	.0357	.0388	.0416
-.7	.0074	.0140	.0197	.0249	.0295	.0336	.0374	.0408	.0439
-.6	.0075	.0142	.0202	.0257	.0306	.0351	.0392	.0430	.0465
-.5	.0076	.0145	.0208	.0265	.0318	.0367	.0413	.0455	.0494
-.4	.0077	.0147	.0213	.0274	.0332	.0385	.0435	.0482	.0527
-.3	.0077	.0150	.0219	.0284	.0346	.0405	.0460	.0513	.0564
-.2	.0078	.0153	.0225	.0295	.0362	.0426	.0489	.0549	.0607
-.1	.0079	.0156	.0232	.0306	.0379	.0450	.0521	.0589	.0657
0	.0080	.0159	.0239	.0318	.0398	.0477	.0557	.0637	.0716
.1	.0080	.0162	.0246	.0332	.0419	.0508	.0599	.0692	.0787
.2	.0081	.0166	.0254	.0346	.0442	.0543	.0648	.0758	.0873
.3	.0082	.0169	.0262	.0362	.0468	.0582	.0705	.0838	.0981
.4	.0083	.0173	.0271	.0379	.0497	.0628	.0774	.0936	.1117
.5	.0084	.0177	.0281	.0398	.0531	.0682	.0857	.1061	.1302
.6	.0085	.0181	.0291	.0419	.0568	.0746	.0960	.1224	.1557
.7	.0086	.0185	.0302	.0442	.0612	.0823	.1092	.1447	.1936
.8	.0087	.0189	.0314	.0468	.0663	.0918	.1266	.1768	.2558
.9	.0087	.0194	.0327	.0497	.0723	.1038	.1506	.2274	.3769

NATIONAL ADVISORY
COMMITTEE FOR AERONAUTICS

TABLE IV.- CORRECTIONS APPLIED TO UNCORRECTED COEFFICIENTS OF REPRESENTATIVE MODEL FOR THREE END CONDITIONS

Correction	Reflection plane			End plate			No end plate		
	Jet boundary	Plan form	Total	Jet boundary	Plan form	Total	Jet boundary	Plan form	Total
$\Delta\alpha/C_L$	1.019	-0.038	0.981	1.219	-1.127	0.092	1.305	-3.014	-1.709
$\Delta C_D/C_L^2$	.0154	-.0006	.0148	.0185	[a]-.0141	.0044	.0198	-.0348	-.0150
$\Delta C_m/C_L$	---------	.0344	.0344	---------	.0586	.0586	---------	.0936	.0936
[b]$\Delta C_l/C_{l_u}$	-.082	-.104	-.186	-.082	-.098	-.180	-.082	-.083	-.165
$\Delta C_n/C_L C_l$	-.0405	-.0005	-.0410	-.0405	.0005	-.0400	-.0469	.0058	-.0411

[a]Includes ΔC_{D_e} (see text).

[b]For purpose of this table $\frac{\Delta C_l}{C_{l_u}} = \frac{C_l}{C_{l_u}} - 1 = \frac{\Delta C_{l_j}}{C_{l_u}} + \frac{\Delta C_{l_p}}{C_{l_u}}$.

NATIONAL ADVISORY
COMMITTEE FOR AERONAUTICS

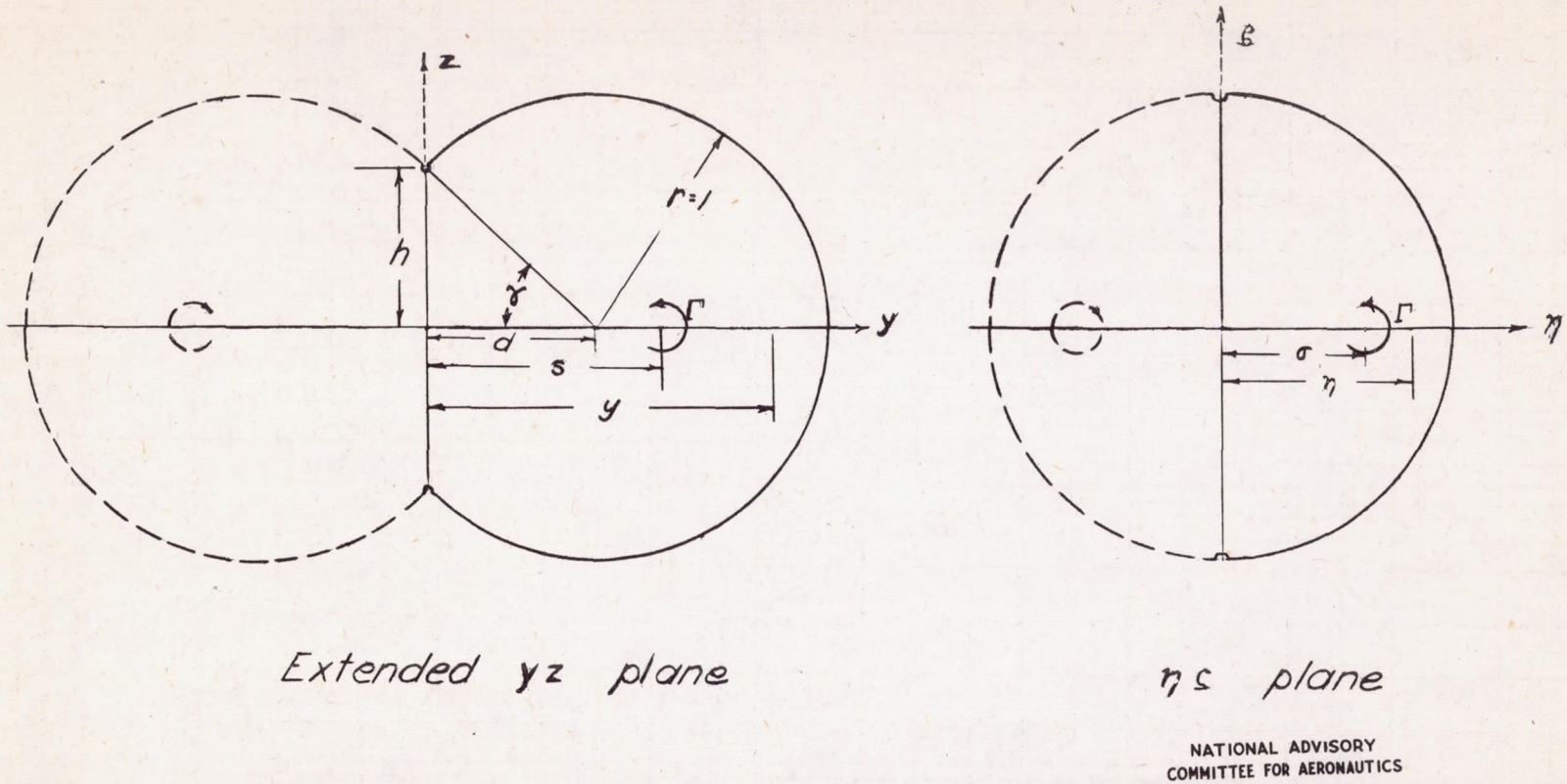


Figure 1.- Diagram of the bipolar tunnel including the reflected half of the jet and the complete transformed jet.

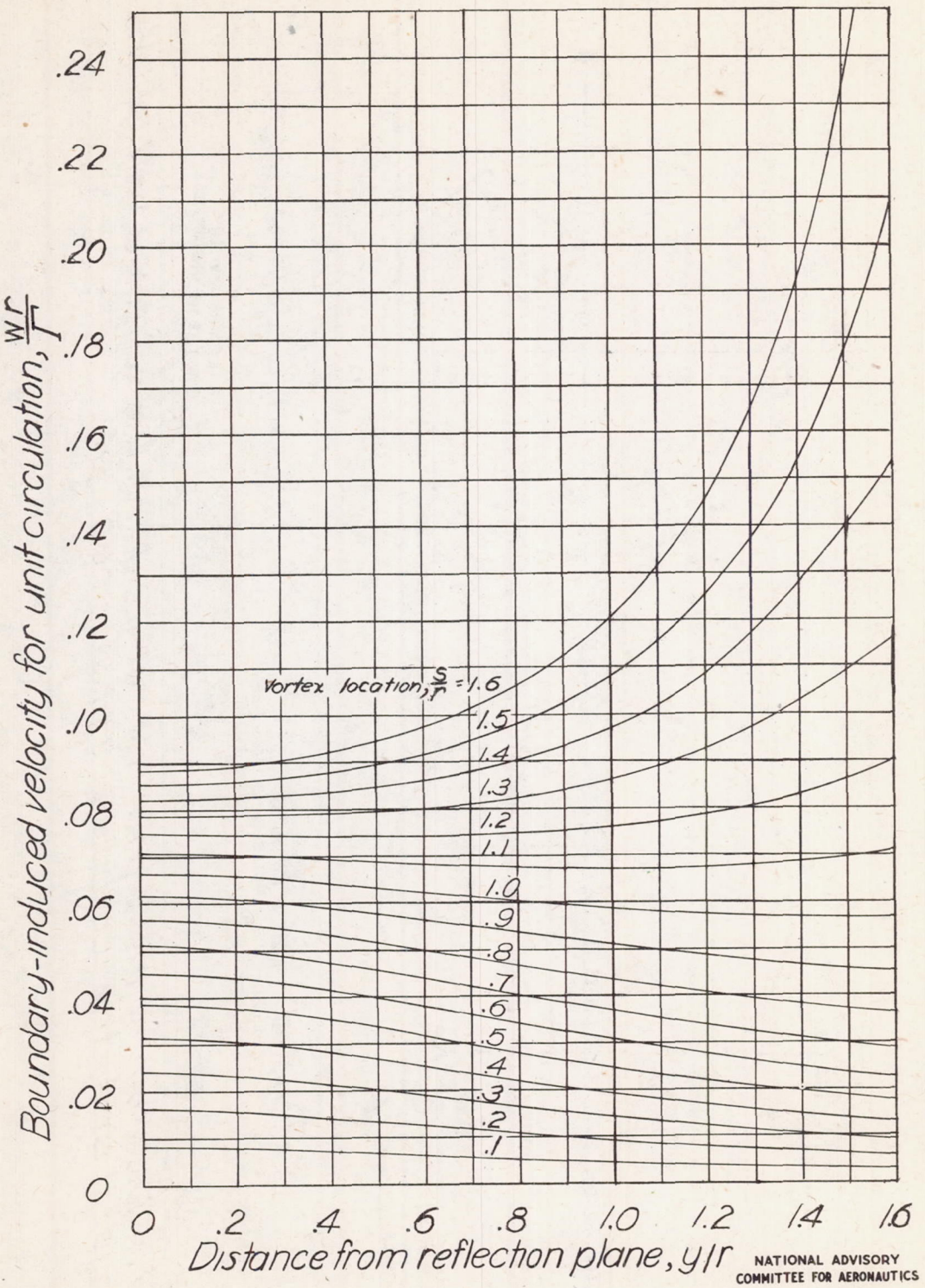


Figure 2.-Boundary-induced velocity along the horizontal center line due to a unit counterclockwise vortex at various distances $\frac{s}{r}$ from the reflection plane. $\frac{d}{r}$ = 0.73026.

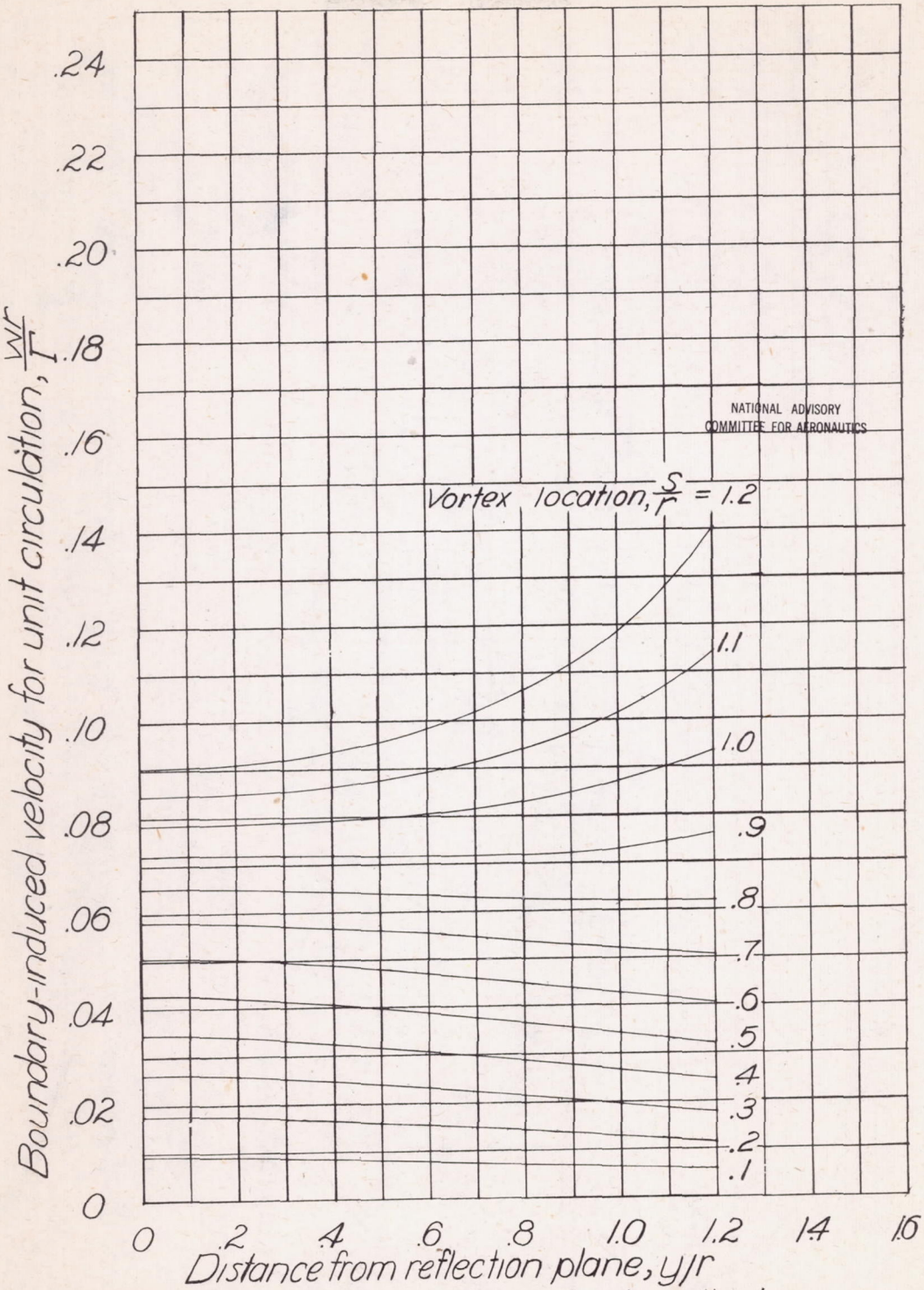


Figure 3.-Boundary-induced velocity along the horizontal center line due to a unit counterclockwise vortex at various distances $\frac{s}{r}$ from the reflection plane. $\frac{d}{r}$=0.49781.

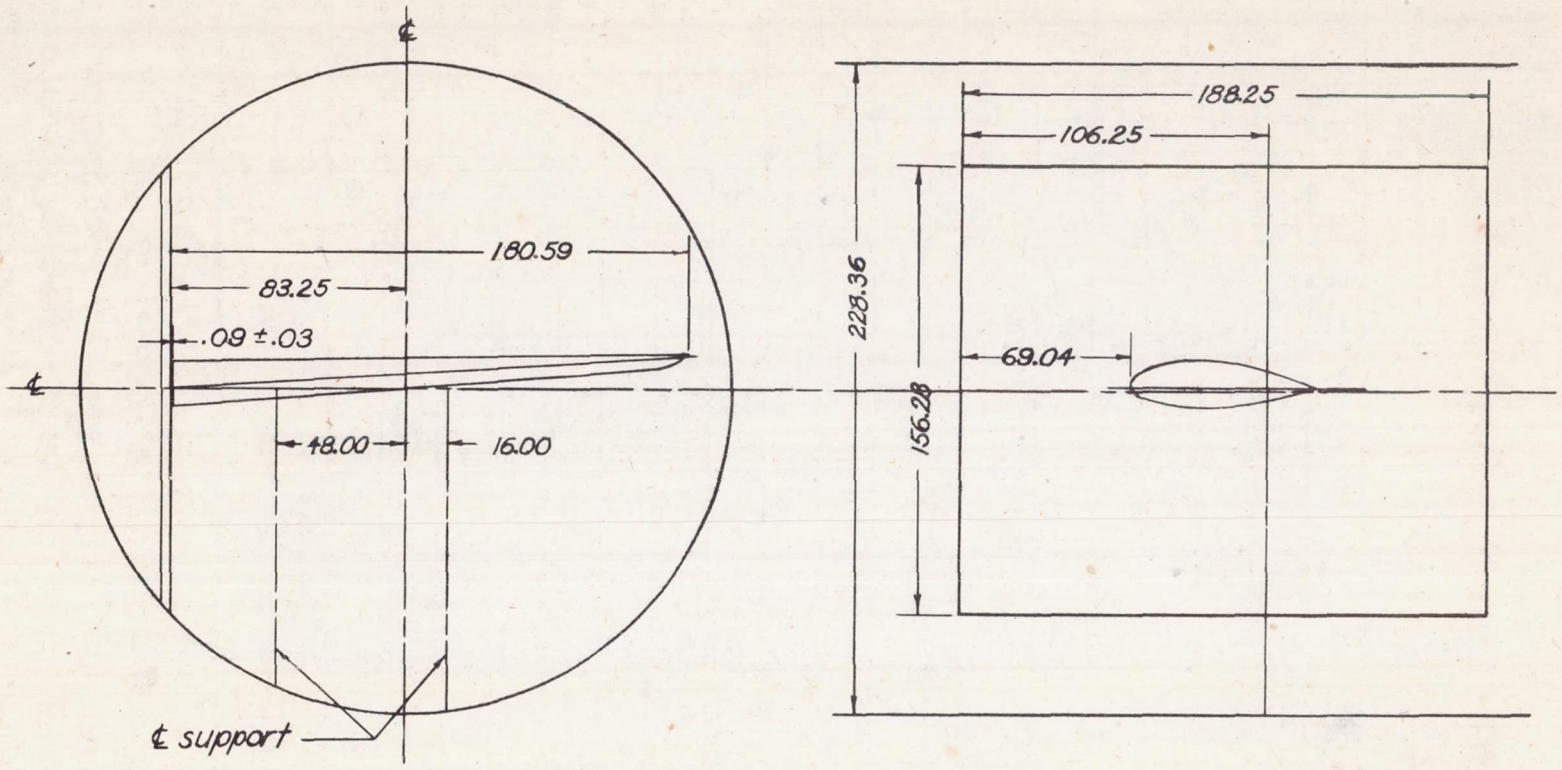


Figure 4.-General arrangement of the tapered-wing model and the reflection plane in the Langley 19-foot pressure tunnel. (All dimensions in inches.)

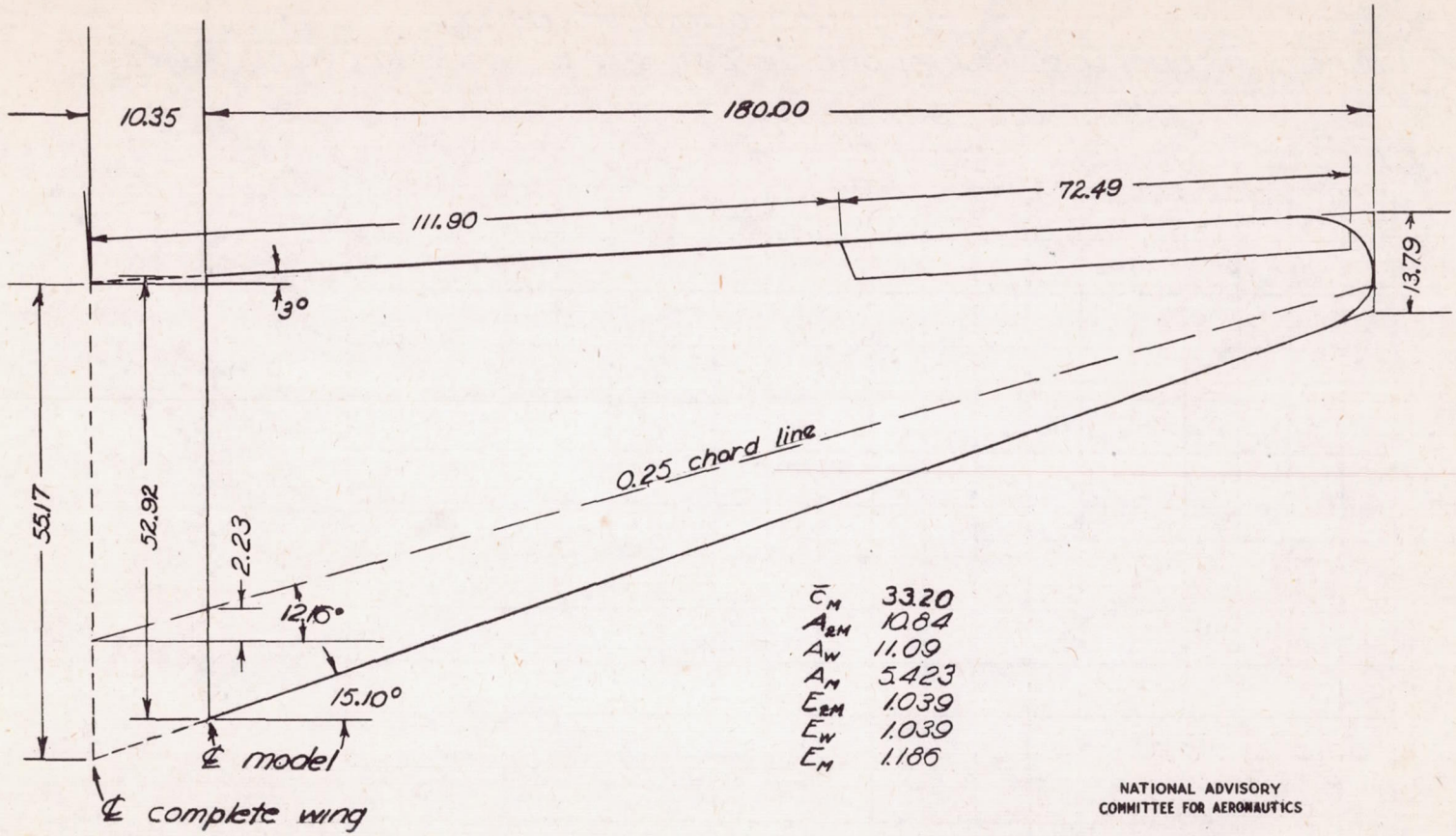


Figure 5.-Plan view and general dimensions of the tapered-wing model.
(All dimensions in inches.)

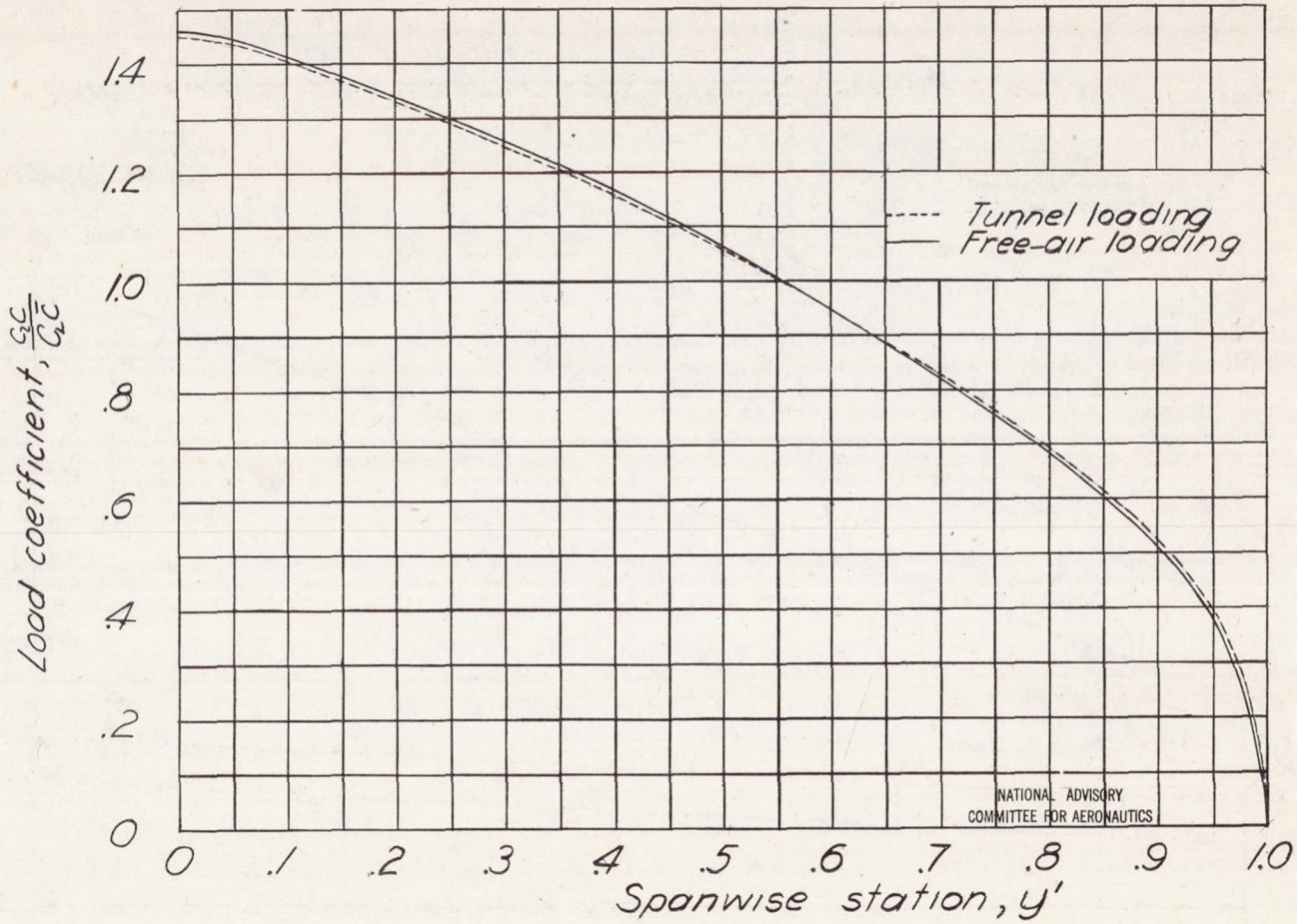


Figure 6.-Comparison of the free-air and tunnel span load distribution. Reflection-plane condition.

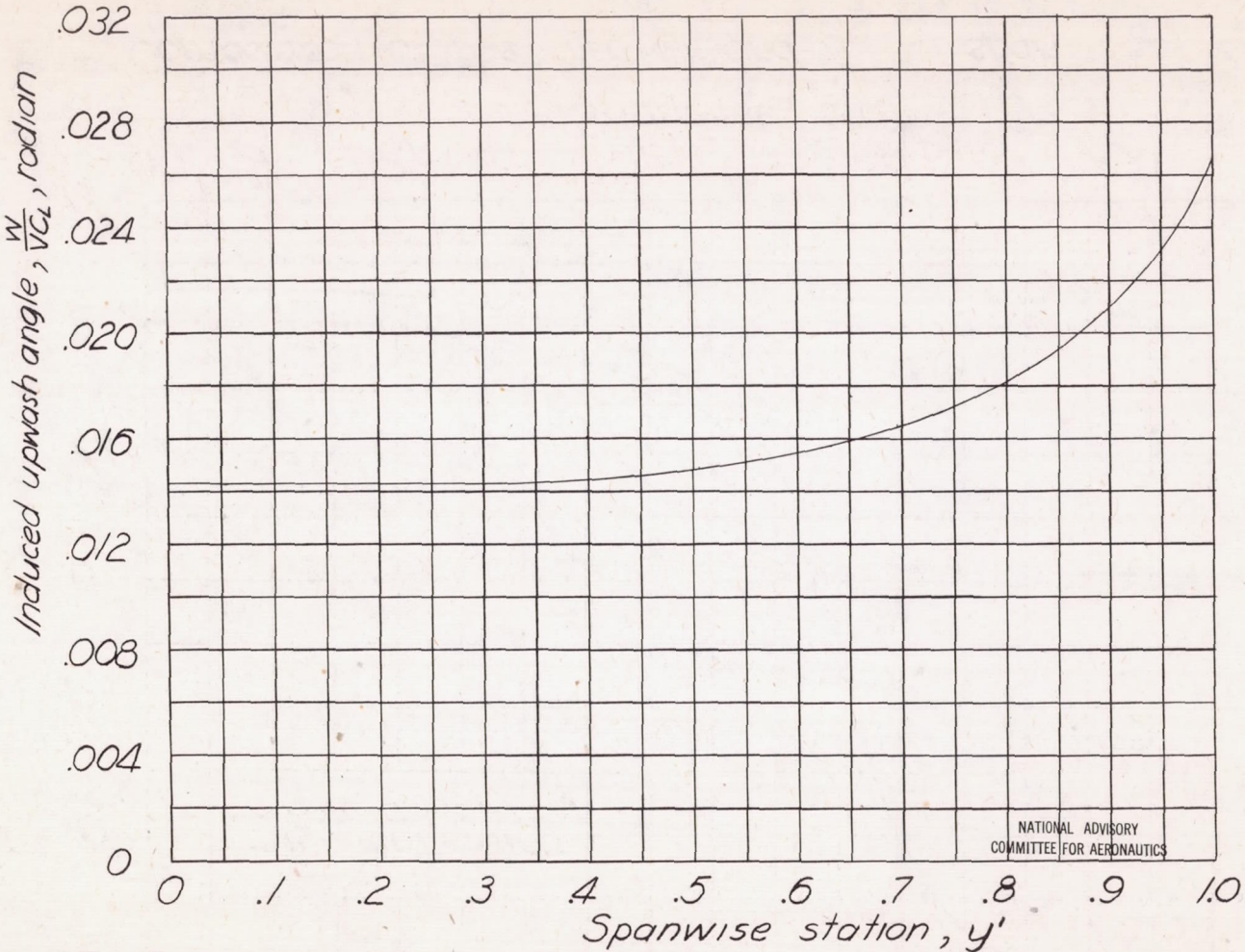


Figure 7.-Spanwise distribution of the boundary-induced upwash angle. Reflection-plane condition.

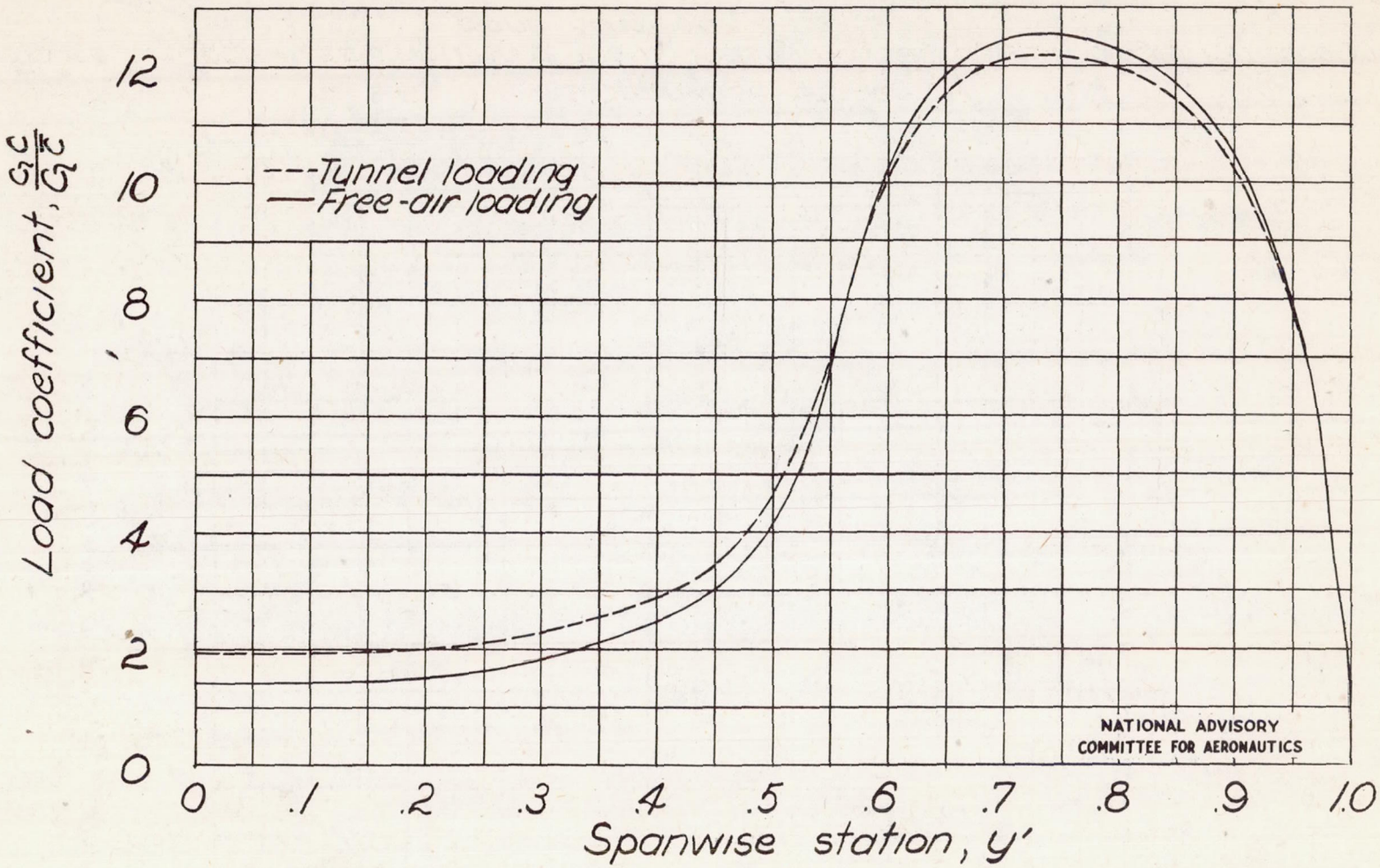


Figure 8.- Comparison of the free-air and tunnel span load distribution due to the aileron deflection. Reflection-plane condition.

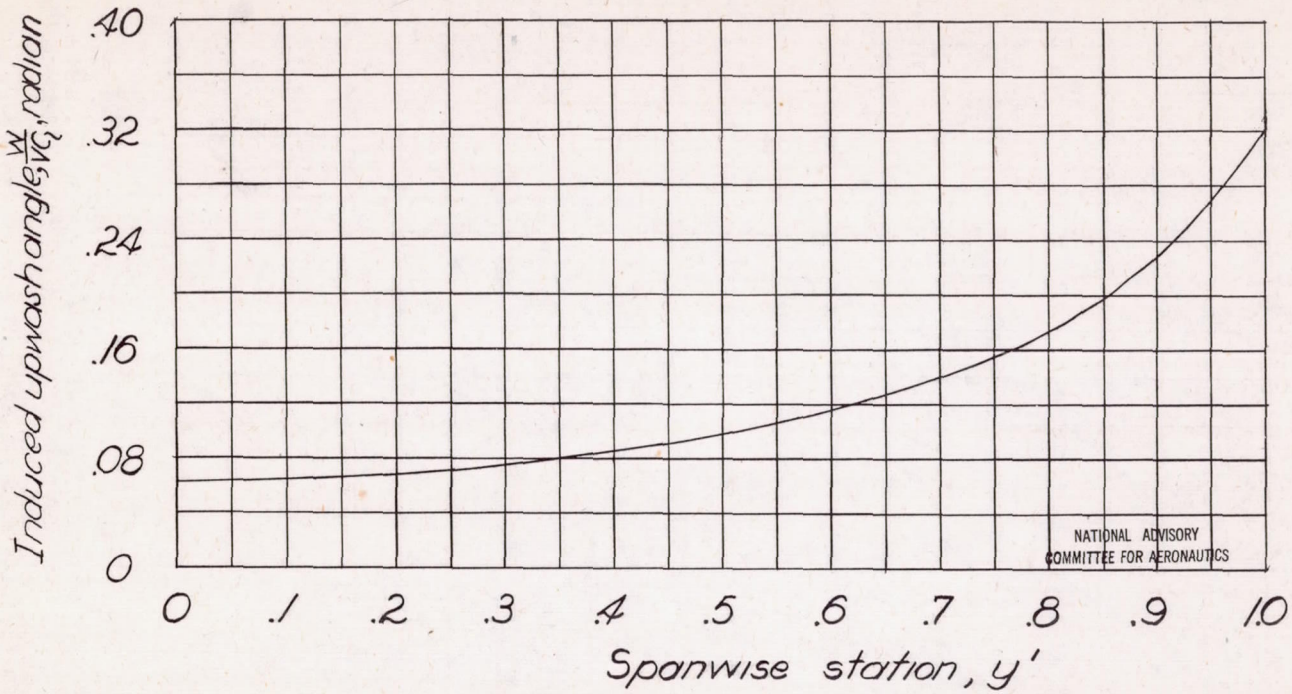


Figure 9.- Spanwise distribution of the boundary-induced upwash angle due to the aileron deflection. Reflection-plane condition.

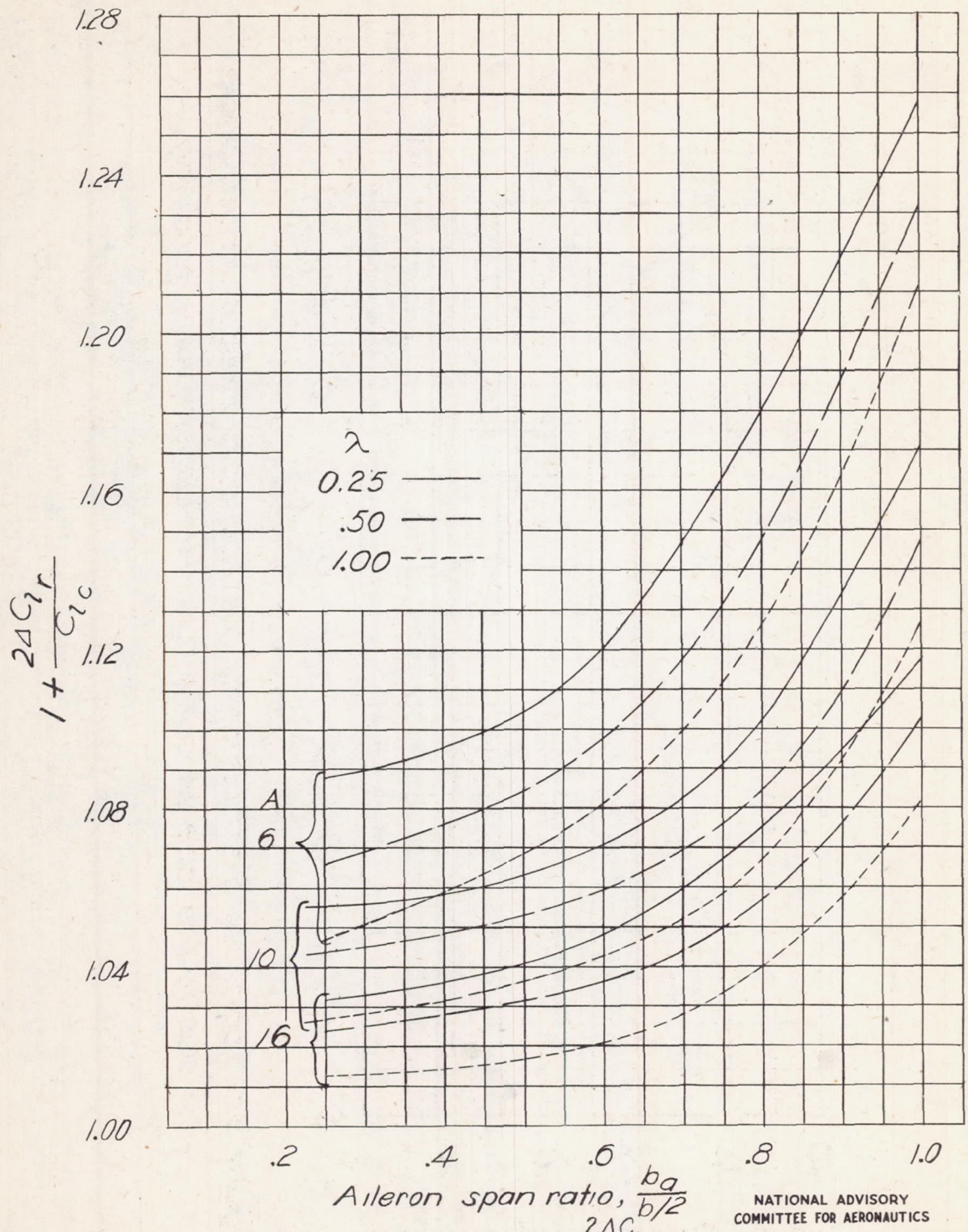


Figure 10.-Values of the factor $1+\frac{2\Delta C_{l_r}}{C_{l_c}}$ used to account for the effect of the reflection plane on the rolling-moment coefficient for ailerons extending inboard from the tips of the wings of reference 8. (From reference 3.)

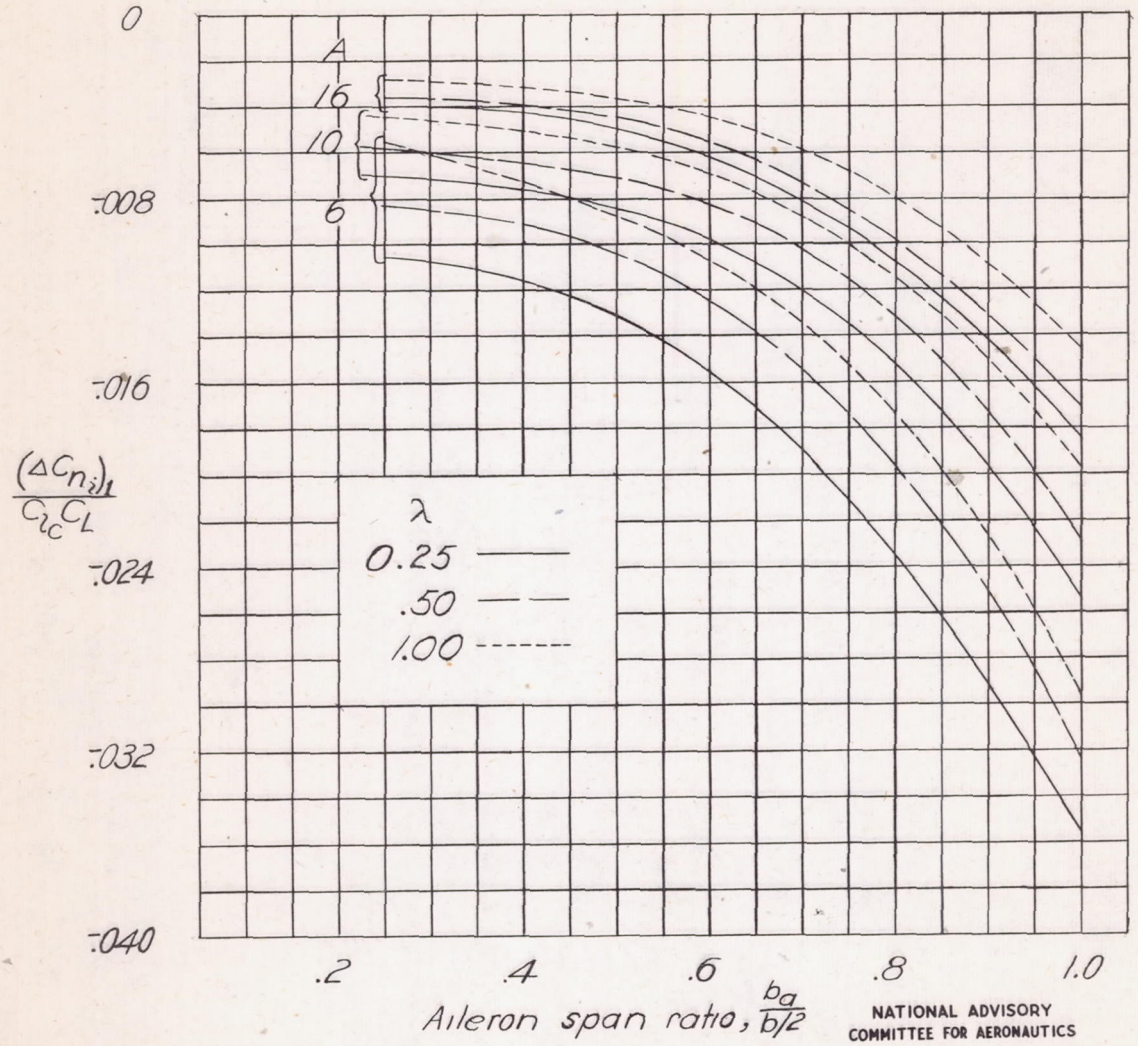


Figure 11.- Increment of yawing-moment-coefficient correction due to the reflection plane for ailerons extending inboard from the tips of the wings of reference 8. (From reference 3.)

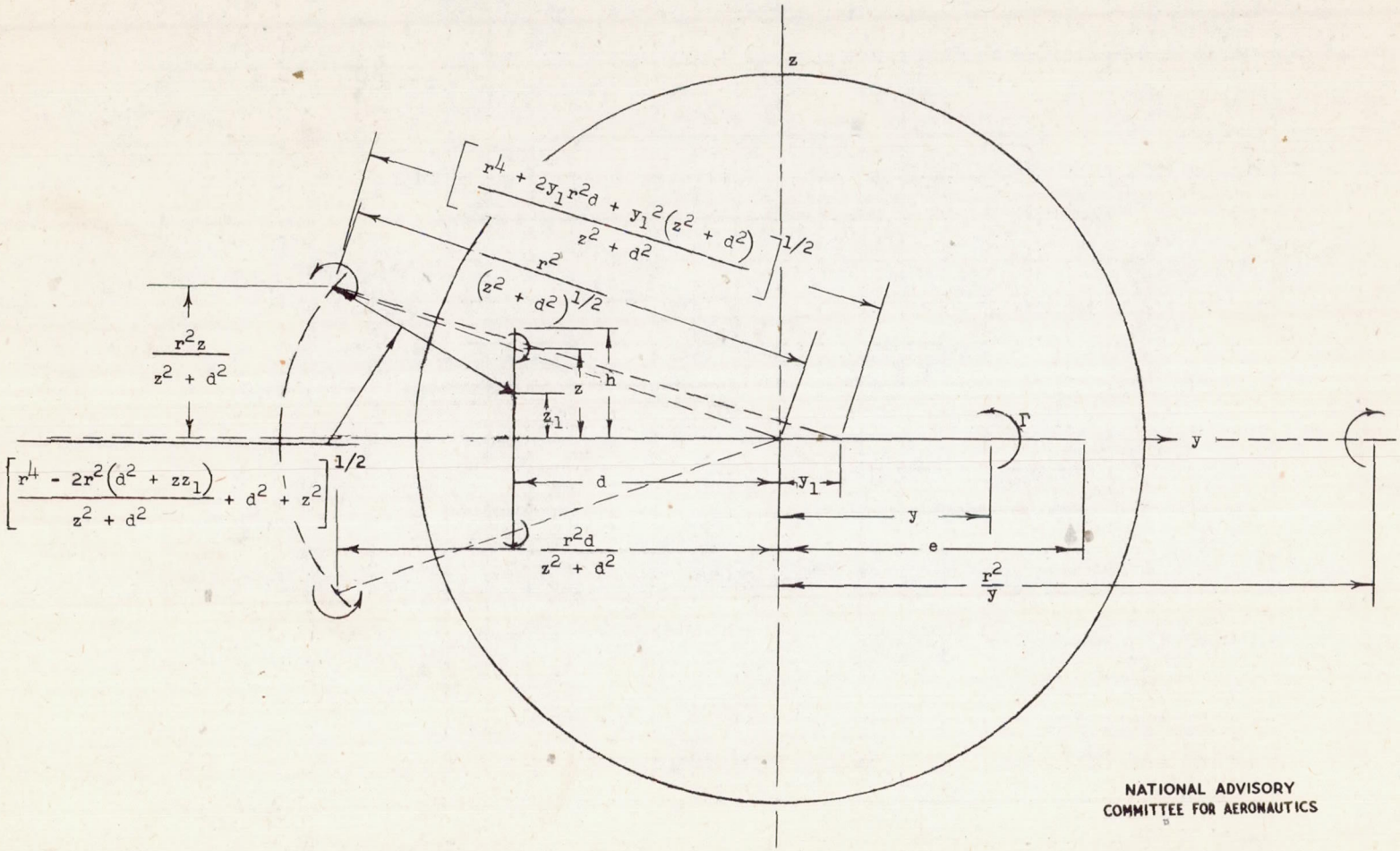


Figure 12.- Diagram of the model and end-plate trailing-vortex system and the corresponding reflected images.

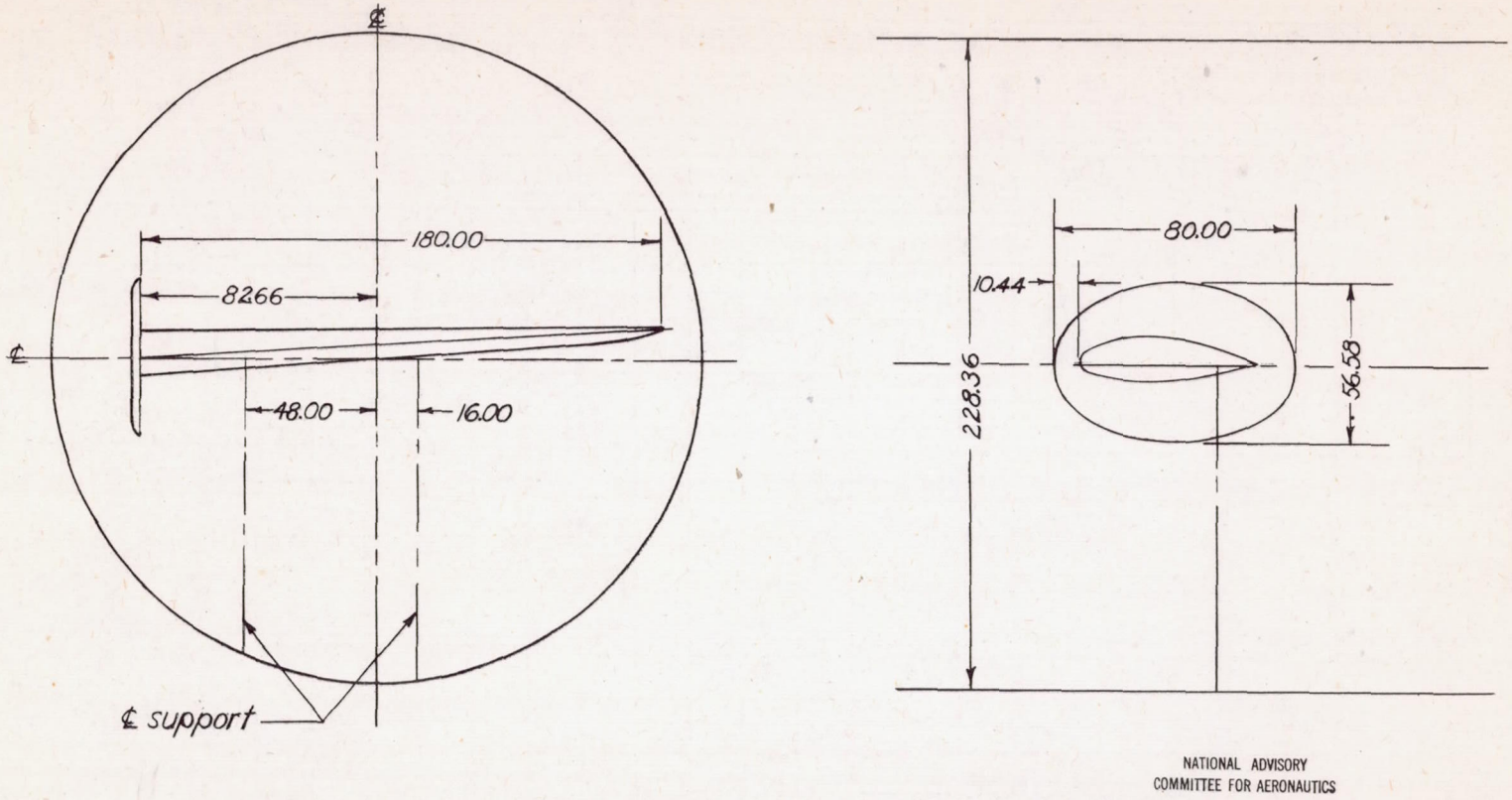


Figure 13.- General arrangement of tapered-wing model and the end plate in the Langley 19-foot pressure tunnel. (All dimensions in inches.)

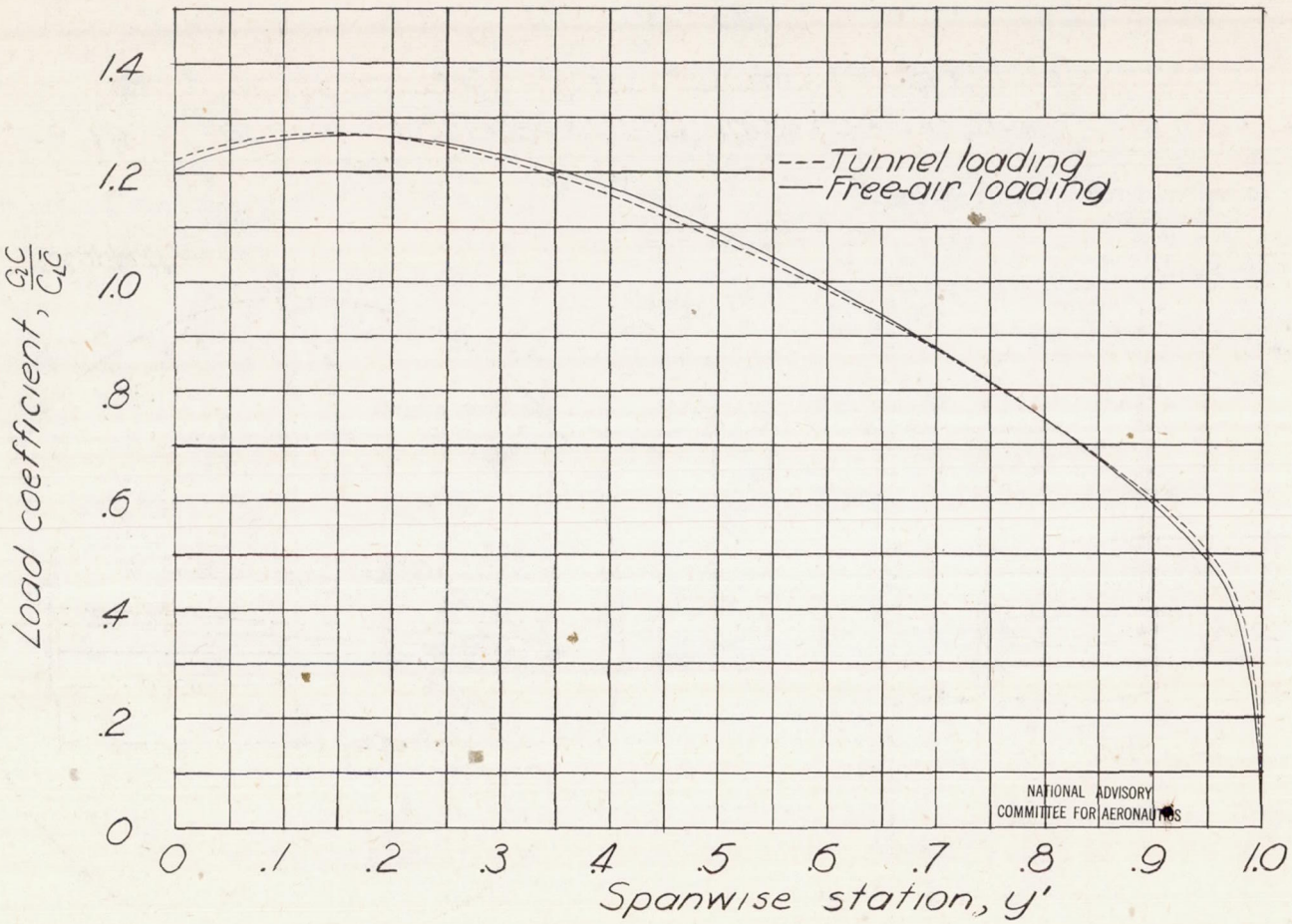


Figure 14.- Comparison of the free-air and tunnel span load distribution. End-plate condition.

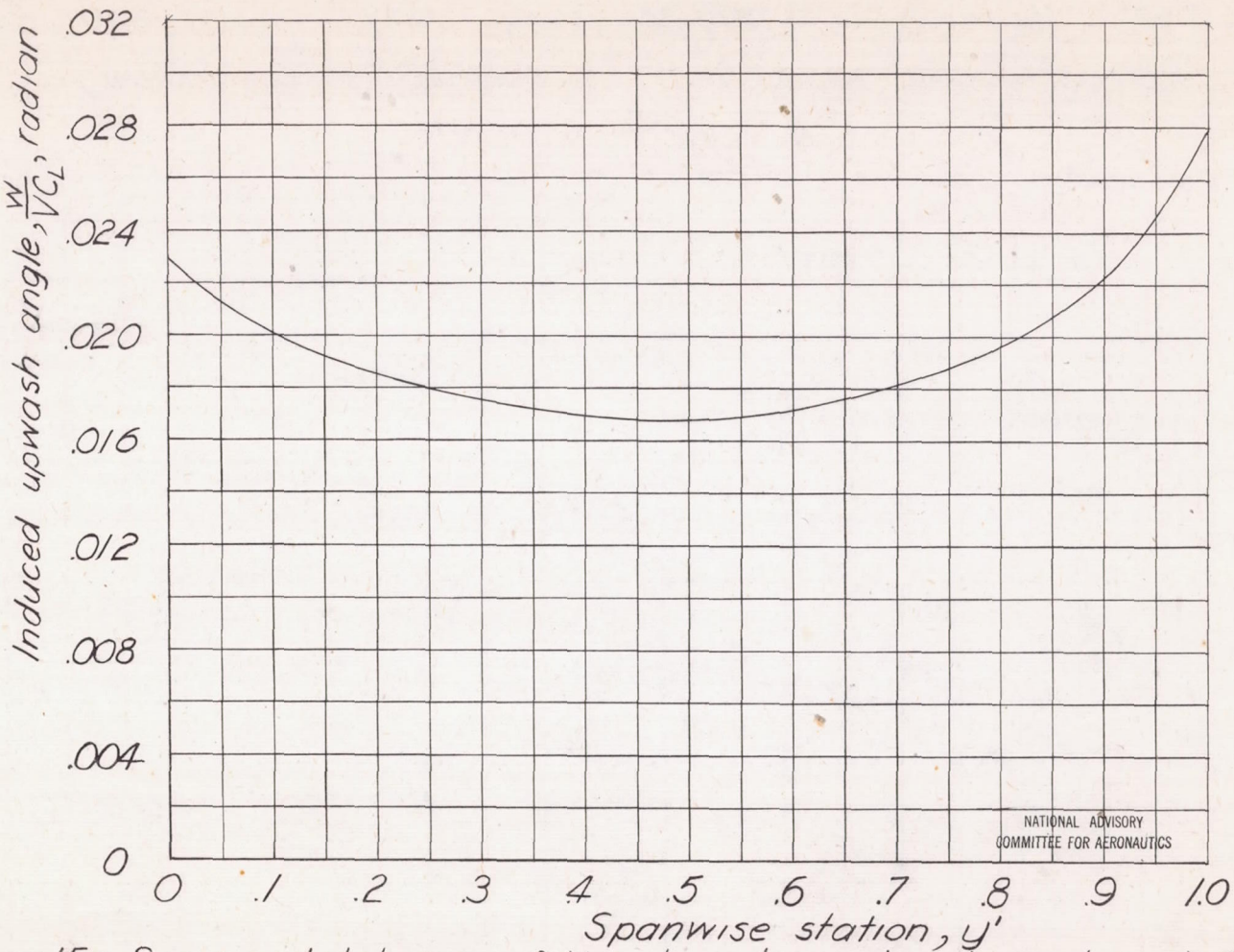


Figure 15.- Spanwise distribution of the boundary-induced upwash angle. End-plate condition.

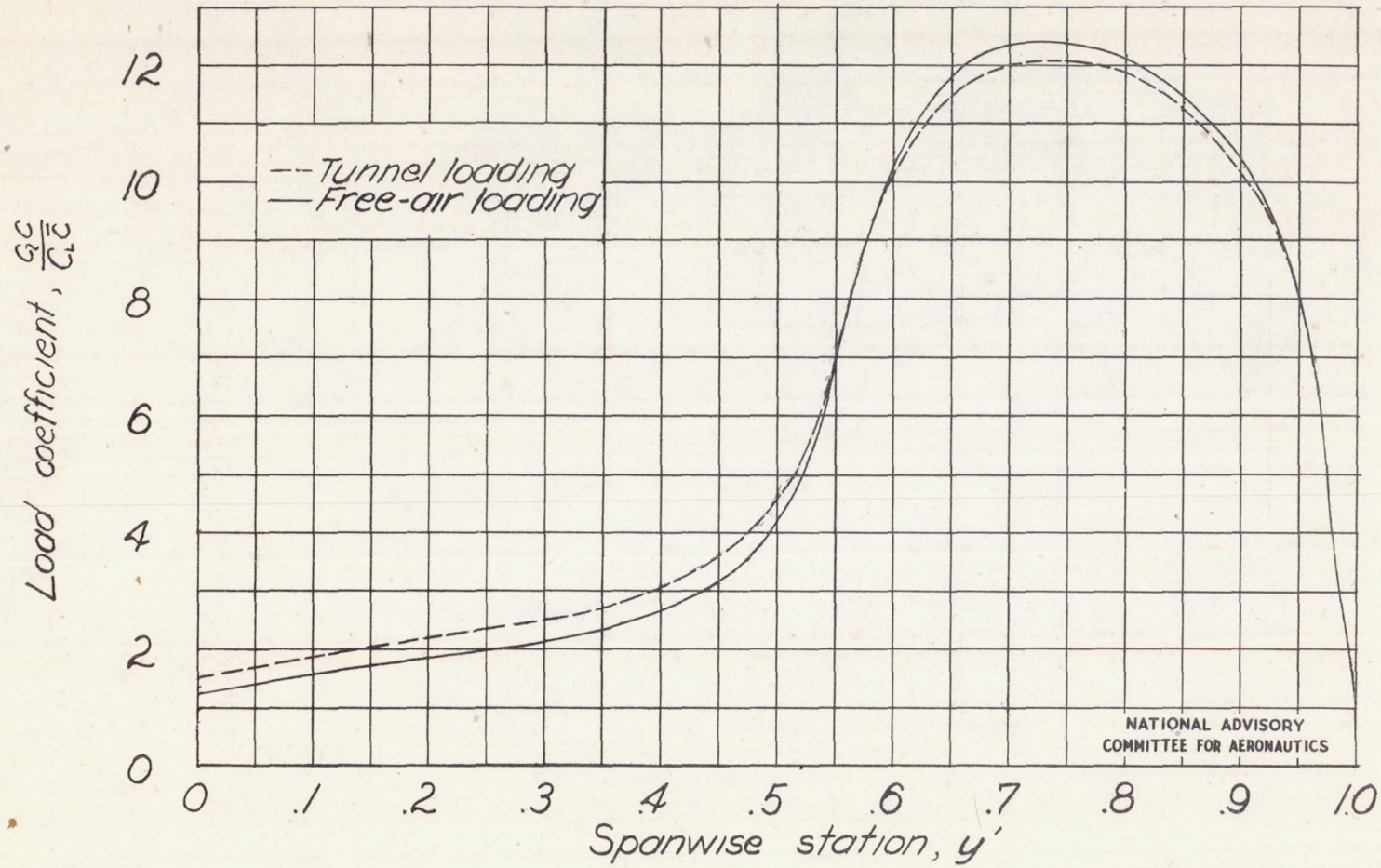


Figure 16.- Comparison of the free-air and tunnel span load distribution due to the aileron deflection. End-plate condition.

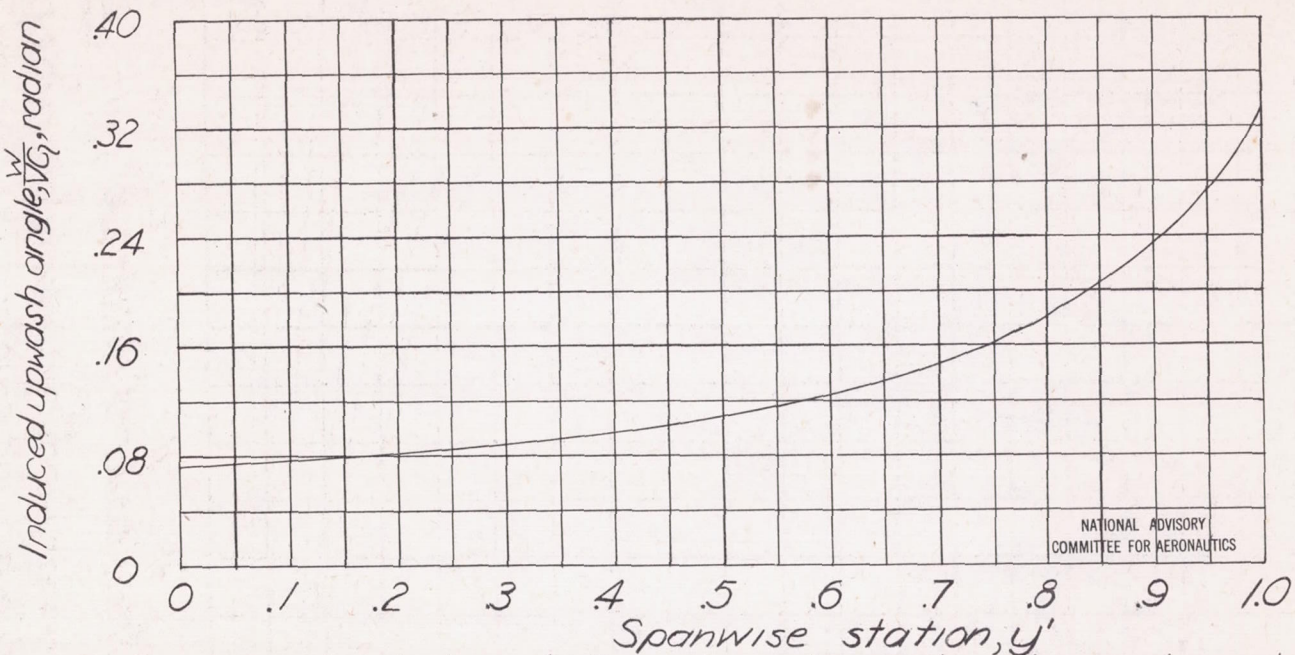


Figure 17.- Spanwise distribution of the boundary-induced upwash angle due to the aileron deflection. End-plate condition.

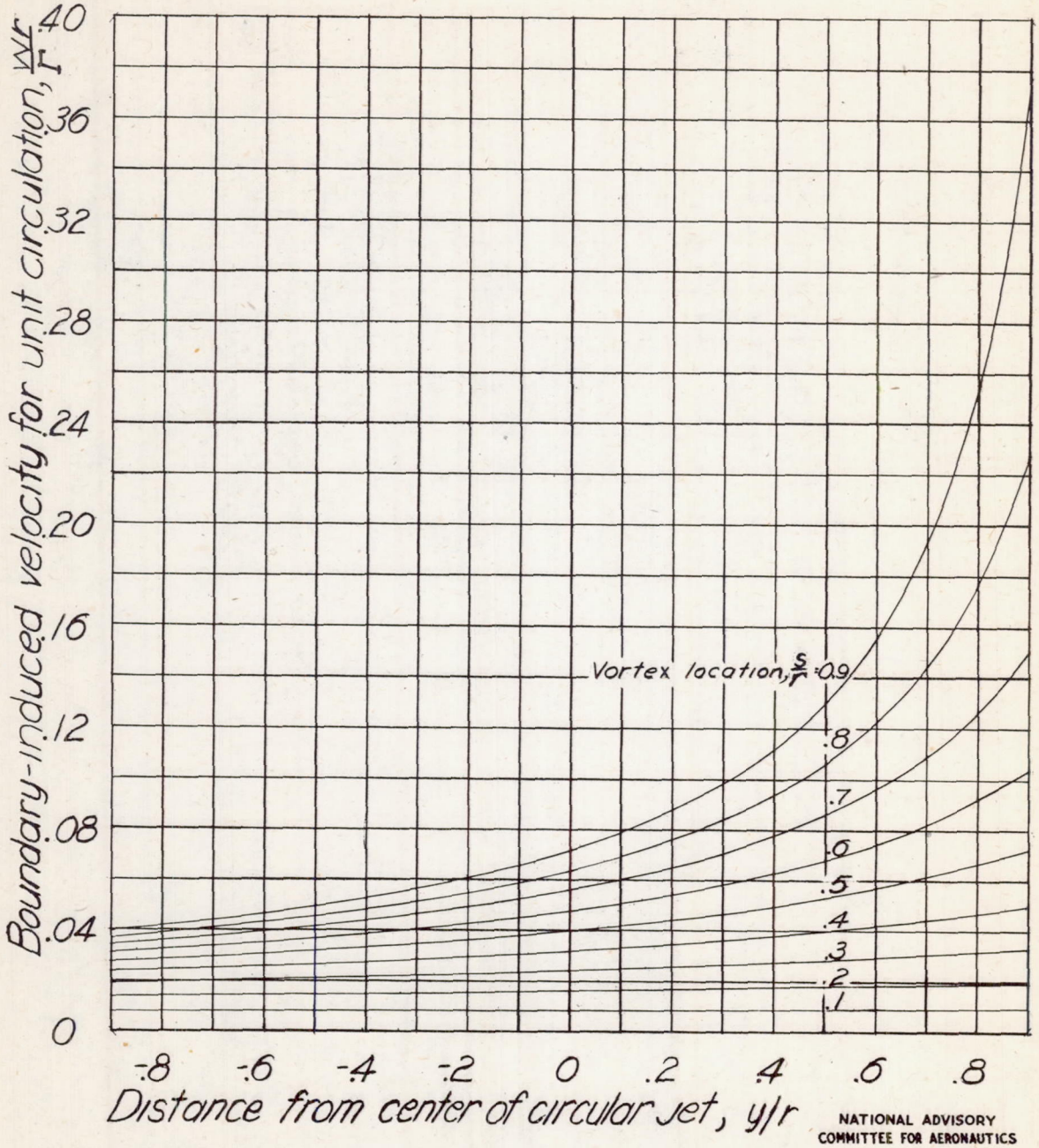


Figure 18.-Boundary-induced velocity along the horizontal center line due to a unit counterclockwise vortex at various distances $\frac{s}{r}$ from the center of a circular jet.

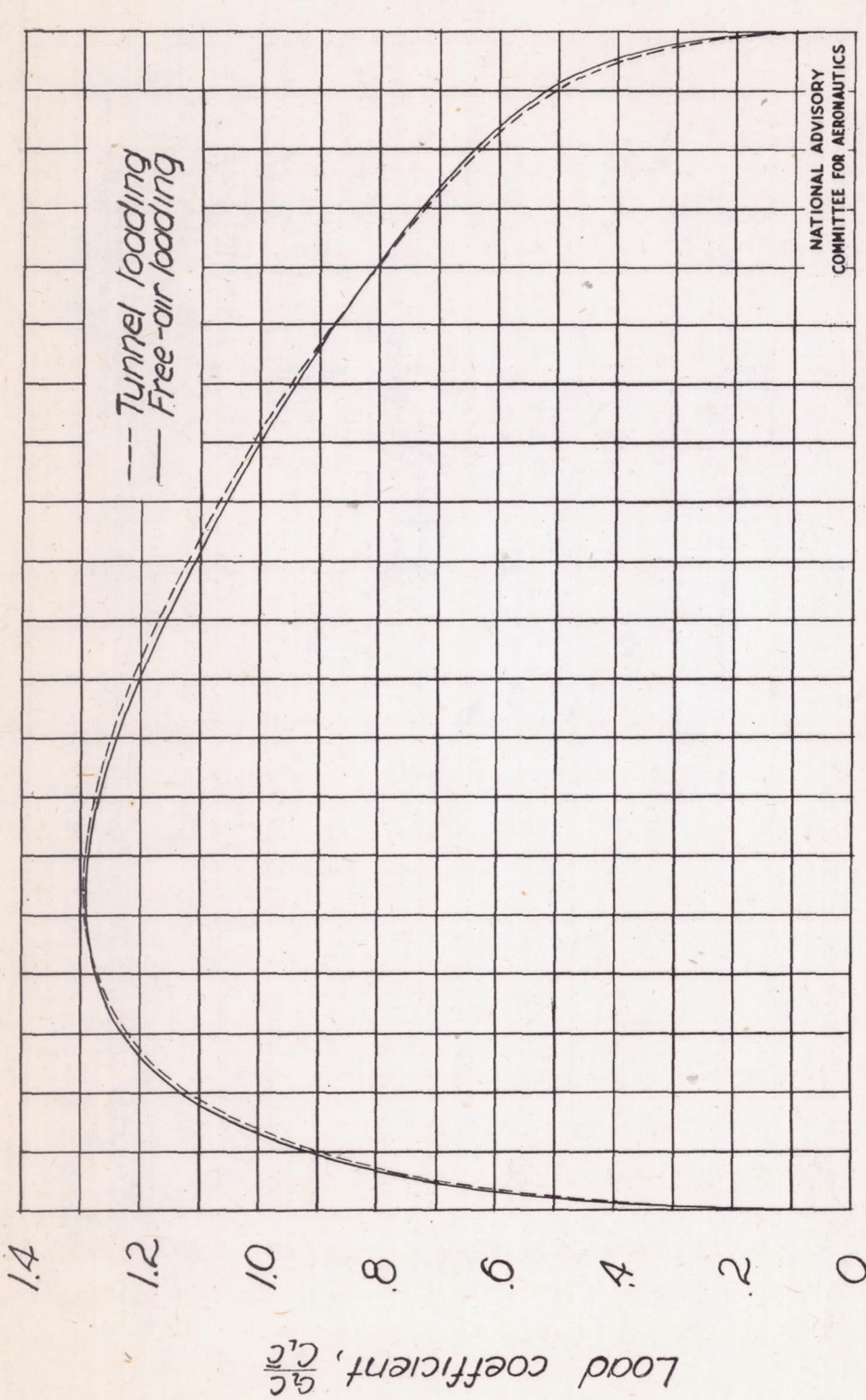


Figure 19.- Comparison of the free-air and tunnel span load distributions. No end plate.

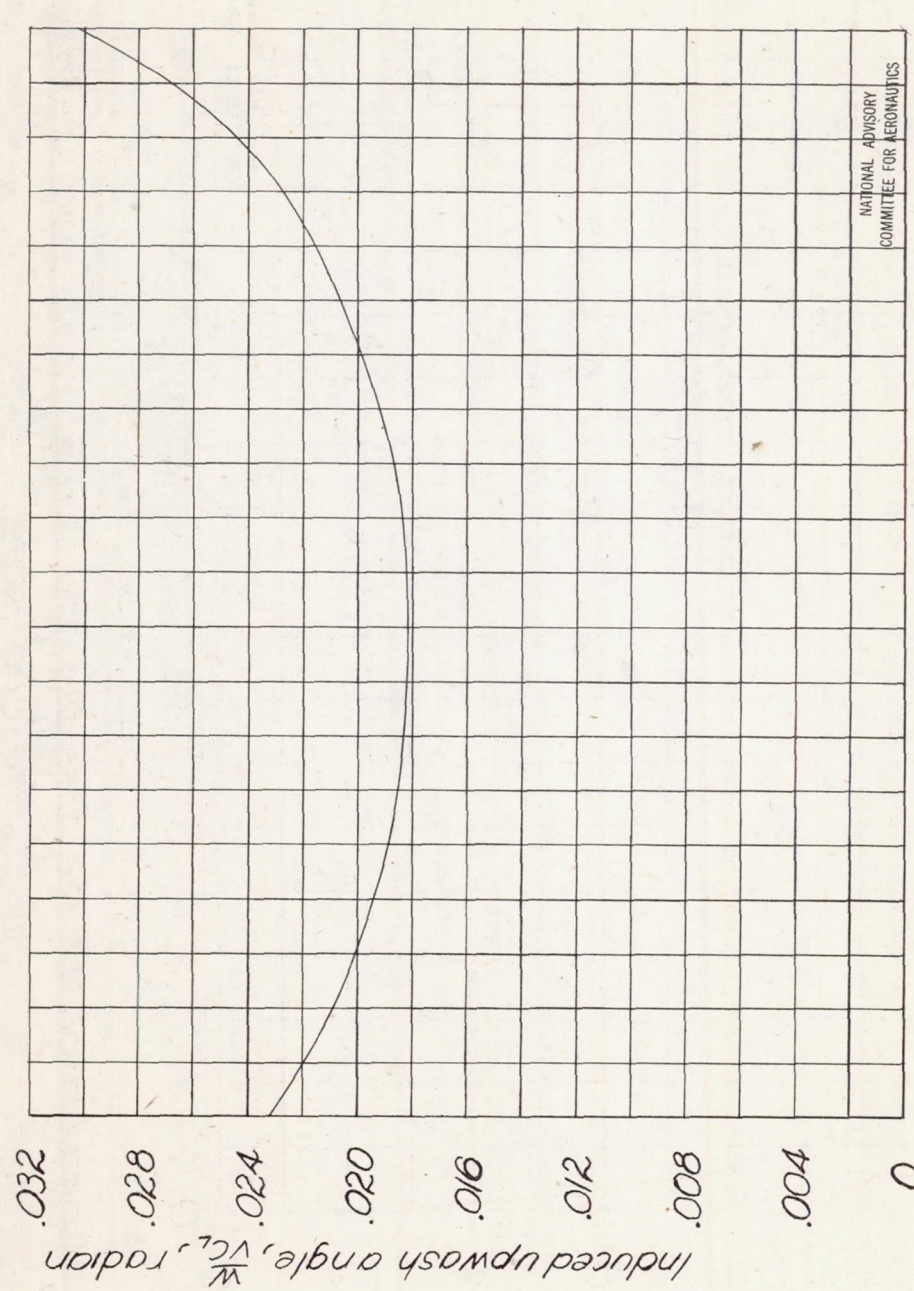


Figure 20.-Spanwise distribution of the boundary-induced upwash angle. No end plate.

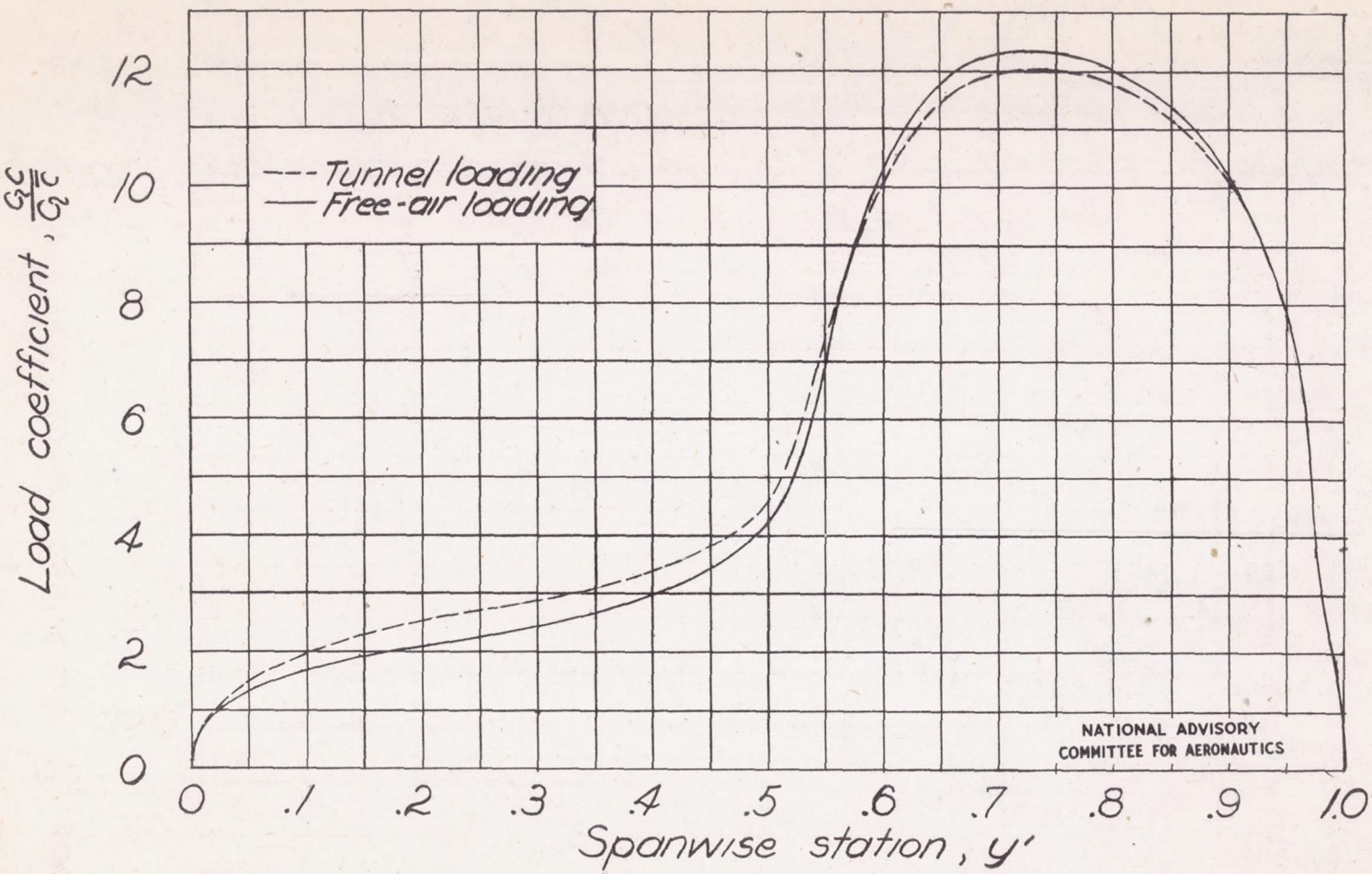


Figure 21.- Comparison of the free-air and tunnel span load distribution due to the aileron deflection. No end plate.

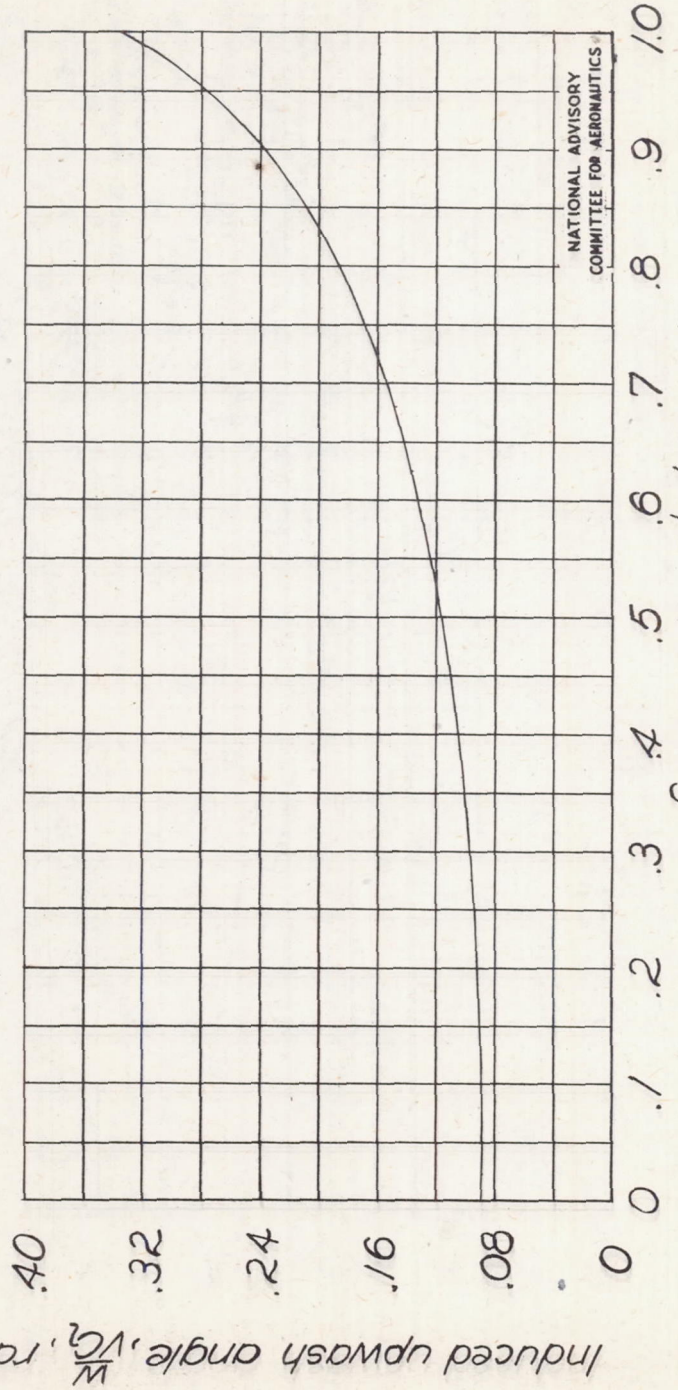


Figure 22.- Spanwise distribution of the boundary-induced upwash angle due to the aileron deflection. No end plate.

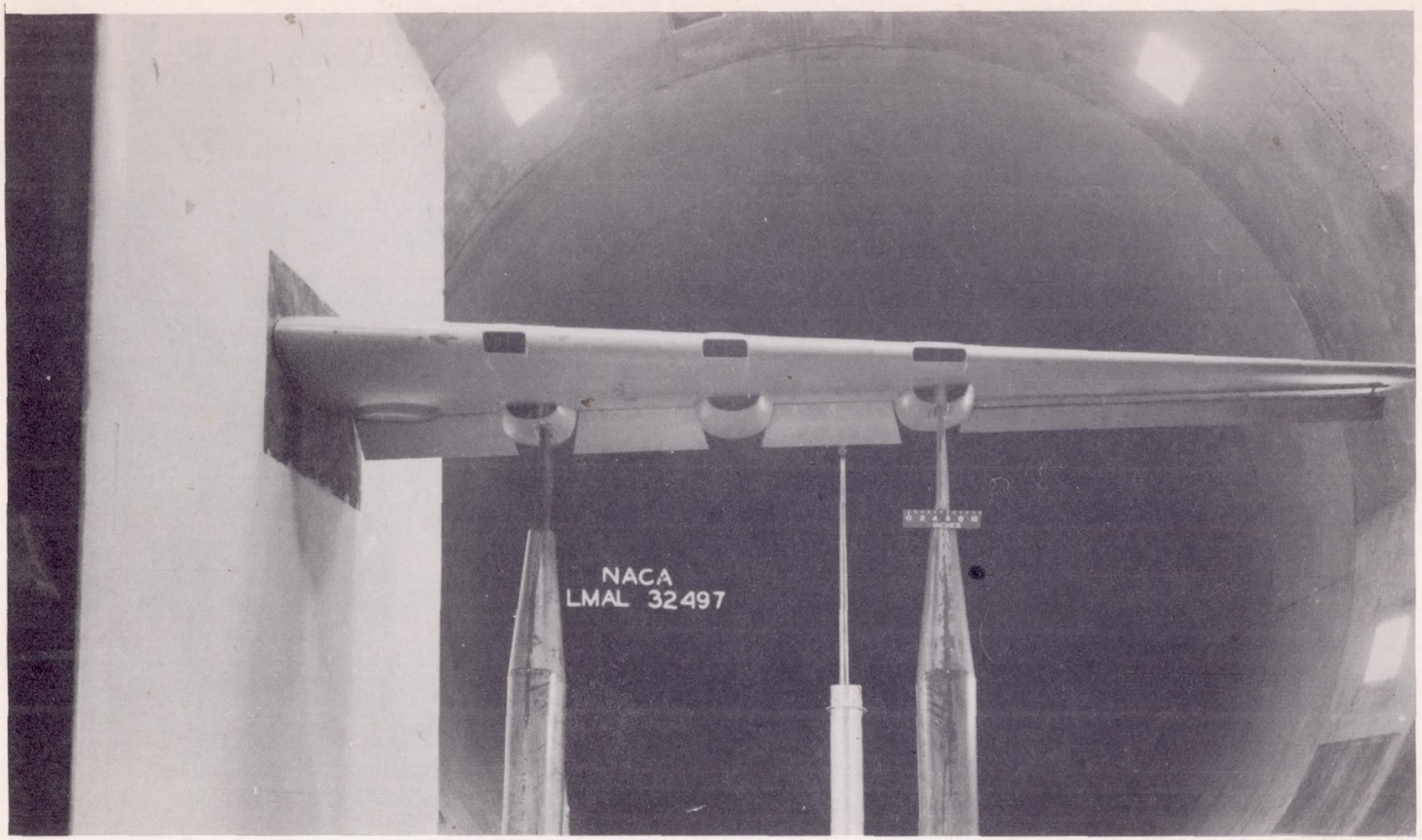


Figure 23.- Partial-span tapered wing model with reflection plane mounted in Langley 19-foot pressure tunnel.

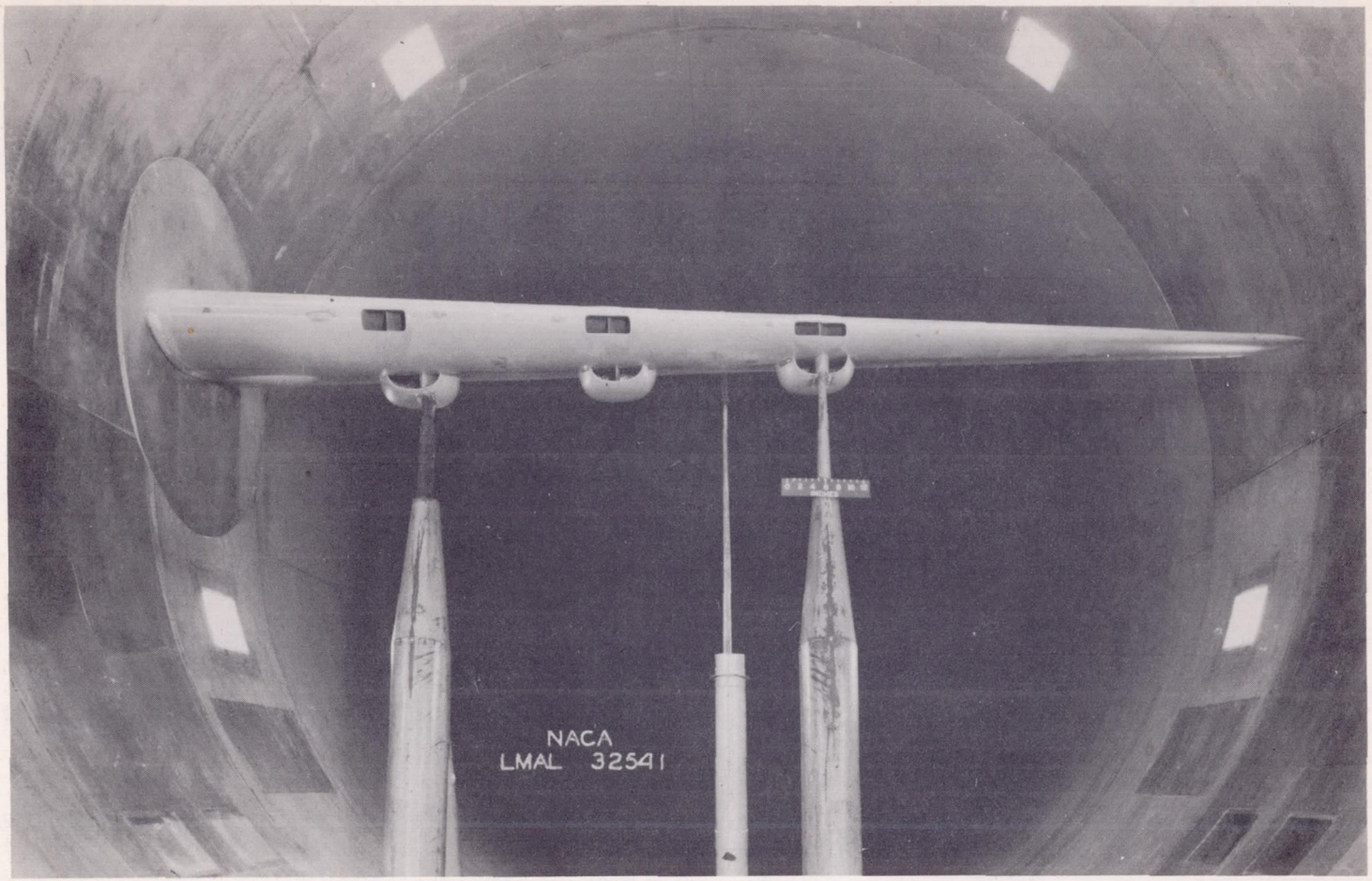


Figure 24.- Partial-span tapered wing model with end plate mounted in Langley 19-foot pressure tunnel.

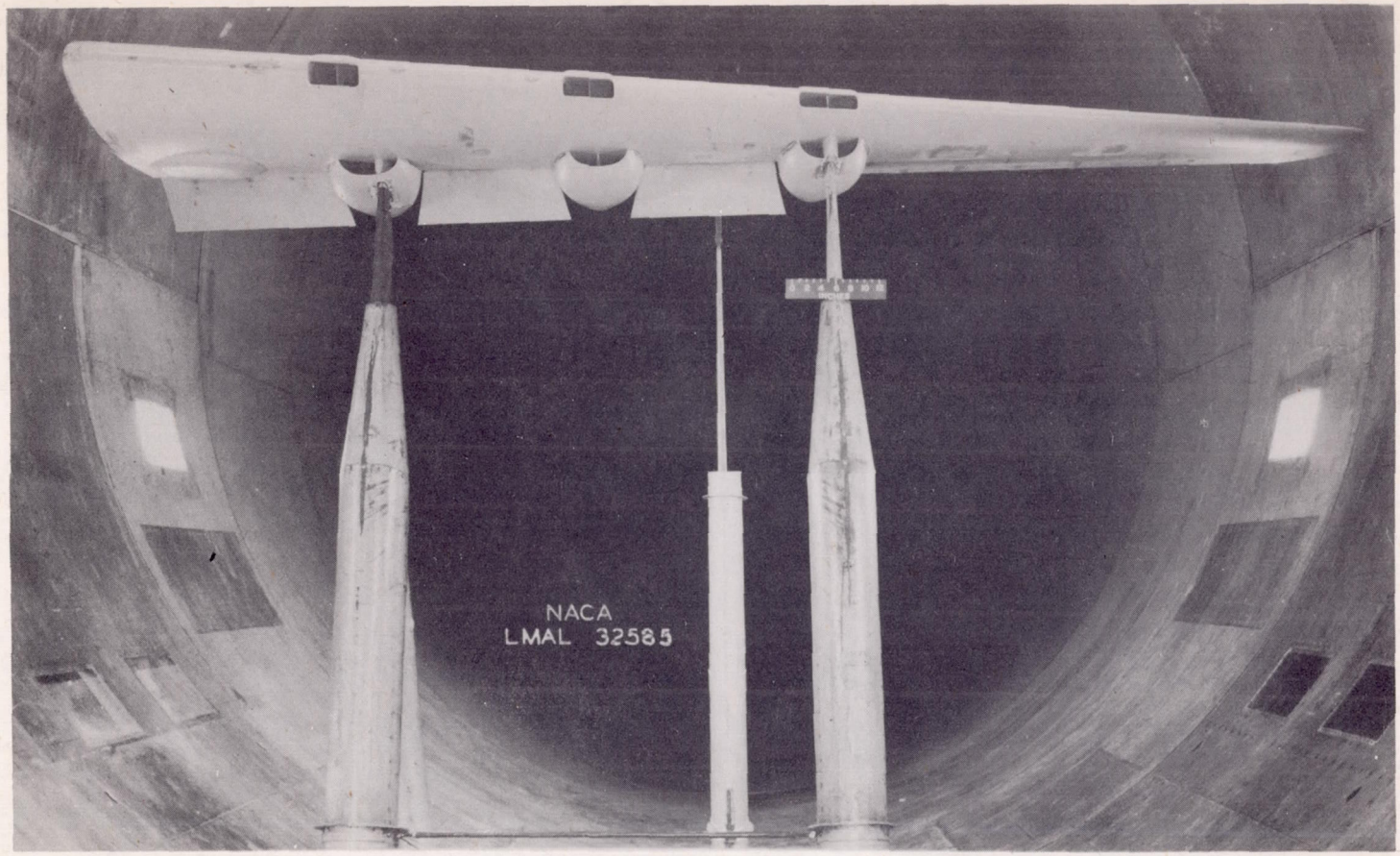
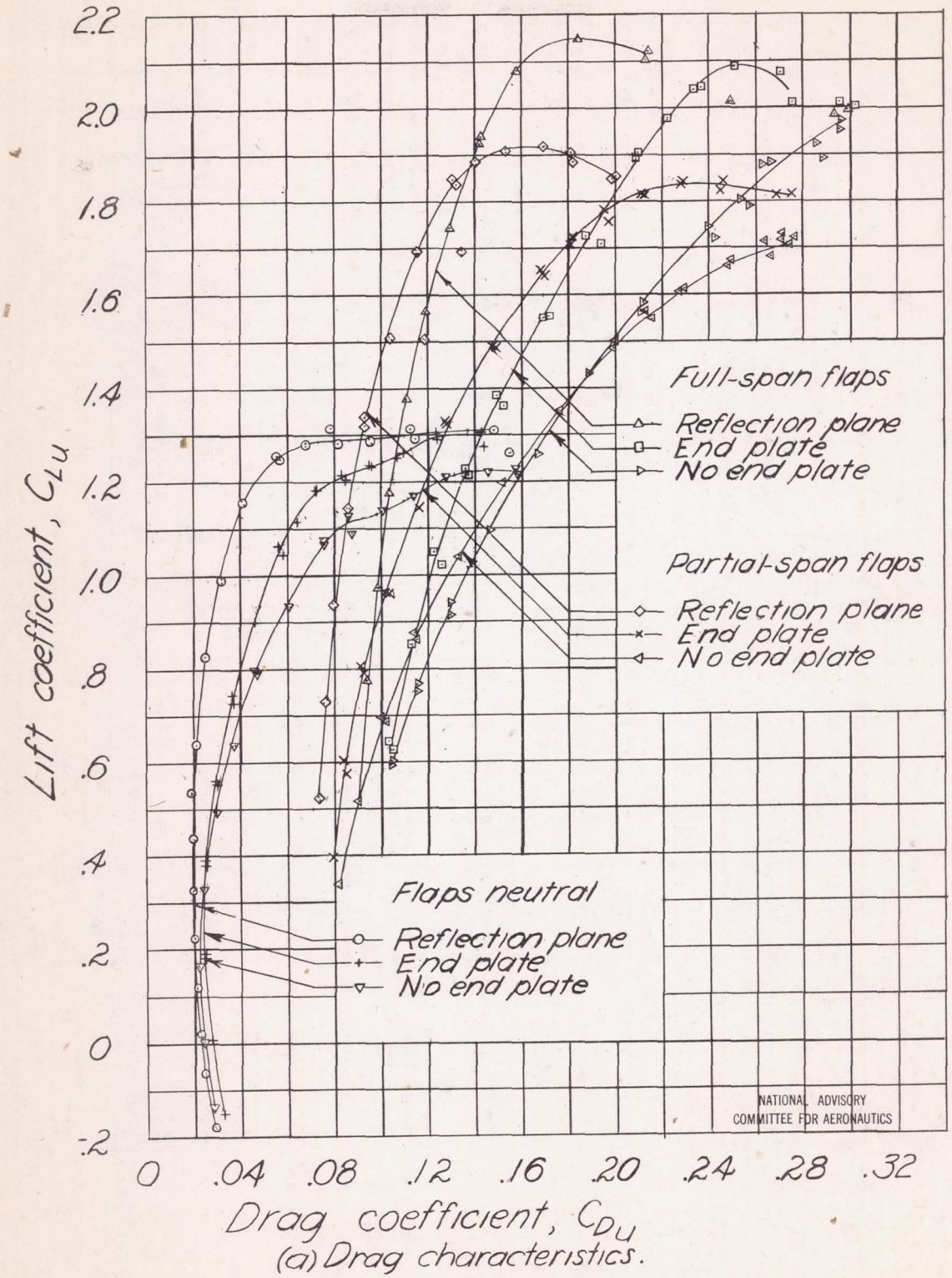
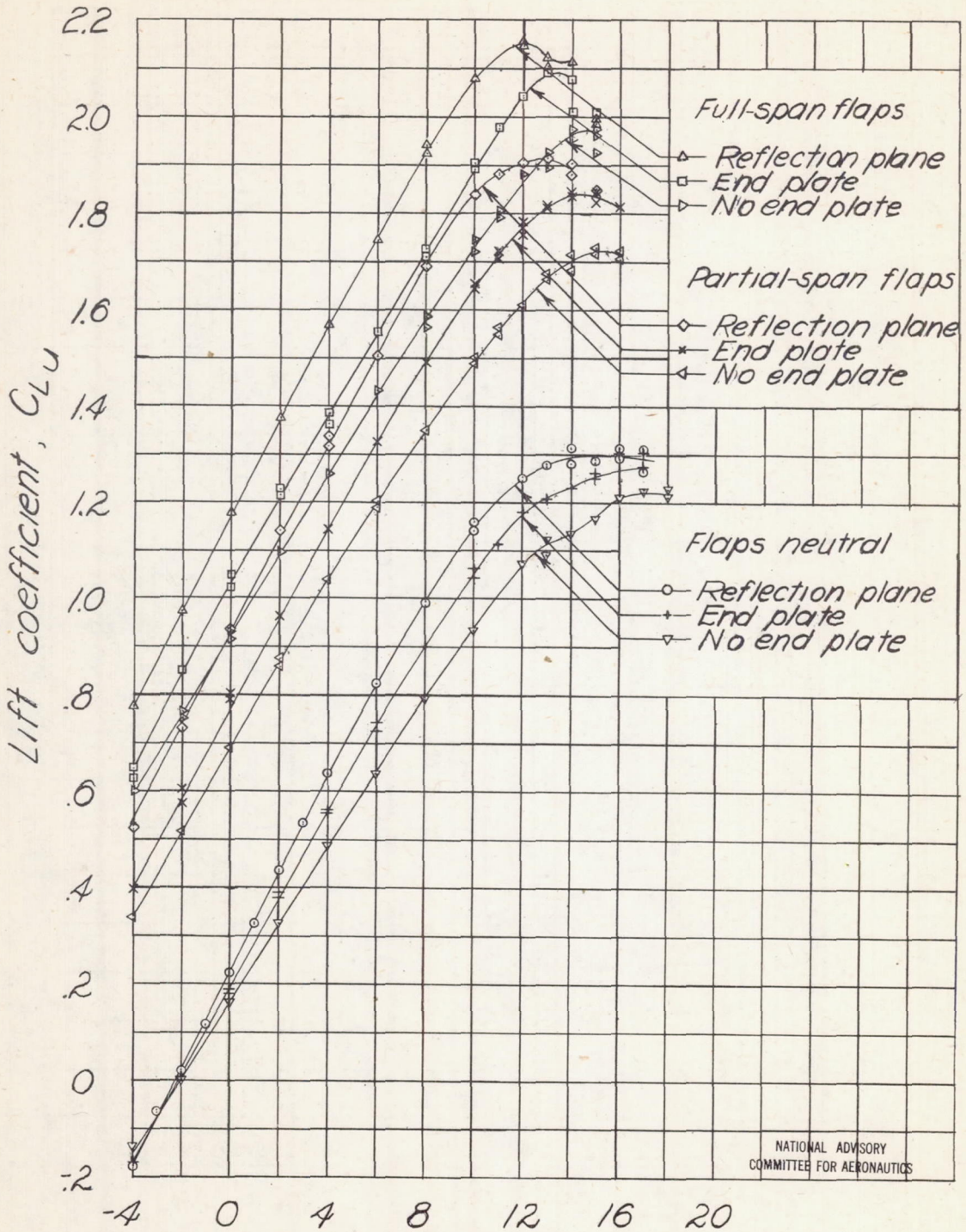


Figure 25.- Partial-span tapered wing model with no end plate mounted in the Langley 19-foot pressure tunnel.



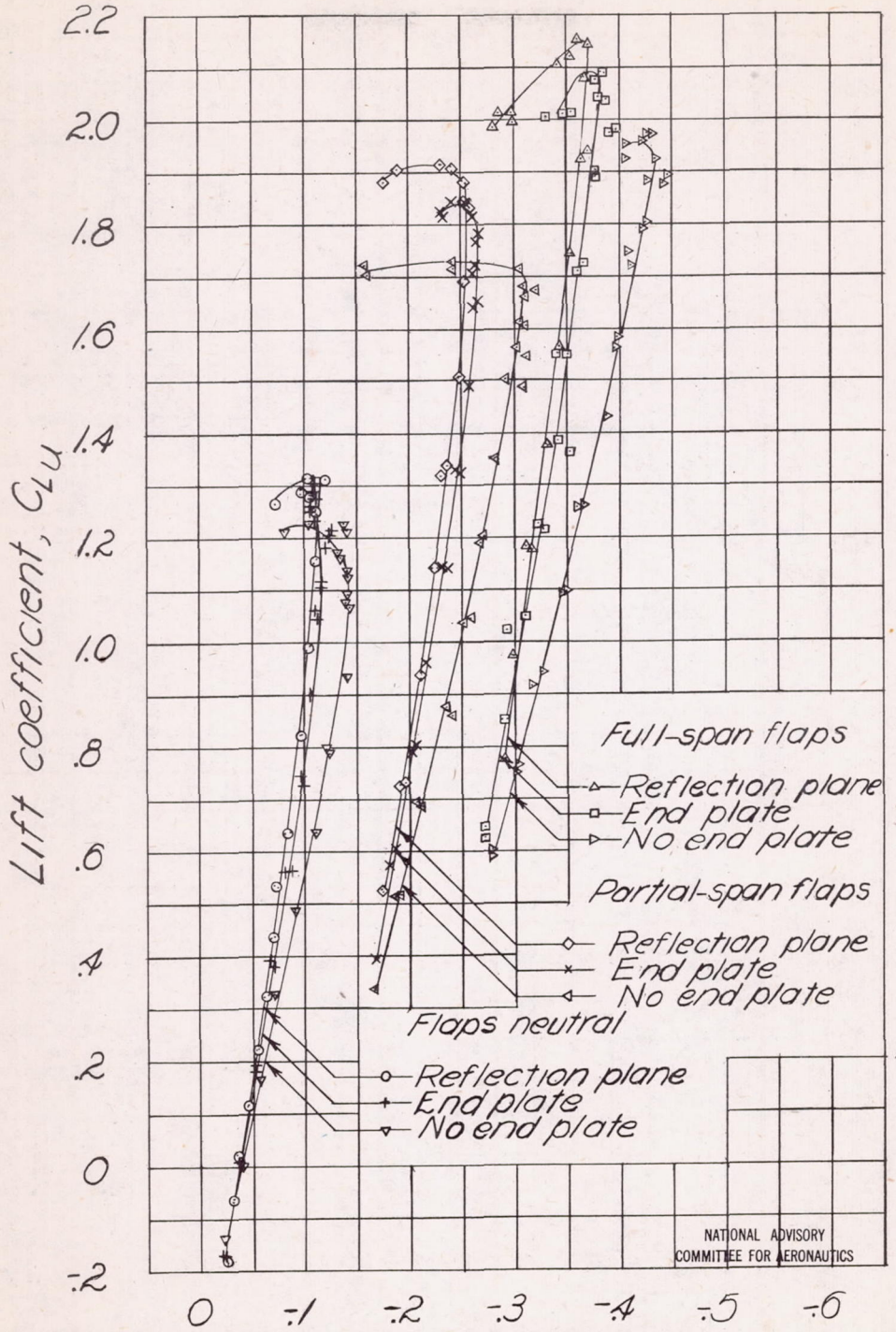
(a) Drag characteristics.

Figure 26.- The uncorrected aerodynamic characteristics of the tapered-wing model for three flap arrangements and three end conditions. $R \approx 8.9 \times 10^6$; $M \approx 0.17$.



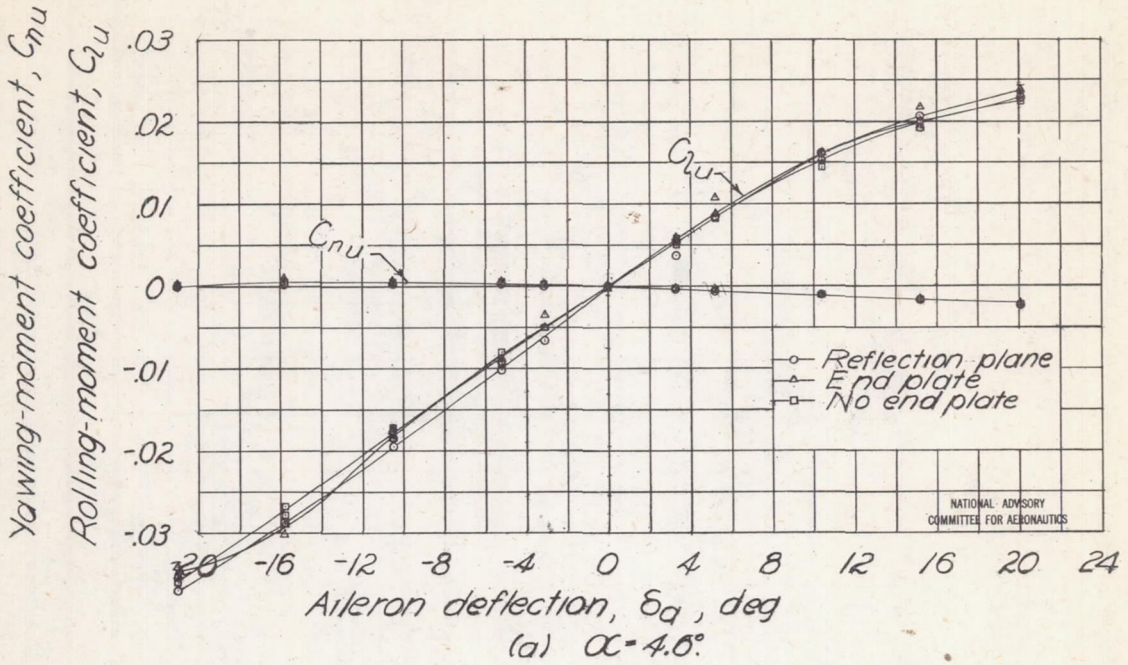
(b) Lift characteristics.

Figure 26.- Continued.

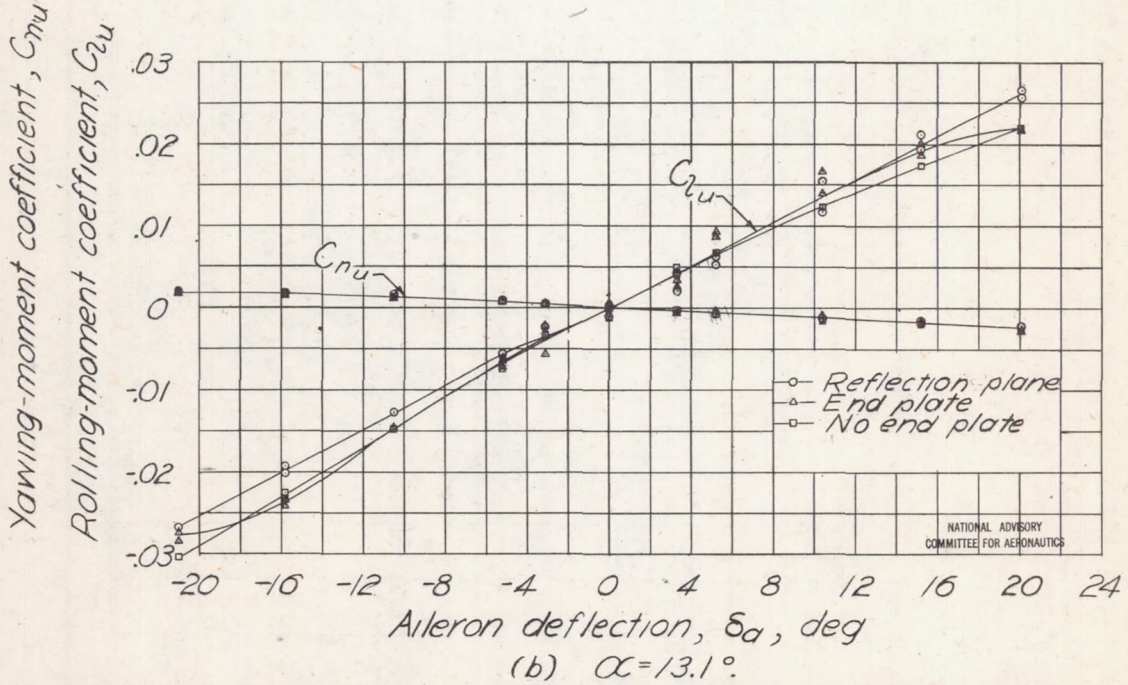


(c) Pitching-moment characteristics.

Figure 26.- Concluded.

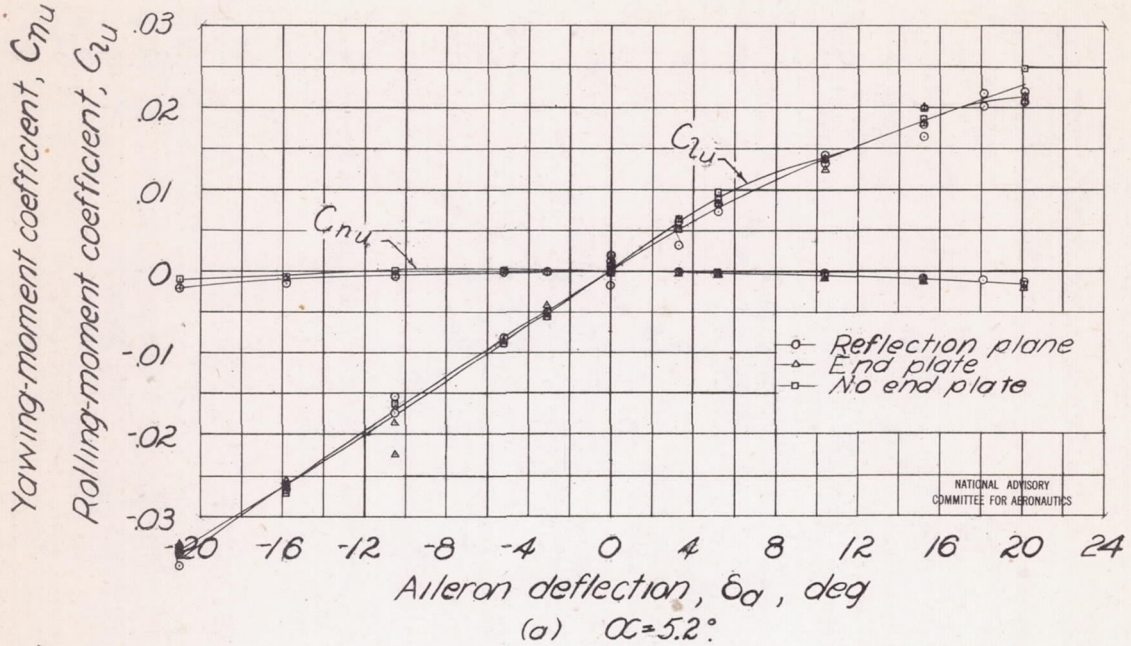


(a) $\alpha = 4.6°$.

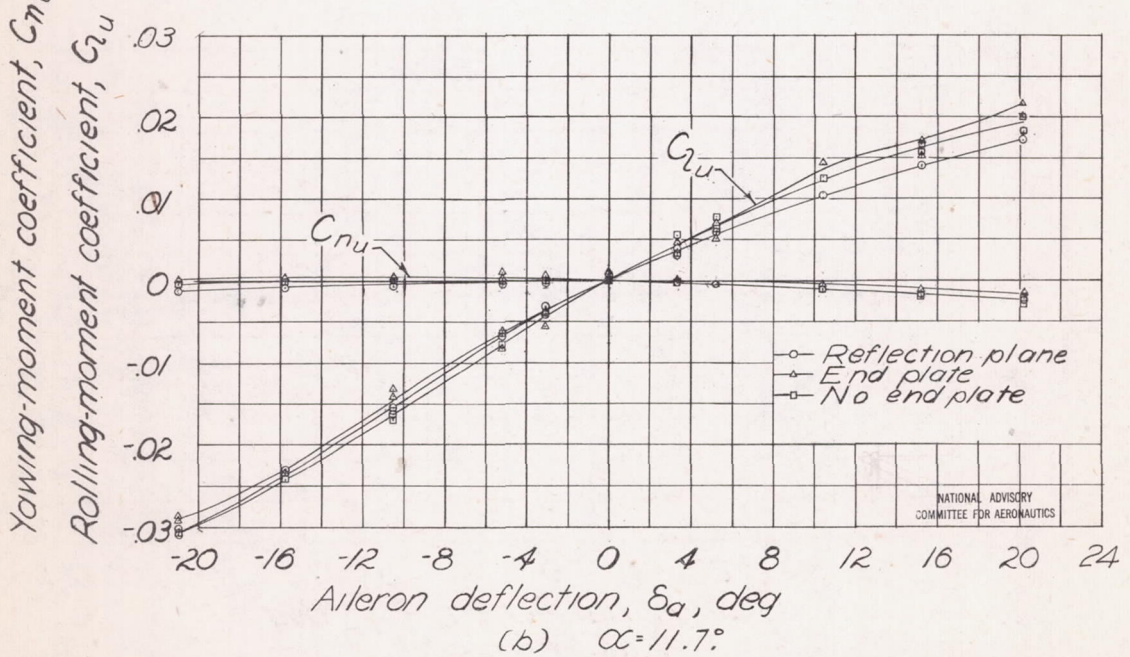


(b) $\alpha = 13.1°$.

Figure 27.-The uncorrected aileron characteristics of the tapered-wing model for three end conditions. Flaps neutral; $R \approx 8.9 \times 10^6$; $M \approx 0.17$.

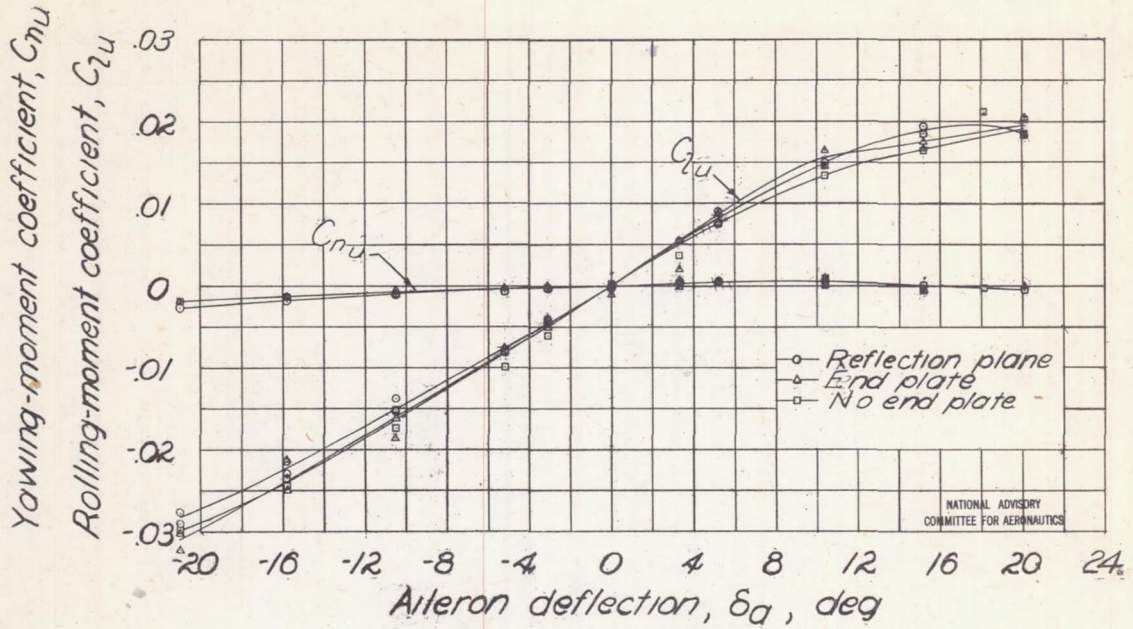


(a) $\alpha = 5.2°$.

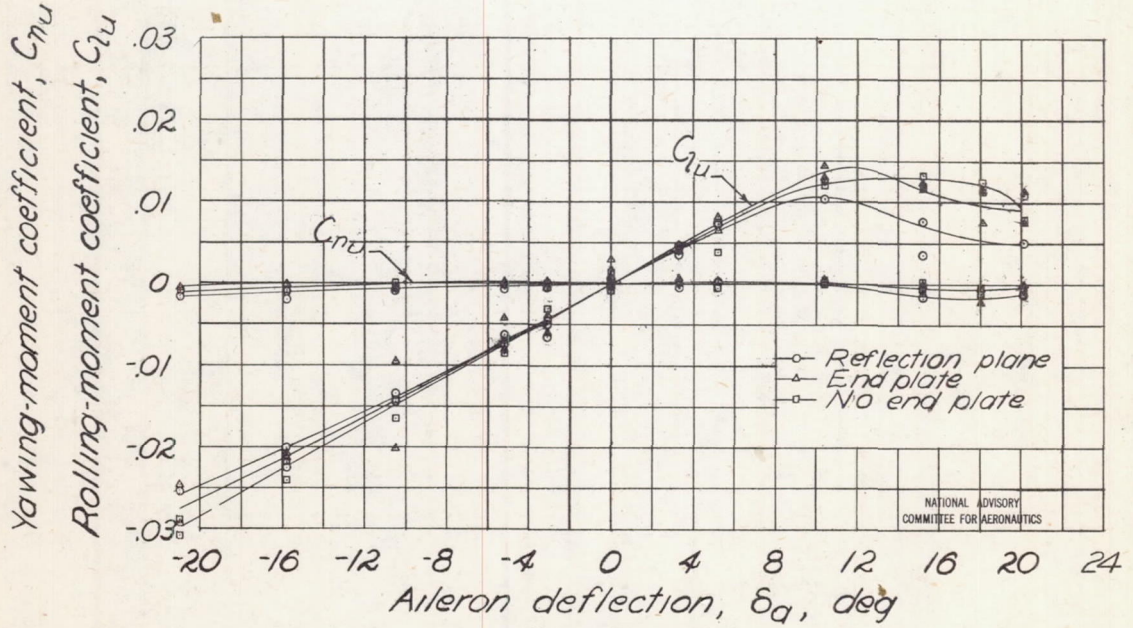


(b) $\alpha = 11.7°$.

Figure 28.–The uncorrected aileron characteristics of the tapered-wing model for three end conditions. Partial-span flaps; $R \approx 8.9 \times 10^6$; $M \approx 0.17$.

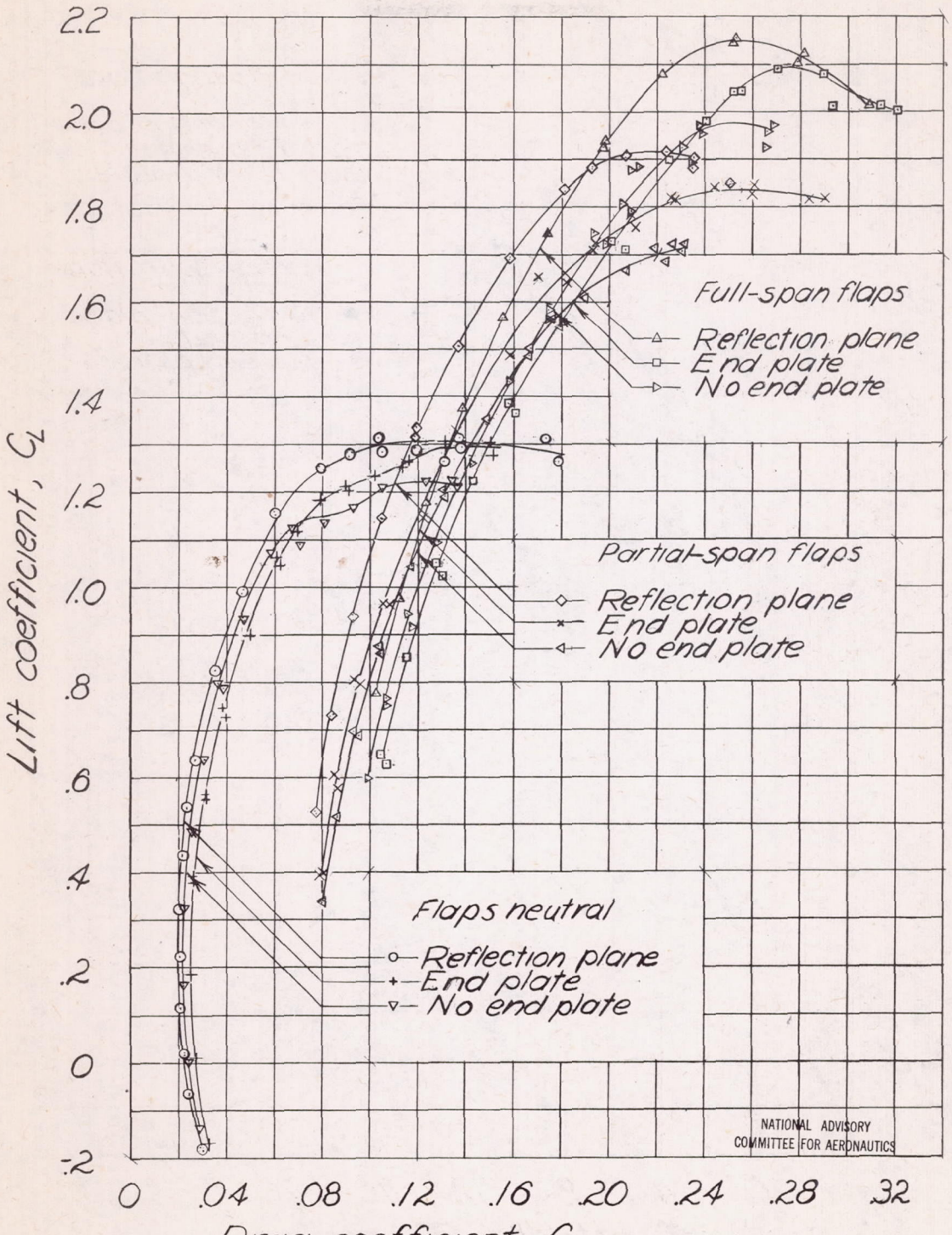


(a) $\alpha = 5.4°$.



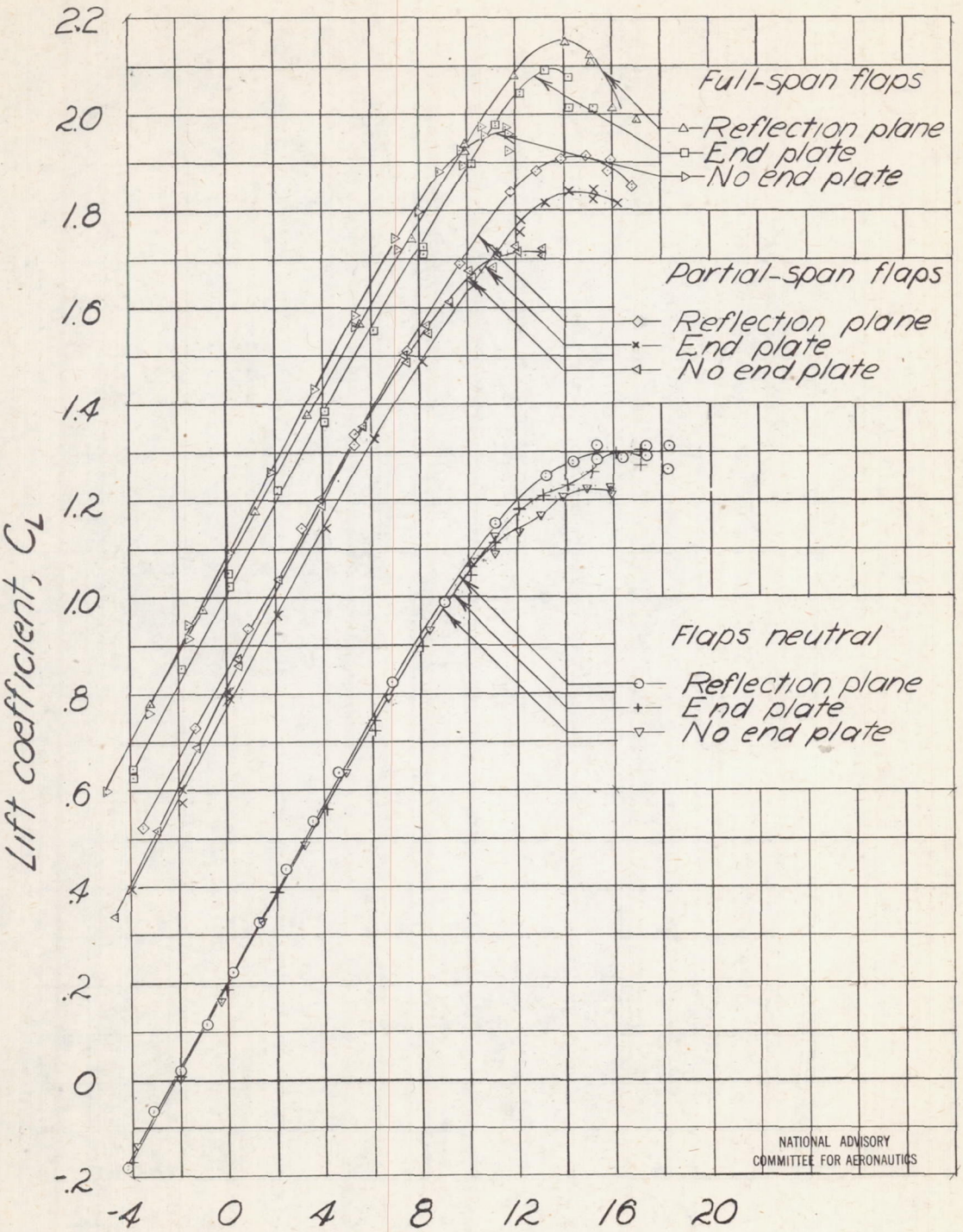
(b) $\alpha = 11.9°$.

Figure 29.-The uncorrected aileron characteristics of the tapered-wing model for three end conditions. Full-span flaps; $R \approx 8.9 \times 10^6$; $M \approx 0.17$.



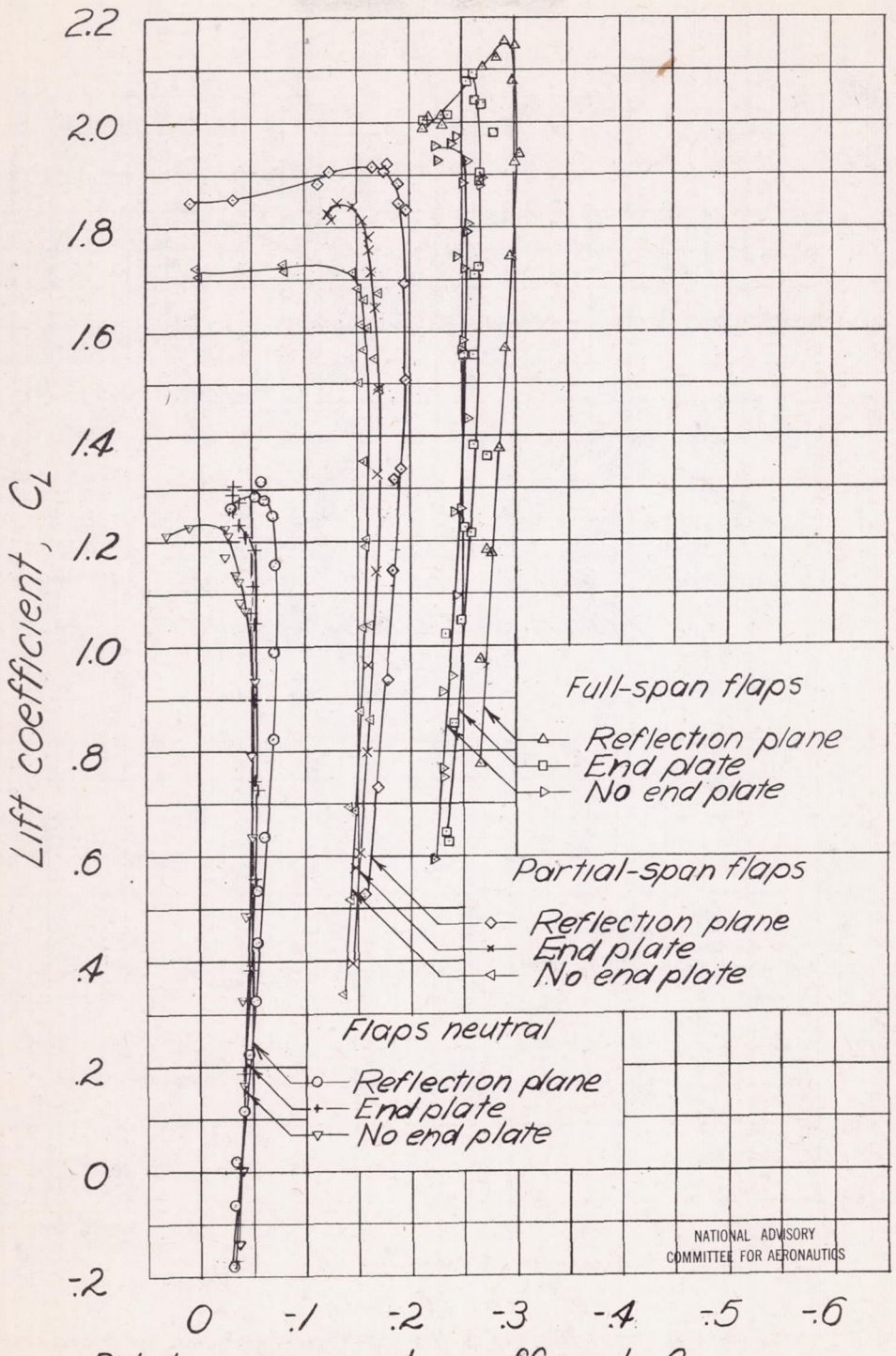
(a) Drag characteristics.

Figure 30.- The corrected aerodynamic characteristics of the tapered-wing model for three flap arrangements and three end conditions. $R \approx 8.9 \times 10^6$; $M \approx 0.17$.



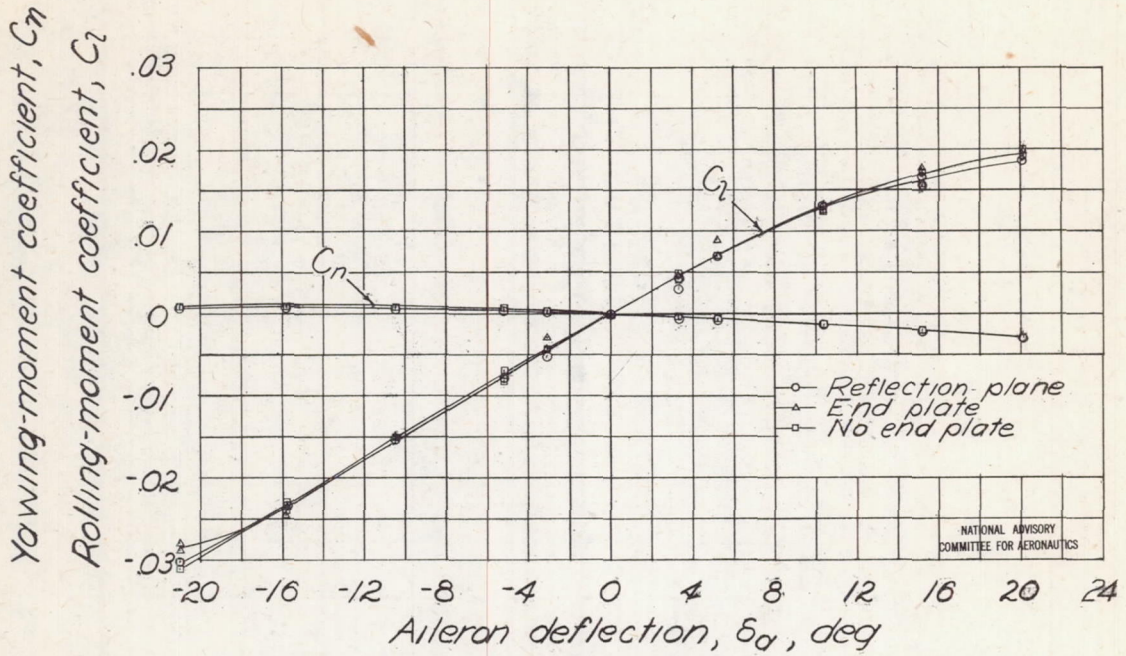
(b) Lift characteristics.

Figure 30.-Continued.

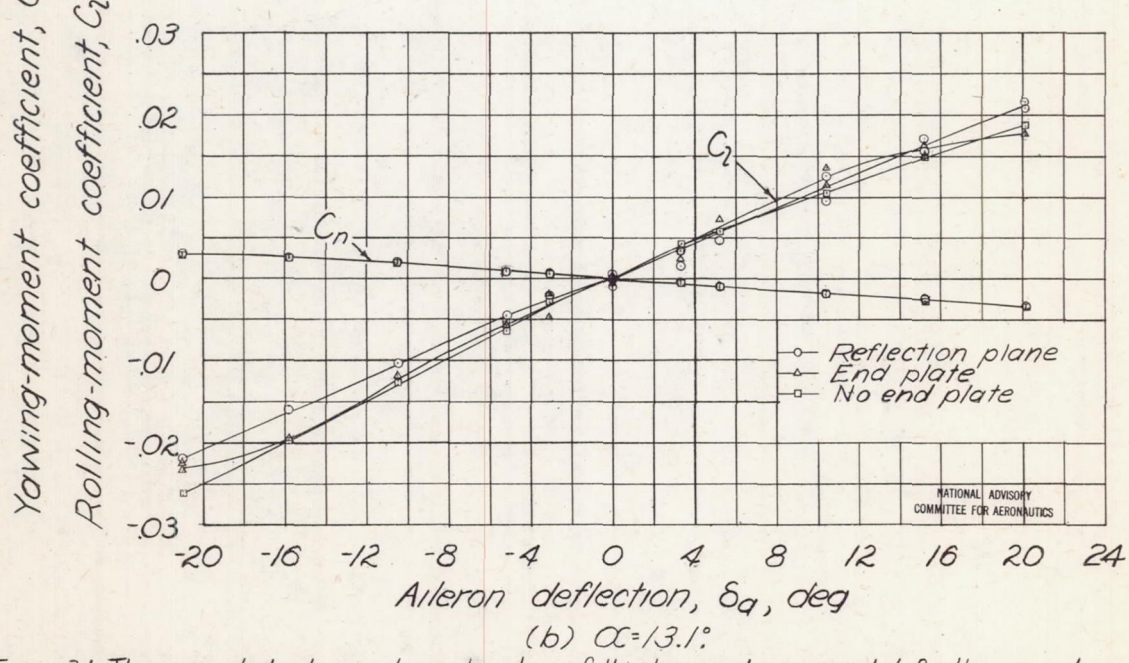


(c) Pitching-moment characteristics.

Figure 30.- Concluded.

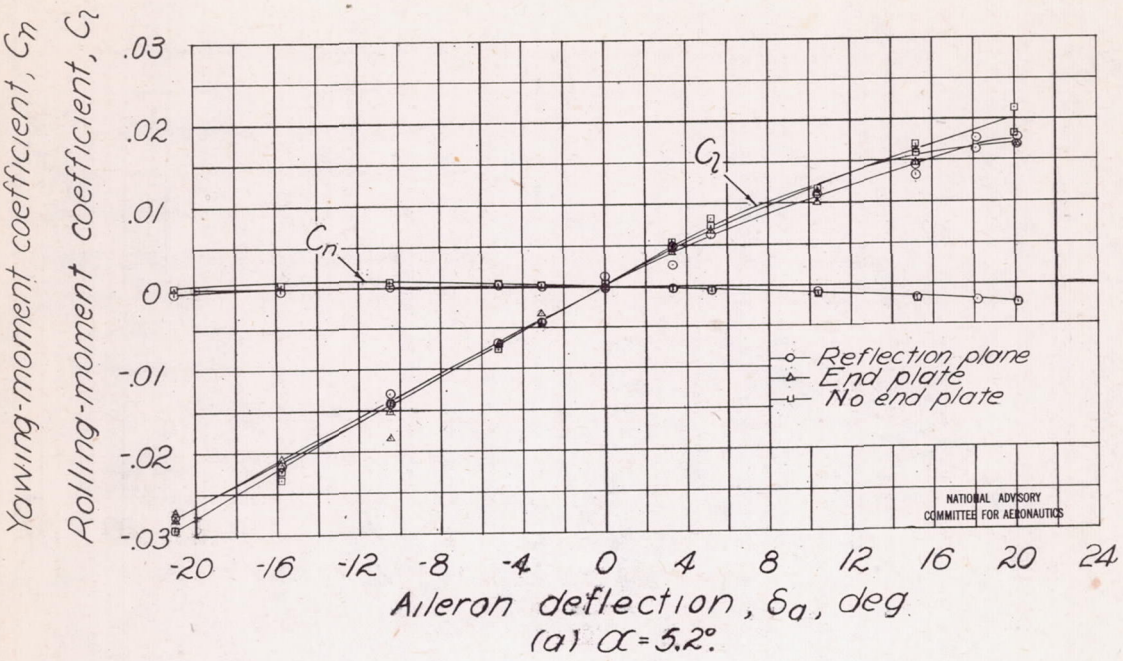


(a) $\alpha = 4.6°$.

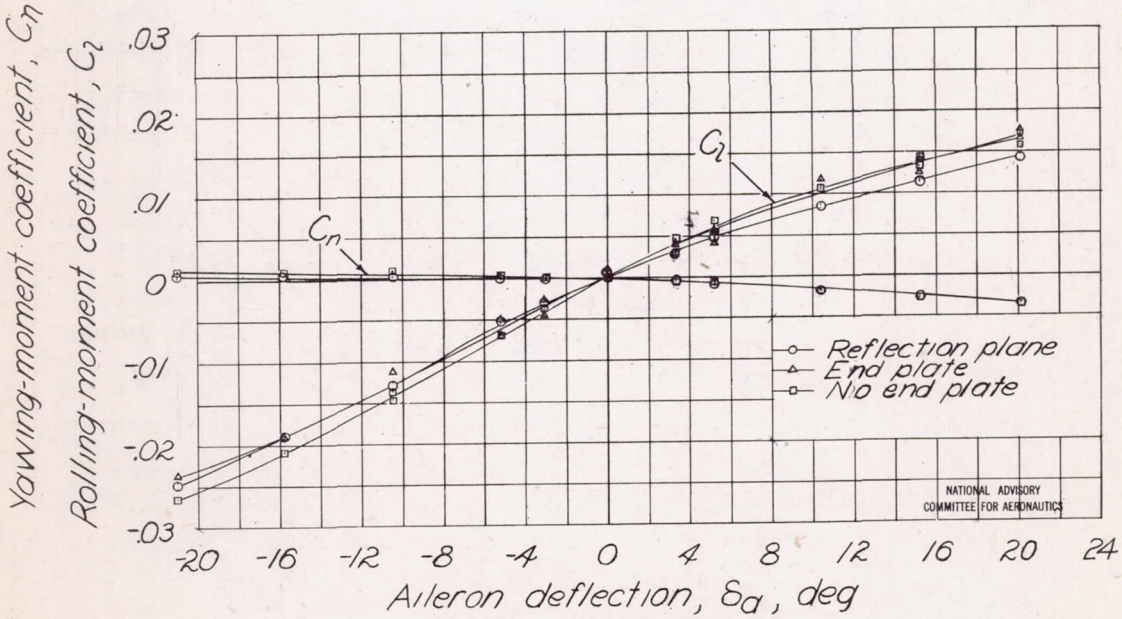


(b) $\alpha = 13.1°$.

Figure 31.-The corrected aileron characteristics of the tapered-wing model for three end conditions. Flaps neutral; $R \approx 8.9 \times 10^6$; $M \approx 0.17$.

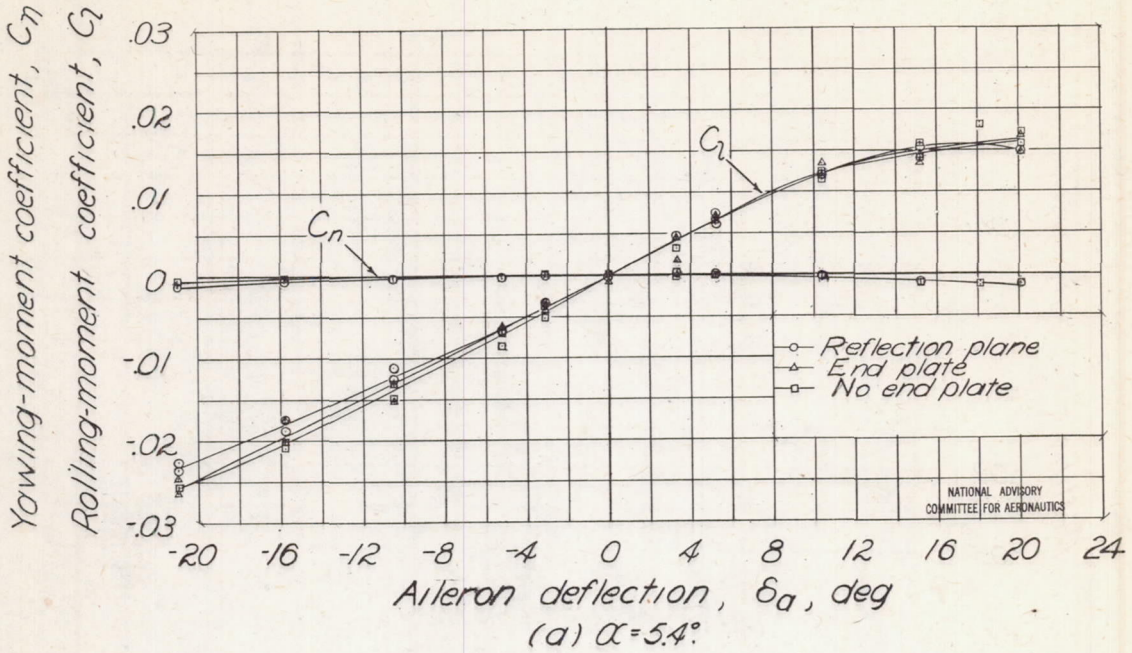


(a) $\alpha = 5.2°$.

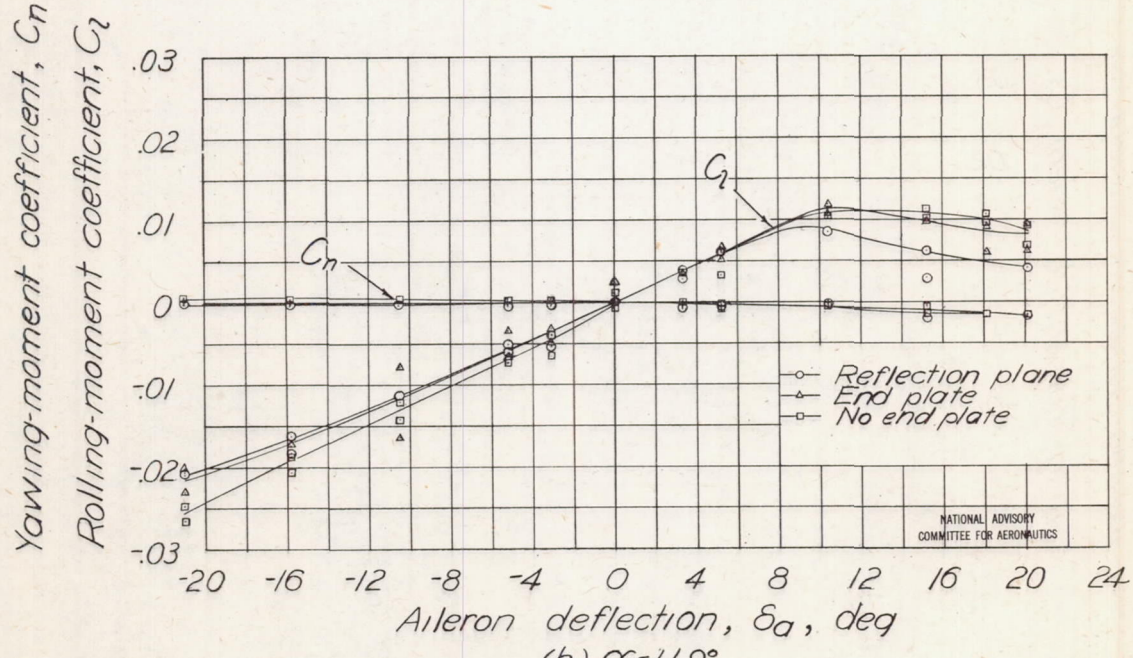


(b) $\alpha = 11.7°$.

Figure 32.- The corrected aileron characteristics of the tapered-wing model for three end conditions. Partial-span flaps; $R \approx 8.9 \times 10^6$; $M \approx 0.17$.

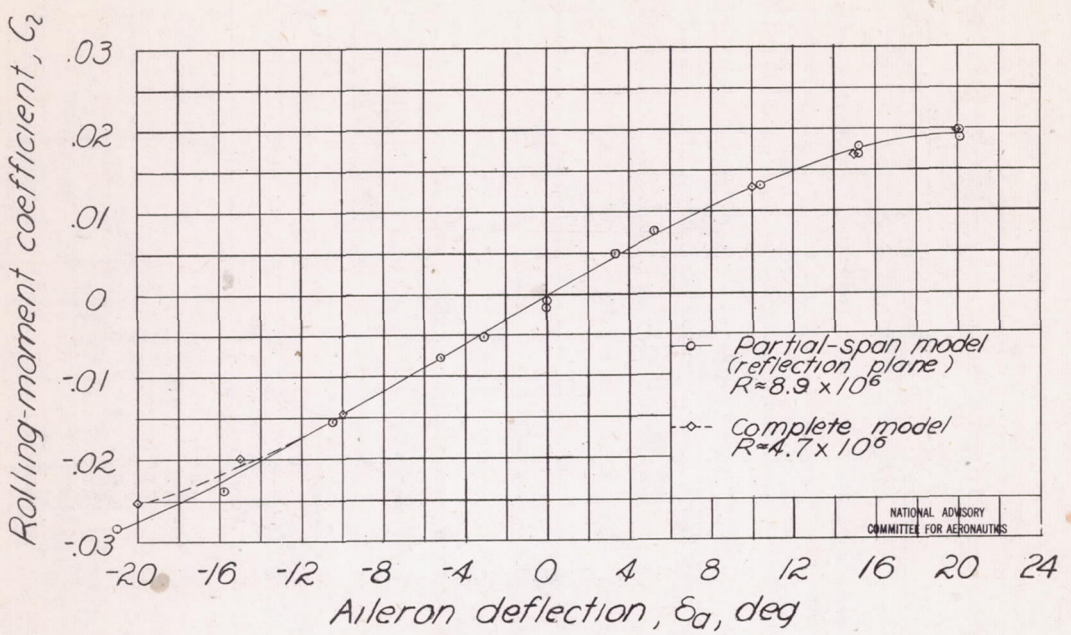


(a) $\alpha = 5.4°$.

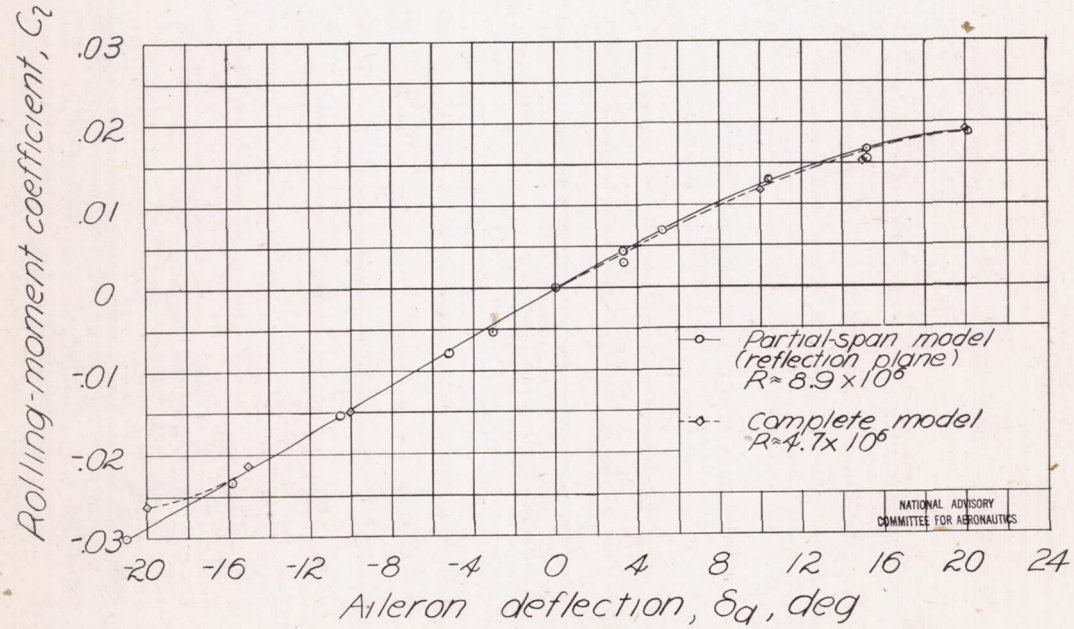


(b) $\alpha = 11.9°$.

Figure 33.- The corrected aileron characteristics of the tapered-wing model for three end conditions. Full-span flaps; $R \approx 8.9 \times 10^6$; $M \approx 0.17$.

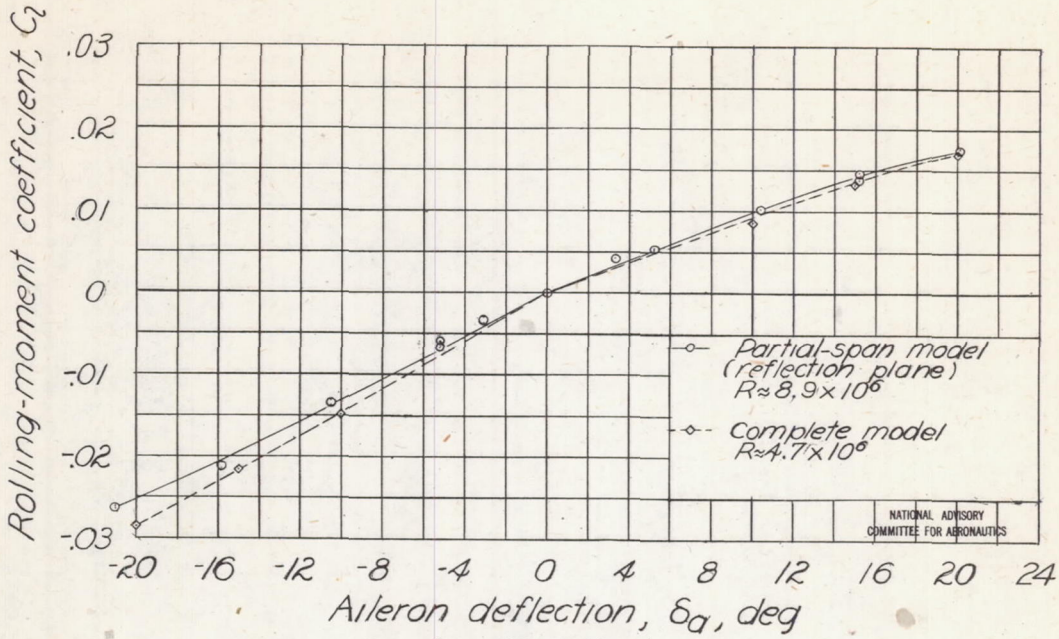


(a) $\alpha = 0.2°$.

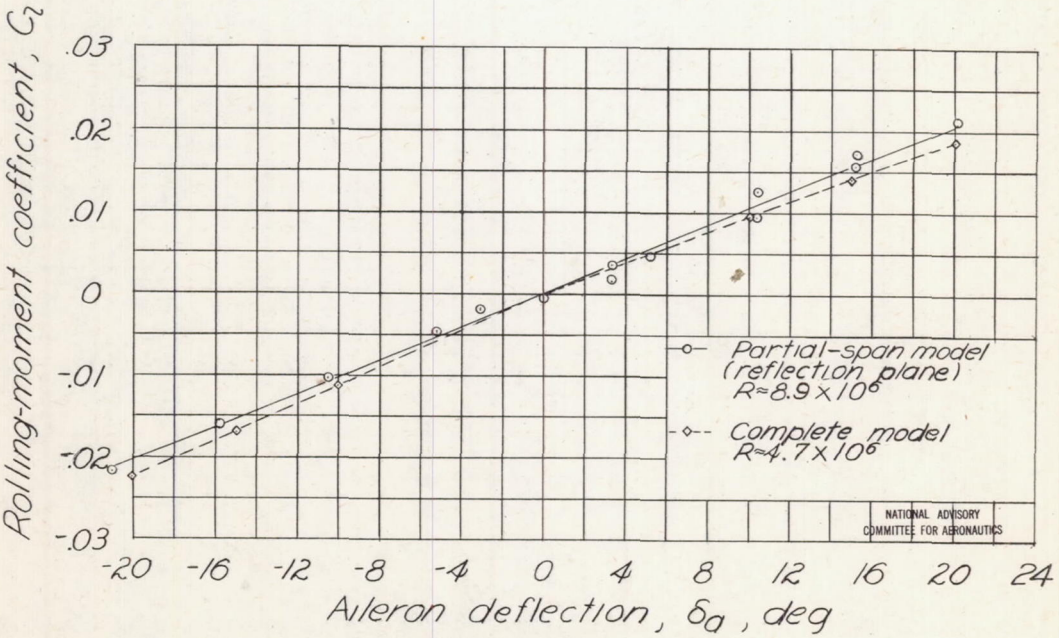


(b) $\alpha = 4.6°$.

Figure 34.-Comparison of the aileron effectiveness of the partial-span tapered-wing model and the complete-span model. Flaps neutral, $M \approx 0.17$.

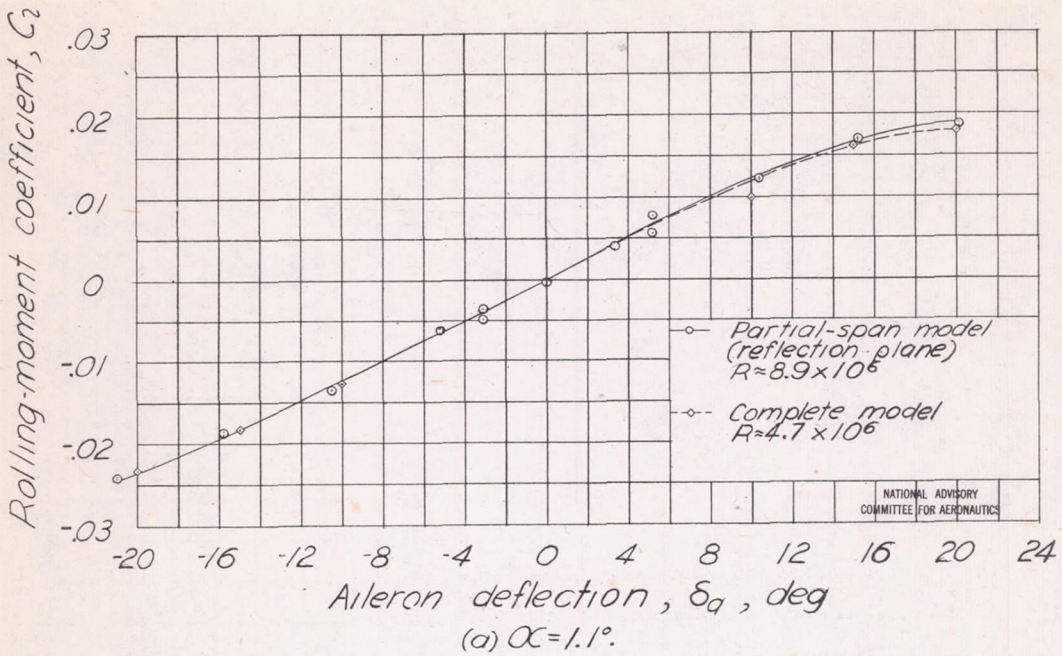


(c) $\alpha = 8.9°$.

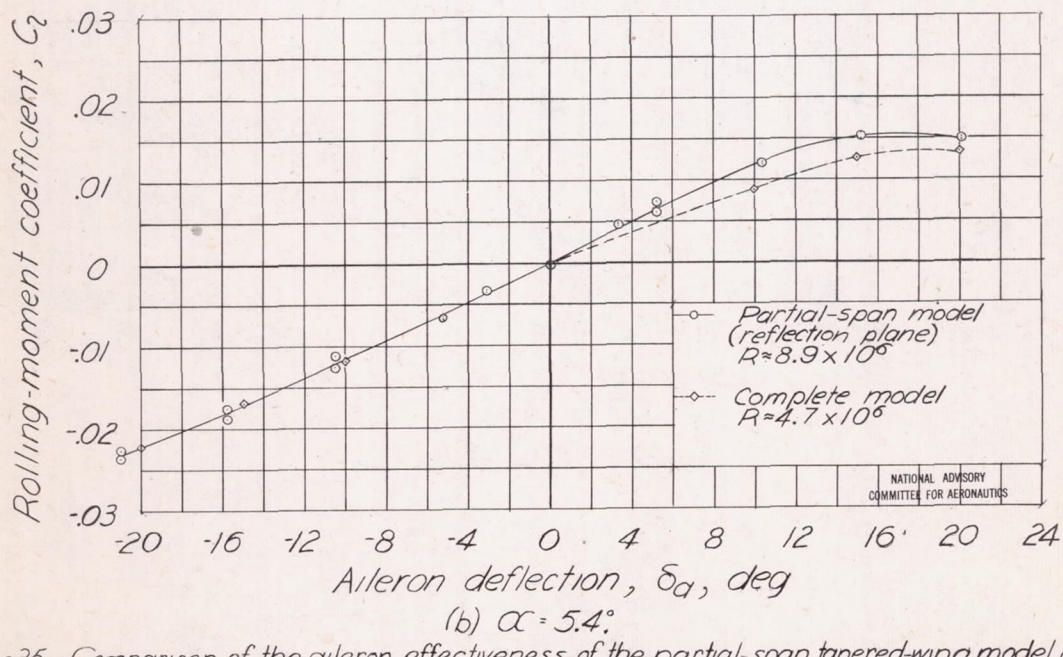


(d) $\alpha = 13.1°$.

Figure 34.- Concluded.

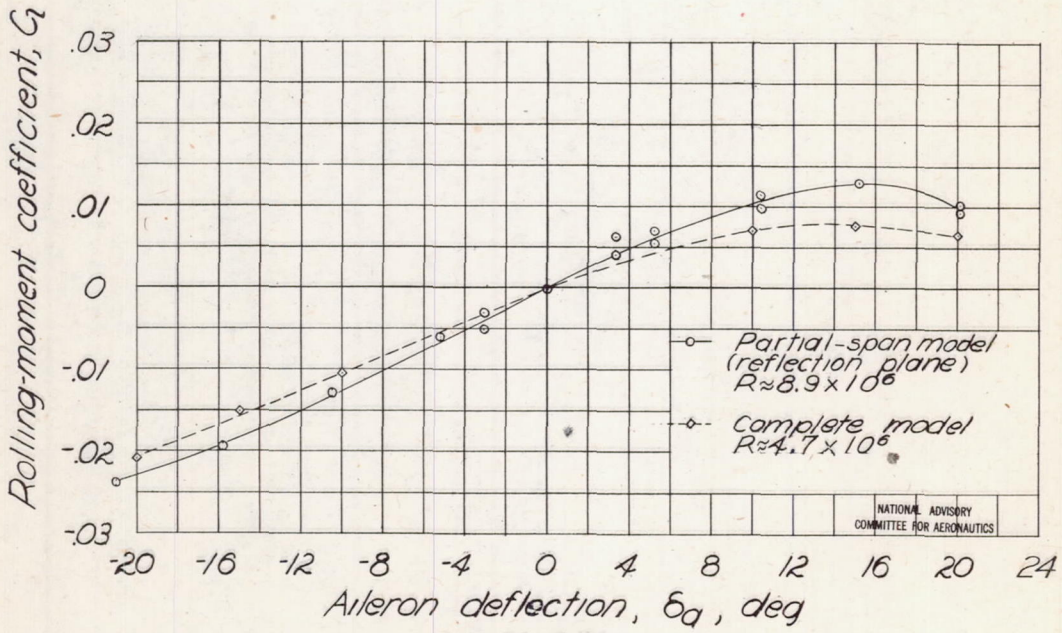


(a) $\alpha = 1.1°$.



(b) $\alpha = 5.4°$.

Figure 35.– Comparison of the aileron effectiveness of the partial-span tapered-wing model and the complete-span model. Full-span flaps deflected, $M \approx 0.17$.



(c) $\alpha = 8.7°$

Figure 35.- Concluded.